DETECTION AND ANALYSIS OF LOW FREQUENCY MAGNETOTELLURIC SIGNALS

by

THOMAS CANTWELL

S.B., Massachusetts Institute of Technology

(1948)

M.B.A., Harvard University

(1951)

SUBMITTED IN PARTIAL FULFILLMENT
OF THE REQUIREMENTS FOR THE
DEGREE OF DOCTOR OF
PHILOSOPHY

at the

MASSACHUSETTS INSTITUTE OF TECHNOLOGY

February, 1960

Signature of Author .....
Department of Geology and Geophysics
January 25, 1960

Certified by.....
Thesis Supervisor

Accepted by.....
Chairman, Departmental Committee
on Graduate Students

TABLE OF CONTENTS

TABLE OF TABLES

TABLE OF FIGURES

ABSTRACT

Title: Detection and Analysis of Low Frequency Magnetotelluric Signals

Author: Thomas Cantwell

Submitted to the Department of Geology and Geophysics on January 25, 1960 in partial fulfillment of the requirements for the degree of Doctor of Philosophy at Massachusetts Institute of Technology

The thesis is an investigation of the earth's natural electromagnetic field in the frequency range from 0.005 cps to 1 cps. This electromagnetic field is the so-called magnetotelluric field. The investigation deals with four problems: first, detection of the magnetotelluric signals; second, methods of analysis assuming the signals represent stationary time series; third, the effects of anisotropy or two-dimensional inhomogeneities in the conductivity structure of the earth, or elliptical polarization of the magnetotelluric field; and fourth, interpretation of the field data.

The detector for the magnetic signal consisted of a 90,000 turn coil wound on a 5-foot Permalloy bar. Sensitivity was 4 millivolts/gamma at 1 cps. The signal was amplified, bandpassed, and chopped before AM recording on magnetic tape. The electric signal was measured over a kilometer distance, perpendicular to the magnetic signal. The electric signal was amplified, bandpassed, chopped, and AM recorded. Signal amplitudes were of the order of a few microvolts for the magnetic field and of the order of a few millivolts for the electric. Bandpassing the signal preserved linearity and gave the overall system a dynamic range of better than 60 db. The pass bands generally used were .005 - .02 cps, .02 - .06 cps, .06 - .2 cps, .2 - .6 cps, and .6 - 1 cps.

The magnetic tapes were processed in the laboratory, and paper records made. These paper records were hand digitalized, and statistically analyzed to obtain the power spectra of the signals. Coherency analysis was also carried out to get coherency between electric and magnetic signals as well as phase shift. In this analysis the records were treated as stationary time series.

Based on the statistical analysis each record was assigned a figure of merit, with the most coherent records being 1, intermediates 2, and the least coherent 3.

Analysis of twenty-five records is included in this thesis.

Investigation of the effects of anisotropy and two-dimensional inhomogeneities centered on how to detect their existence and how to decompose signals so further interpretation could take place. Elliptical polarization of the magnetotelluric field was also considered.

In the general case the magnetic and electric fields may be related by $H_i = \alpha_{ij}E_j$. Along the axes of symmetry of the anisotropy or two-dimensional inhomogeneity, this becomes $H_1 = \alpha_1 E_2$ and $H_2 = \alpha_2 E_1$. The analysis was confined to plane low frequency magnetotelluric waves, and only the horizontal fields entered the analysis.

A summary table of the results is shown below:

Conductivity Structure	Magnetotelluric Field Structure	Diagnostic Feature	Number of Independent Measurements Needed
Horizontally Stratified	Elliptically Polarized	E-H have constant phase at given frequency	1
Anisotropic	Linearly Polarized	Both fields linear	2
Inhomogeneous	"Linearly" Polarized	One field linear, one elliptic	2
Anisotropic	Elliptically Polarized	Solve equations check phases of α_1 and α_2	2
Inhomogeneous	Elliptically Polarized		

Finally the data taken at Littleton, Massachusetts during the fall of 1959 were analyzed and a two-layer interpretation using the method of Cagniard (1953) done. It is shown that the two-layer interpretation agrees well with the data. On the basis of this interpretation a resistivity discontinuity at a depth of 70 km has been postulated. The resistivity in the upper layer has been taken as 8000 ohm-meters and that in the lower layer as less than 80 ohm-meters.

Such a resistivity discontinuity can be explained on the basis of temperature effects. Using the ionic conductivity-temperature data of Hughes (1953) and temperature-depth estimates by MacDonald (1959), it is shown that such a resistivity discontinuity is to be expected.

Thesis Supervisor: T. R. Madden
Assistant Professor of Geophysics

ACKNOWLEDGMENTS

It is the author's pleasant duty to acknowledge the aid of T. R. Madden during this thesis investigation. Without his counsel the topic might not have been discovered, and because of his continued interest and advice the study was a stimulating and enjoyable experience. In addition to all other contributions he programmed the statistical analysis for the IBM 704.

Others who have offered valuable counsel include E. N. Dulaney and J. P. Downs. E. N. Dulaney helped in a variety of ways from field work to theoretical discussions. J. P. Downs offered advice on the IBM 704.

Support for the investigation came from the National Science Foundation's Grant NSF-G6602. The statistical analysis computations were performed at the M.I.T. Computation Center on the IBM 704.

During the major part of this investigation the author was supported by the Department of Geology and Geophysics. The constant interest shown by Dr. R. R. Shrock and others in the Department was much appreciated.

For a brief period at the beginning of this study, the author was supported by the Nuclear Engineering Department, and the interest of T. J. Thompson during this time was gratifying.

A. M. Hauck made available preliminary results from his own resistivity measurements and from his interpretation of available deep resistivity measurements. This made possible a more accurate magnetotelluric interpretation.

Mrs. E. Levingston typed the manuscript and R. Parks drafted the figures. Their assistance is gratefully acknowledged.

CHAPTER I

INTRODUCTION

Purpose of the thesis

This thesis is an investigation of the earth's natural electromagnetic field in the frequency range from 0.005 cps to 1 cps. This electromagnetic field is the so-called magnetotelluric field. The investigation has been limited to several problems: first, detection of the magnetotelluric signals at a number of frequencies, second, methods of statistically treating the detected signals to get them in a form suitable for a conductivity interpretation, third, analysis of the effects of anisotropy and inhomogeneity in the earth, and lastly, interpretation of the field data obtained.

Most studies of the magnetotelluric field have used magnetic and electric signals obtained at an observatory site, and only large scale disturbances have been analyzed. Correlations have been done using these disturbances. For the most part, the records obtained can be analyzed only during these large disturbances, which may occur 10-20% of the time or less.

In contrast to this, a geophysical field tool should be functional a major portion of the time. In using magnetotellurics to study the regional crustal structure, it is desired to go to the chosen location, make a measurement, and be reasonably certain that the data obtained

will be useful. The development of magnetotellurics into a reliable field geophysical tool is a major object of this thesis.

Historical

The term magnetotellurics was coined by Cagnaird (1953) and is used to designate the combined variable electric and magnetic fields of the earth; that is, the electromagnetic field of the earth. The term is usually restricted to variable fields with periods of several minutes or less. Traditionally these fields have been studied as separate phenomena, with the electric fields known as telluric fields and the magnetic fields known as geomagnetic pulsations. Many workers; for example, Rikitake (1951), Holmberg (1951), Duffus and Shand (1958), Maple (1959), Campbell (1959) and Watanabe (1959); have studied these fields as separate phenomena, and it is from their investigations that the properties of these fields have been deduced. Others; for example, Hatakeyama and Hirayama (1934), Burkhart (1955), Scholte and Veldkamp (1955), Enenshtein and Aronov (1957), Lipskaia (1953), and Tikhonov (1956); recognized that some events on telluric and geomagnetic records could be correlated as to phase and amplitude, and this information could in theory be used to determine the conductivity structure of the earth's crust. The results in the literature so far are not encouraging to

this method since the resistivities obtained seem unreasonable. Observations were made at observatory sites, and to date no use of the magnetotelluric method to determine crustal structure over a broad area has appeared in the literature.

The source of the oscillations up to 1 cps seems to be located in the ionosphere. For the higher frequencies, sub-audio and audio, the likely source seems to be lightning and other local atmospheric disturbances. That the sources of the magnetotelluric field is outside the earth is dictated by their high frequencies and consequent shallow skin depth.

While little attempt has been made on an organized basis to use the frequencies below 1 cps for determining the earth's conductivity structure, the audio frequencies have been made the basis of a prospecting tool known as AFMAG. As described by Ward et al (1958) and Ward (1959), this method determines the plane of polarization of the magnetic field by measuring two of its components. Since a good conductor "attracts" the telluric current, an anomalous magnetic field exists in the vicinity of the conductor causing a "crossover" or in other words, giving a vertical component to the otherwise horizontal variable geomagnetic field.

Recent progress in magnetotellurics has been reported by Webster (1957) and Niblett (1959),but useful magneto-

telluric data is still scarce.

Uniformity of the field

Even though the causes of the magnetotelluric field are felt to be known, the locations and strengths of these fields are not and very likely never will be. In order to treat the fields and their interaction with the earth, it is necessary to assume them to be plane fields. This assumption depends on the experimental fact that these fields are uniform over wide areas, or in other words we are dealing with uniform current sheets.

The evidence for such uniformity is strong, especially for major disturbances. Since the location and distribution of the sources is very likely the same for disturbances of any magnitude, uniformity is a very reasonable assumption. Simultaneous measurements over distances up to hundreds of kilometers are reported by Schlumberger and Kunetz (1946), Kunetz (1952), Kunetz (1953), and Duffus et al (1959). A summary of the evidence is given by Cagniard (1956). In all of these references excellent visual correlation is reported for records made at distant points, and as we shall point out, the eye is a sensitive correlator.

With this evidence, the magnetotelluric fields may be assumed to be uniform over distances on the order of hundreds of kilometers. This allows treatment of the fields as plane and avoids the difficulties in having to identify the sources and establish their properties.

Direction of propagation of the magnetotelluric field in the earth

It is of interest to note that because of the great conductivity contrast from the air to the earth, an electromagnetic wave incident at any angle propagates essentially downwards. This can be demonstrated by considering the governing equation

$$\nabla^2 \phi + k^2 \phi = 0$$

This is essentially the wave equation with $k \sim 10^{-9}$ for air and $k \sim 10^{-4}$ for the ground. Application of Snell's law shows the downward propagation.

Independence of individual measurements

Before presenting a summary of the theoretical results for a stratified earth it is well to note that the magnetotelluric method allows each measurement to be independent of other measurements and independent of any base station measurement. If we define, as is usually done, the impedance normal to the earth as the ratio of the tangential electric field intensity to the tangential magnetic field intensity, then the independence of measurements becomes evident, as it is just these quantities that are measured at any one location.

From these measured quantities, tangential E and H, it is possible to construct a plot of apparent resistivity against frequency. Variations of apparent resistivity with

frequency can be explained for a stratified earth in terms of varying conductivity at depth. The lower frequencies will penetrate more deeply and "see" more of the deeper conductivity structure.

Stratified earth model

These concepts can be put in a quantitative form by summarizing the results given by Cagniard (1953). We must first establish a coordinate system and we will use the one shown below where the x-y plane is the earth's surface and z increases downwards. This system will be used throughout this thesis.

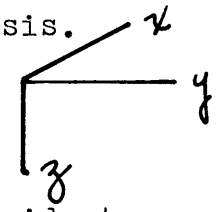

For a plane wave incident on a uniform earth the ratio of tangential E to tangential H is given by

$$E_x/H_y = (\rho_a \mu \omega)^{1/2} e^{i\pi/4}$$

where ρ_a is the resistivity in ohm-meters, μ is the permeability in henry/meter, ω is the radial frequency, E_x is the electric field in the x-direction, and H_y is the magnetic field in the y-direction. Determining this ratio for a uniform earth gives an interpretation of the conductivity, since μ is generally constant. The units throughout this thesis will be rationalized MKS unless otherwise noted.

The skin depth can be expressed as

$$\delta = \sqrt{\frac{2}{\mu w \sigma}}$$

and the dependence of this quantity on frequency appears.

In the two layer case the previous formula is modified to

$$E_x/H_y = (\rho_a \mu w)^{1/2} e^{i(\pi/4 + \psi)}$$

where ρ_a is an apparent resistivity, and the angle ψ modifies the previous 45° shift for the uniform earth. Master curves for this two layer case were worked out by Cagniard and are presented in Figure 13. Plotting the apparent resistivity or phase versus $(\text{period})^{\frac{1}{2}}$ on the same scale as the master curves, the plot is moved to coincide with one of the master curves. This establishes the resistance of the lower layer and its thickness since the resistivity value lying on $\rho_a = 1 \Omega m$ is ρ_1 and multiplying this by the contrast gives ρ_2. The thickness is found by considering the projection of point A on the $(T)^{1/2}$ axis. This thickness $h = \frac{x}{8}\sqrt{10 \rho_1}$ km letting x be the value of this projection. This method will be used in Chapter IV.

Cagniard also demonstrates the general n-layered case.

Real earth complications

The real earth complications stem from two sources; the earth is not always horizontally stratified, and the signals are not always noise-free, linearly polarized waves. The stratified model may not approximate the real earth closely enough and our magnetotelluric signals are corrupted

with noise.

Attempts to remove the first restriction and consider even two-dimensional structures lead to a classic problem of theoretical physics; the wave equation and the finitely conducting wedge. In the past, many workers have attempted to solve this problem. Clemmow (1953), Karp (1959), and Karal and Karp (1959) are among those to have considered this problem recently, but using special restrictions such as infinite conductivity or high frequency electromagnetic waves. So far the general case remains unsolved. Neves (1957) and Kunetz and d'Erceville (1959) have treated the magnetotelluric problem with success as long as the electric field was across strike. That is, as long as current was flowing across the two-dimensional feature. Calculations by Madden (1959) show that for this case, with a resistivity contrast of 16, phase shifts up to 135° can be observed, and apparent resistivities will vary by a factor of 30 in crossing the contact. This is shown in Figure 14.

An excellent summary of the problem of diffraction of electromagnetic waves by a finitely conducting wedge appears in Neves (1957).

Although the general problem has not yielded to analytic treatment, it is possible to use finite difference equations to approximate the differential equations. The finite difference equations can then be solved either by a digital computer or by an analogue computer, and both of these approaches are being taken by others in the Geophysics Group

at M.I.T. The calculations referred to by Madden above were done using the digital computer to solve the finite difference equations.

In the one-dimensional case discussed previously, a magnetotelluric measurement, or sounding, at one spot was sufficient to establish the sub-surface conductivity structure. In the two-dimensional case a line of data across the two-dimensional feature will be necessary in order to make an interpretation.

This thesis will not treat the two-dimensional problems in detail. However, the case in which the earth conductivity can be treated as a second order tensor will be considered as it affects the magnetotelluric field. The attempt is made to show how the properties of this tensor can be determined, given field measurements on the surface.

The other real earth complication, that the signals are noisy, only becomes evident on taking data. For example, Figure 9 shows a record with some apparent correlation but the quantitative questions of the amplitude ratios and phase shifts are not so apparent. We say that such a record is a noisy record, although the precise source of the noise is not identified.

The treatment of signals corrupted by noise has been given by a number of authors; Davenport and Root (1958), Bendat (1958), Blackman and Tukey (1958), and Robinson (1954). The technique of autocorrelation and crosscorrelation

followed by taking the Fourier transforms of these correlations to get the power spectra is used to analyze the signals as discussed in the chapter on analysis. The last record shown in Figure 9 has the power spectra shown in Figure 12 with the coherency analysis, a measure of the correlation between the traces, shown in Appendix I. Statistical techniques allow a quantitative measure to the amount of correlation.

The requirements on the signals being analyzed are that they be part of a stationary time series. We assume that the noise is random and incoherent on both traces so that it will disappear in the cross correlation. The final step is to use the ratios of the power autospectra to determine E/H and calculate the apparent resistivity. The odd and even parts of the power cross spectra are used to determine the phase angle between the two signals.

A further complication could be that the magnetotelluric field is elliptically polarized and that the relation between E and H can be represented by a second order tensor as $H_i = \alpha_{ij} E_j$. These further complications can be divided into three categories:

i) The earth has vertical conductivity variations only and the field is elliptically polarized.

ii) The relationship of E to H can be represented by a second order tensor and the field is linearly polarized.

iii) The relationship of E to H can be represented by a second order tensor and the field is elliptically polarized.

Complications ii) and iii) could arise from anisotropy in the ground or from inhomogeneities; contacts and the like. Anisotropy would give rise to measurements constant over the surface. Inhomogeneities would cause varying measurements and possible characteristic phase shifts.

Methods of handling the field data for each of the above cases will be suggested, as well as methods for obtaining the data.

Outline of the thesis

The chapters are organized as follows:

Chapter I - Introduction: The purpose of the thesis, brief historical review, and summary of past important work is presented. The complications found in the real earth and the investigations followed to remove these complications are discussed.

Chapter II - Detection: The equipment and field techniques to obtain the electric and magnetic signals are described.

Chapter III - Analysis: The records are discussed, methods of analysis proposed, and the correlation techniques used are presented. The treatment of elliptically polarized magnetotelluric fields is discussed, as is the representation of the conductivity by a second order tensor.

Chapter IV - Results: Records and computer correlation results are presented and discussed. Conductivity-depth relationships are shown, and a discontinuity in resistivity at 70 km is postulated.

Chapter V - Further work: Recommendations for means of obtaining data are presented. A program for crustal exploration is outlined. The need for determining the geographical correlation of all frequencies of the magnetotelluric field is discussed. Theoretical work is requested in certain phases of the problem.

CHAPTER II

DETECTION OF MAGNETOTELLURIC SIGNALS

General

The problem of detection of magnetotelluric signals subdivides into detection of the electric field and of the magnetic field. The headings in this chapter are divided thus, with additional sections to describe the field recording method and the playback method used in the laboratory to restore the signals to a form suitable for analysis.

The frequency range covered by the signals measured in this work runs from a lower limit of 0.005 cps to an upper of 2 cps. The amplifiers are direct coupled, and as will be shown, in the case of the magnetic signal the equivalent input noise to the amplification equipment has to be at the sub-microvolt level. The general scheme of handling the signals is to amplify, filter, chop, and record the chopped signal directly on magnetic tape. In the laboratory the tape signal is either filtered and demodulated or demodulated directly and the restored signals fed to a paper recorder.

Although the theoretical treatment of the magnetotelluric method has been in the literature for a number of years no satisfactory measurements have appeared. We can only speculate as to why this is so, since the physical characteristics of the field seem to be advantageous to such measurements. One limiting factor in the past has very likely

been instrumentation. Several of the instruments used in this investigation have only recently become available, for example the very low frequency band pass filters, and the low noise amplifiers. One other technique that helps to discriminate signal from noise is the statistical treatment described in the next chapter. These two factors contributed heavily to the successful results of this investigation.

The quantities to be measured are the electric and magnetic field amplitudes and the phase angle between them.

The electronic instrumentation was purchased whenever possible. This philosophy is based on the observation that purchased equipment is more reliable and generally less expensive. This also allowed us to do a better design and construction job on the equipment built.

Magnetic field instrumentation

A schematic of this equipment is shown in Figure 1.

The coil consists of 90,000 turns of #26 copper magnet wire wound in pi-sections of 6000 turns each. This coil is slipped over a five-foot Permalloy bar. The whole assembly is placed in a wooden box for ease in handling.

The resonant frequency of the coil is 250 cps equivalent to a shunt capacitance of 100 $\mu\mu$f. The inductance of the coil is 4000 henries and the resistance at zero frequency is 1830 ohms.

The coil was detuned to a resonant frequency below 60 cps by shunting with a condenser. The following table shows the measured resonant frequencies obtained and the nominal shunt capacitance.

Table I - Shunt Capacitance and Coil Resonant Frequency.

Shunt Capacitance	Resonant Frequency
mfd	cps
0.1	8.5
1.0	2.5
10.0	0.75

The coil is placed on a three-legged stand at a distance of 100 feet from the recording truck. The portable 60 cps gasoline generator is placed about 100 feet from the truck in the opposite direction. No coupling between the generator and the coil system has been detected. The power supply includes a voltage regulator from which all equipment draws power.

The signal from the coil is fed through a shielded cable to a low noise, direct coupled amplifier. We use the Offner 190 differential data amplifier. The maximum output of this amplifier is $\pm$ 10 volts with 0.05% linearity. Laboratory tests using mixed signals of 70 cps and 1 cps showed that signals of .7 μv of 1 cps could be picked out of 7 mv of 70 cps with proper filtering, after this amplifier. The sources used in this test were low impedance, about 1000 ohms each.

The input impedance of this amplifier is 100,000 ohms and the output impedance a few ohms. The source impedance is suggested as limited at 1000 ohms but the use of a higher source impedance still gives acceptable noise figures for our use.

The signal is then fed to a low pass filter of the type outlined in Jackson (1943), using two m-derived sections separated by a constant - k section. The filter as built starts to cut off about 55 cps and has a 60 cps rejection of 60 db. The iterative impedance of this filter is 1800 ohms.

Following this filter is a potentiometer type voltage bucking system. It was discovered that the coil tuning condensers generate a few tens of microvolts steady voltage. When amplified by a million this becomes tens of volts, and we have tried to limit the input to the band pass filter to ten volts. Therefore, a voltage source, variable from 0 to 1 volt, is inserted in the circuit to null out the consenser voltage.

Final amplification is by a Philbrick USA-3 amplifier with variable gain up to x1000. The input circuit has been modified to give amplification independent of the source impedance.

This signal is fed to a variable band pass filter, Krohnhite 330A, covering the range from .005 cps to 500 cps. The frequency attenuation outside the pass band is 24 db per octave.

The overall performance of the system was checked by putting a 1000 Ω resistor at the end of the 100 foot cable, replacing the coil. The noise behavior of the system is shown below at frequency bands corresponding to Krohnhite settings.

Table II - Noise Behavior of the Magnetic System

Frequency Band	Equivalent Input Noise
.02 - .06 cps	0.20 μv
.06 - .2	0.20
.2 - .6	0.25
.6 - 2.	0.20

Noise here refers to the maximum peak to peak swing occurring during 50 periods of the lowest frequency in the band.

Tests made in the laboratory demonstrated that we could take a 0.5 μv peak to peak signal from a signal generator of 1000 Ω output impedance, process it through the electronic system, and recover it very nearly undistorted. This is with the Krohnhite filter set at the frequency bands listed in the previous table and the signals near the band center.

This brief description concludes the magnetic field instrumentation section, and the coil design and field noise problems will be considered before turning to the electric field system.

Magnetic coil design

The design criteria for the coil can be broadly stated as follows:

For 0.1 γ magnetic variations at 0.02 cps, the output should be in the range 1-10 μV . The resistance of the coil should be 1000-2000 ohms.

The equivalent circuit of the coil will be taken as:

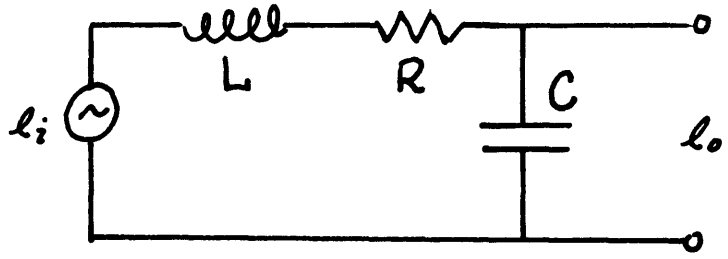

From considerations of voltage induced in a coil of wire by a magnetic field, $B_m = B e^{i\omega t}$,

$$e_i = i \omega B n A_{eff.}$$

where ω is circular frequency in radians/second,
B is the amplitude of magnetic variations in $^{webers}/_{m^2}$,
n is the number of turns in the coil,
and A_{eff} is the effective coil area in meters^2.

The output voltage of the equivalent circuit is

$$e_o = \frac{\omega B n A_{eff}}{(\omega^2 LC - 1) - i RC\omega} = \frac{e_i}{Z_t} \omega C$$

Taking typical orders of magnitude for the various quantities

$$\omega^2 \sim 10^{-3} \ (^{rad}/_{sec})^2$$

$$L \sim 10^3 \text{ henries}$$

$$C \sim 10^{-10} \text{ farads}$$

$$R \sim 10^3 \text{ ohms}$$

We see that a valid approximate expression will be

$$\ell_o = \omega B n A_{eff}$$

For the frequency to be used for design, we have

$$\omega = .06 \ \frac{\text{radians}}{\text{sec}}$$

$$B = 10^{-10} \ \frac{\text{webers}}{2} \ (.1 \ \gamma)$$

$$n = 90{,}000 \text{ turns}$$

$$A_{eff} = 1 \ m^2 \text{ (for a 3/4-inch diameter permalloy bar, 5 feet long)}$$

giving a calculated output voltage of .54 μv or 1.08 μv peak to peak. The output was felt to be adequate.

The coil was calibrated by two methods. A large cube coil as described by Reubens (1945) was constructed, 14 feet on a side. The coil to be calibrated was placed in the center of this cube coil and a field of a given frequency from .03 cps to 1 cps was applied. Knowing the current in the calibration coil. Reuben's formula was used to find the field and Figure 2 resulted.

The second method of calibration suggested by T. R. Madden (1959) was to orient the coil along the north magnetic field and turn it through 90°. The resulting voltage was integrated giving a measure of the effective area of the coil, and a coil constant calculated. This method gave a constant of 5 γ /mv/cps compared with about 4 γ /mv/cps from the graph. The graph has been used because of uncertainties in performing the other measurement.

As previously mentioned, the effective area of the coil was increased by the insertion of the Permalloy rod. The effective permeability of the rod is a function of its length as well as its actual permeability. This effective permeability was calculated using the treatment of an ellipsoid of revolution by Sommerfeld (1952) and letting the major axis become very long. For a one-inch diameter bar the effective permeability as a function of length is shown below.

Table III - Effective μ as a Function of Bar Length

Length (ft)	1	2	3	4	5	6	7	8
Effective μ	60	186	370	610	900	1235	1625	2060

The choice of a five-foot bar is seen to put the effective permeability around 1000. This could be doubled using an eight foot bar, but five feet is the maximum length bar that can be hydrogen-annealed in the Boston area. Also a five-foot length can be more easily transported.

There was a possible problem with Barkhausen noise in the coil. To determine this noise, the Nyquist-Johnson formula was assumed to extend to all real impedance. The impedance of the coil was measured and the Barkhausen noise calculated using

$$E = 2\sqrt{R\,k\,T\,\Delta f}$$

which simplifies to the following equation for T = 298°K, $kT = 4.1 \times 10^{-22}$ and $\Delta f = .5\, f_o$

$$E \sim 3 \times 10^{-11} \sqrt{R f_o}$$

The calculations comparing magnetic signal to Barkhausen noise are shown below:

Table IV - Barkhausen Noise as a Function of Frequency

f_o	R (measured)	E(μv)
.01 cps	2700 ohms	0.00230 μv
.1	3400	0.00055
1	5800	0.00015

The real part of the impedance was measured in the laboratory. It should be noted that the Barkhausen noise as calculated in this manner approaches or exceeds the signal level for audio frequency signals, indicating that coils similar to this would not be suitable as audio frequency detectors.

Magnetic noise

In this section the sources of noise for the magnetic signal will be considered. Broadly, they can be divided into two types, electronic noise and detector noise. In the section on instrumentation it has already been shown that the electronic noise was at an acceptable level. Further we will assume that the part of the field that is uniform is the "signal" and the local source part is "noise".

In considering the detector noise two major sources seem to dominate all others. First, mechanical stability of the

coil is important. If the coil assembly is not stable, the slightest wind or seismic noise is amplified and can cause signals of tens of microvolts. A stand with a three-point ground contact is roughly a ten-fold improvement over placing the coil assembly on the ground. Burial of the pickup might be a further improvement in some cases.

The second source of noise was local disturbances of the field, either by current-carrying wires or by moving conductive objects. Although exhaustive tests were not carried out, a rule of thumb indicated that a safe working distance from a highway is at least 1000 feet and something less than that distance from power lines.

There is still a possibility that local sources corrupt the signals in some way, and to alleviate this problem it was decided to use statistical techniques, treating the signals as stationary time series. This technique will be described in the section on statistical analysis in the next chapter.

A method of checking the magnetic pickup for noise was to use two coils of the same design placed roughly 50 feet apart, and to compare the outputs of these coils. The results of such a test are shown in Figure 3.

A final check on the noise level is to compare the electric and magnetic signals, and Figures 9 and 10 show records taken in different places in New England within the past six months.

Results such as these indicate that we are measuring the magnetic signals of interest.

Electric field instrumentation

Instrumentation for measuring the electric field is shown schematically in Figure 4.

The electrode assemblies were porous ceramic pots containing saturated copper sulfate solution. A copper rod was placed in the solution and the connection to the first stage of the instrumentation was made from this rod. The whole assembly was placed in a shallow hole in the ground after saturating the ground in the immediate vicinity of the hole with salt solution.

The pickup electrode assemblies were placed at least a kilometer apart, with one close to the recording truck and the other connected to the vehicle with magnet wire. The first stage of the electrical field instrumentation consisted of a low pass filter identical in characteristics to that used in the magnetic instrumentation. Since the ground impedance ranged from 1000 up to 8000 ohms in extreme cases, the impedance level of the filter was not high enough, being 1800 ohms, to avoid having to calculate a correction. This correction amounted to taking into account the signal attenuation in this first stage when calculating the overall gain of the electronic system.

Following the filter a variable constant voltage bucking

system was included to buck out the self potential of the electrodes. This self potential can amount to several hundred millivolts.

Amplification is by a Philbrick USA-3 with variable gain from x1 to x3000 using a modified input circuit to make the amplification independent of the source impedance. The electric field signals are at least several millivolts per kilometer so electronic noise is not a severe problem.

Following the amplification the signal goes to a variable bandpass filter made by the Krohnhite Company with bands variable from 0.005 cps to 500 cps. This filter is identical to that described under the magnetic instrumentation section.

Electrical field noise

The noise problems with the electric field could come from a varying self potential, such as a variable electrochemical or thermal potential between the electrodes. The suitability of self potentials as sources of magnetotelluric fields depends on whether these potentials cause current and on their uniformity. The self potentials searched for in ore prospecting are caused by a good conductor; the orebody; connecting together two regions of dissimilar electrochemical potential. Current then flows along the ore body. In other cases no current flow accompanies the self potential.

The scale of investigation is so large for the range of frequencies covered in this study that most ore-body type

conductors would disturb the local fields only. This disturbance would serve to mask regional effects. Non-current causing self potentials also would add to the noise of the system.

The approach to this noise problem was to record co-linear, parallel, and right-angle electrode spreads simultaneously. Records obtained in this manner are shown in Figure 5, and show identical traces.

The evidence is that the electric signals are indeed magnetotelluric signals associated with current flow. The experience of the recording done in this thesis indicates that the electrical measurement is the more reliable of the two field measurements, for freedom from noise.

Local sources will cause "noise" and statistical techniques will be useful in removing this noise.

Recording system

Previous descriptions have taken the signals up to the variable band pass filters. From here both the electric and magnetic signals are treated alike.

The signals from the filters are attenuated to an acceptable level for the tape recorder, biased from a variable direct voltage source to preserve phase information, and chopped at 400 cps. The chopped signals are fed to the stereo tape recorder. The bias used as standard is 5 millivolts and so the signals are attenuated to a 10 millivolt peak-to-peak level or slightly below. Amplitude modulated recording

does not have a large dynamic range, but by filtering before recording a 60 db overall range is obtained. This means that a signal of 1 part in 1000 present in the magneto-telluric field can be detected.

The recorder used is a Gold Crown Stereo X. During the recording a standard 5 millivolt signal is recorded and used to determine the magnitude of the electric and magnetic recorded signals. The recorded signals are divided by the total gain to find the input signal.

Playback system

A schematic of the playback system is shown in Figure 6. The tape signal is amplified x10, demodulated, and sometimes passed through the variable band pass filter again, before giving a visual record on paper. The purpose of the filtering at this stage is two-fold; it reduces the tape noise, and it restores the phases since the signal is played through the filter backwards. At times tape dropout becomes serious enough to cause filter ring, and the filter was not used for the last few sets of records. Examples of the type of records obtained are shown in Figure 9.

Another technique useful for relatively noise-free records is to play the signals on an oscilloscope with one signal on the vertical and one on the horizontal deflection plates. This gives rise to a Lissajou figure from which an average phase and amplitude can be determined. Examples of such a playback scheme are shown in Figure 7.

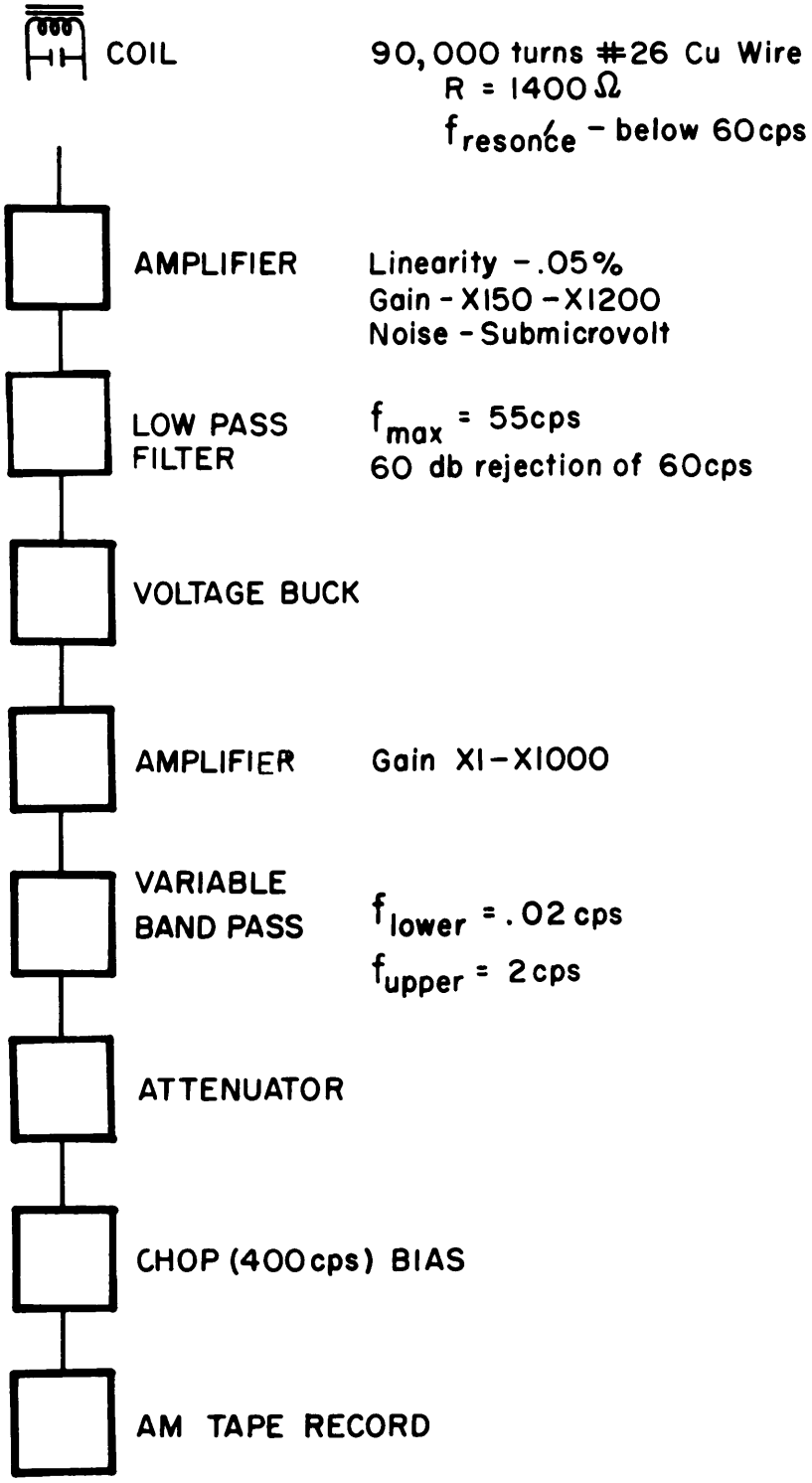

Instrumentation for Magnetic Field Measurement

FIGURE 1

FIGURE 2

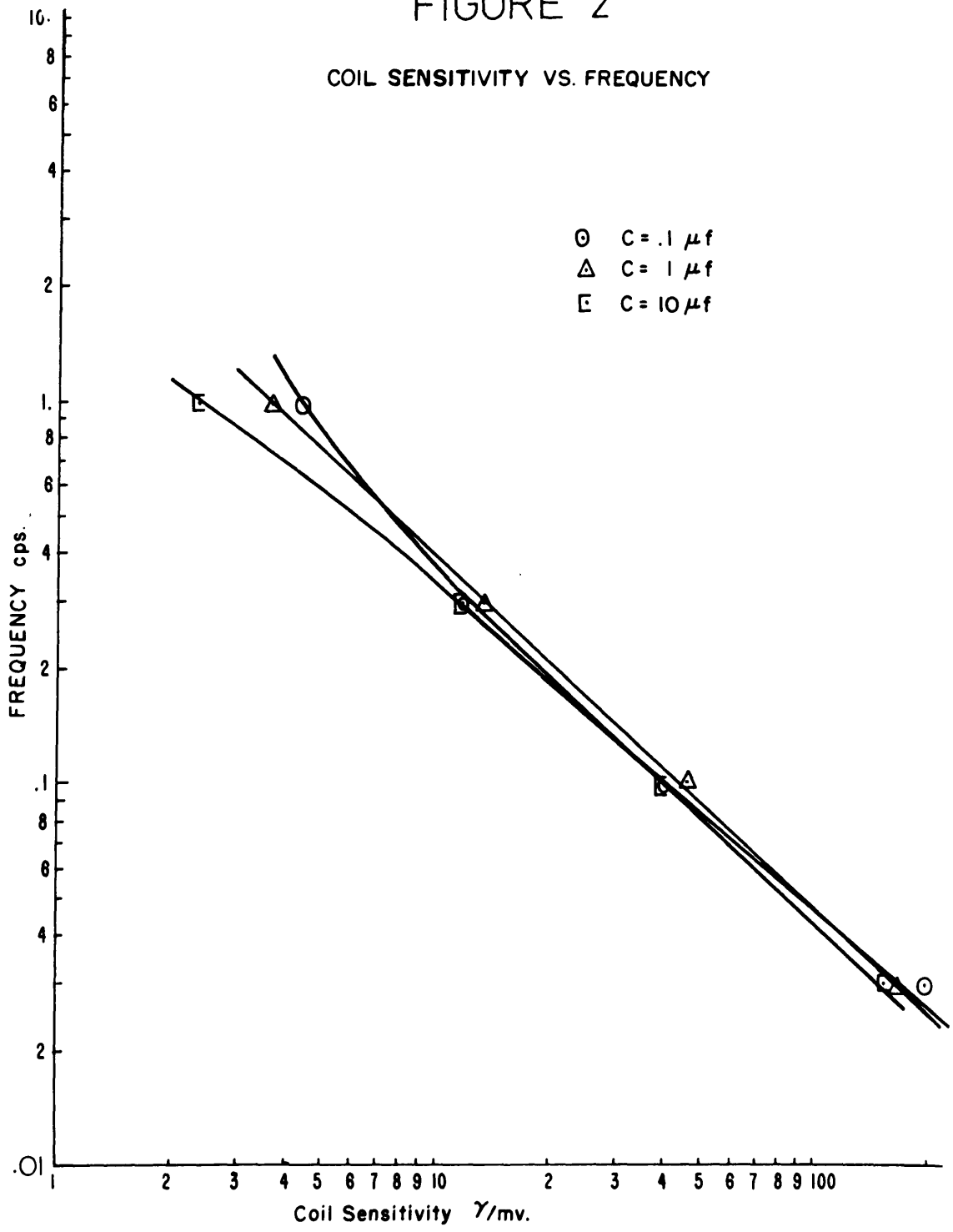
COIL SENSITIVITY VS. FREQUENCY
C = .1 μf
C = 1 μf
C = 10 μf
FREQUENCY cps.
10.
8
6
4
2
1.
8
6
4
2
.1
8
6
4
2
.01
1
2
3
4
5
6
7
8
9
10
2
3
4
5
6
7
8
9
100
Coil Sensitivity γ/mv.

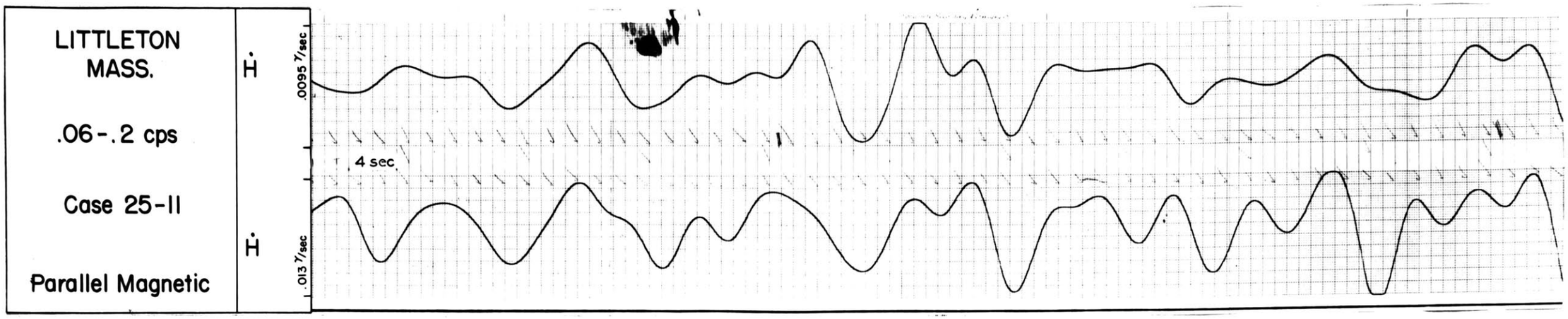

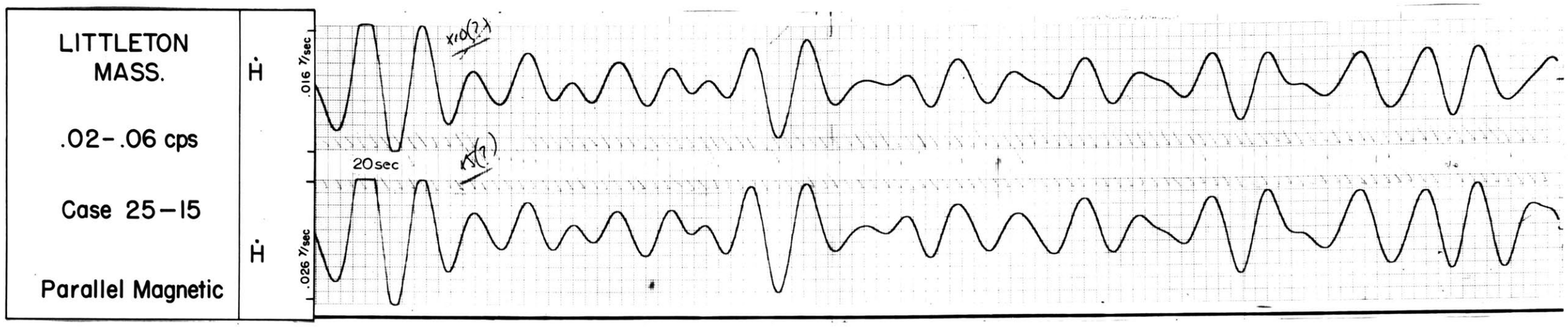

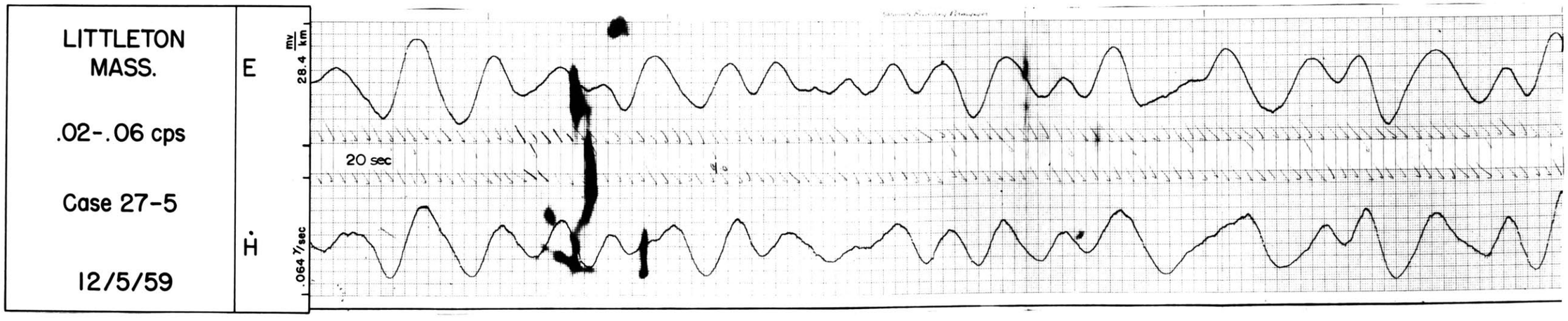

FIGURE 3 MAGNETIC NOISE RECORDS

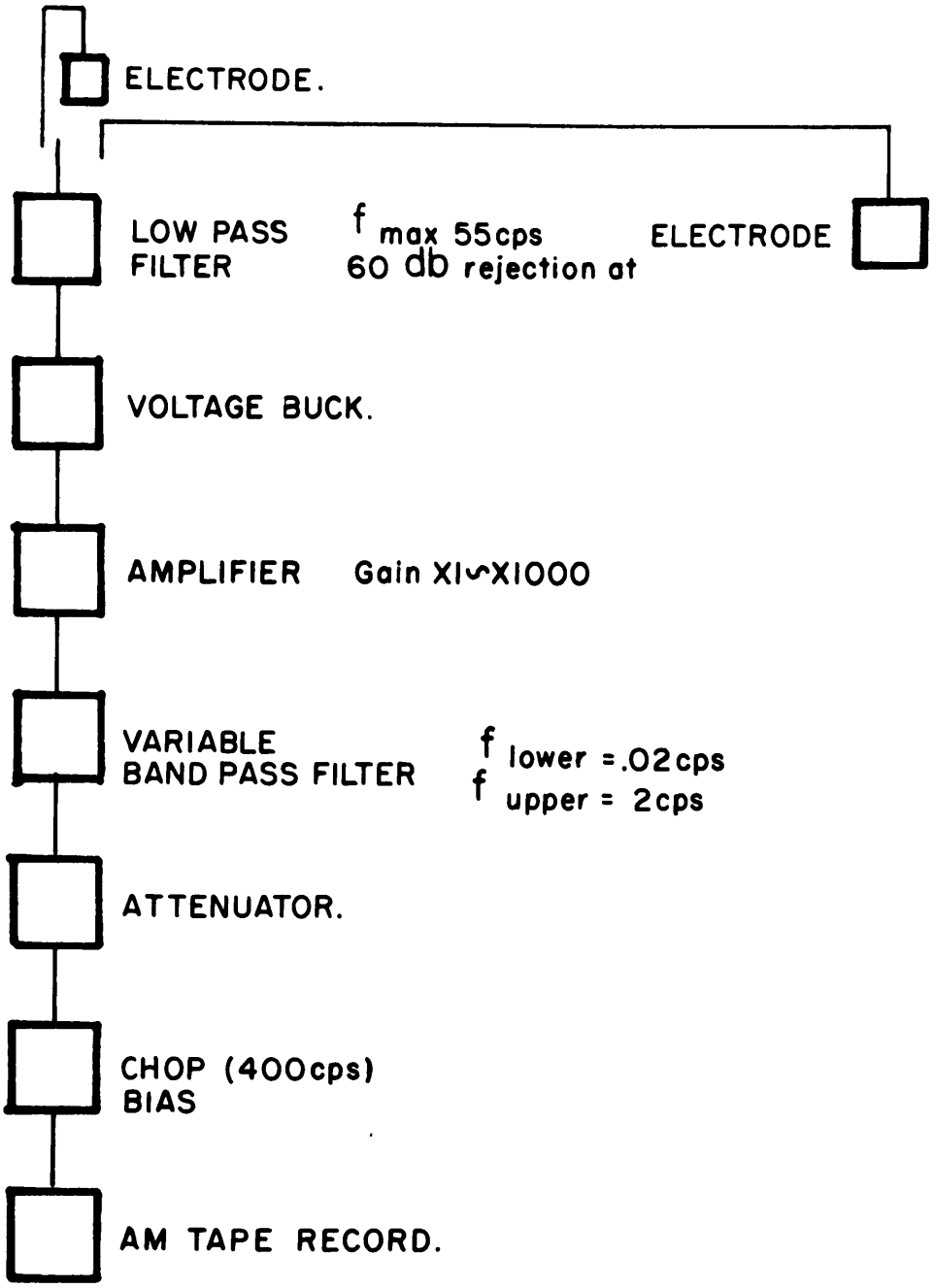

Instrumentation for Electric Field Measurement

FIGURE 4

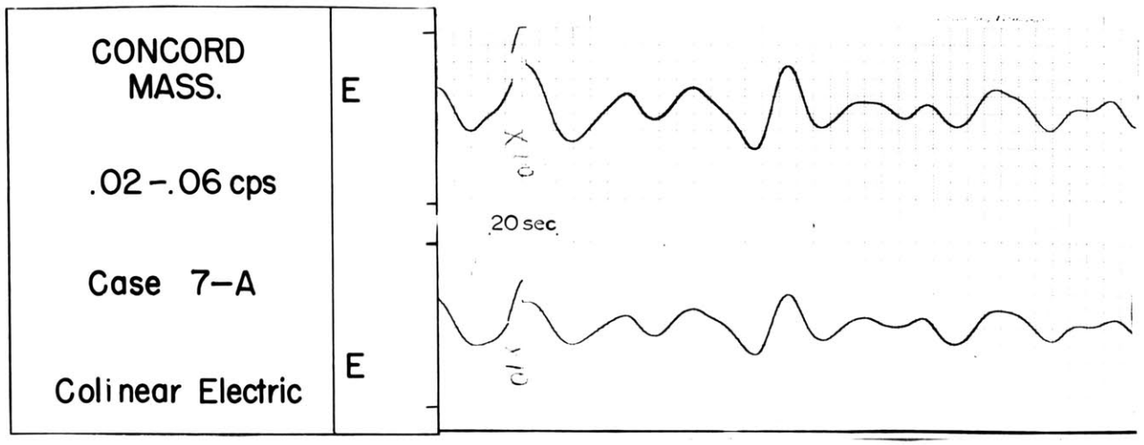

FIGURE 5

ELECTRIC NOISE
RECORDS

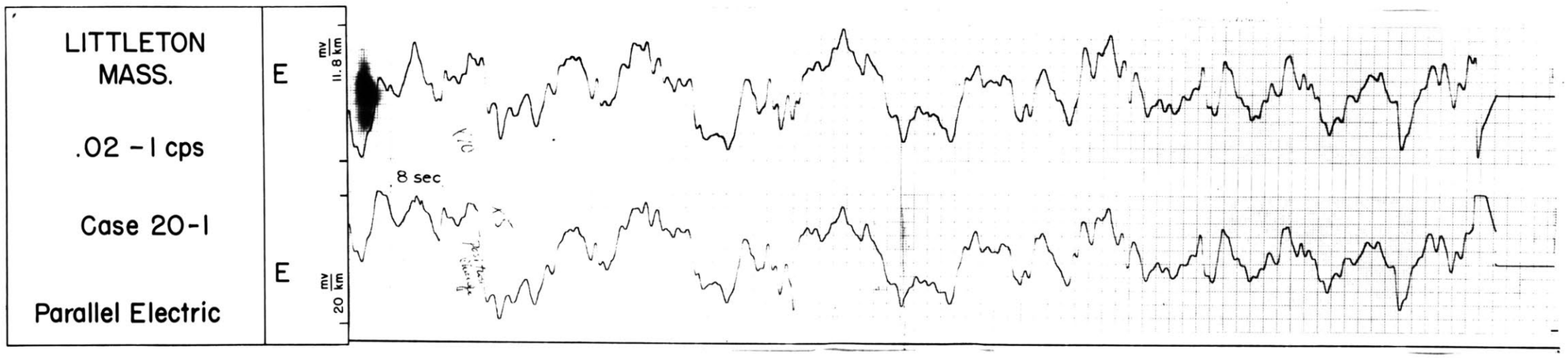

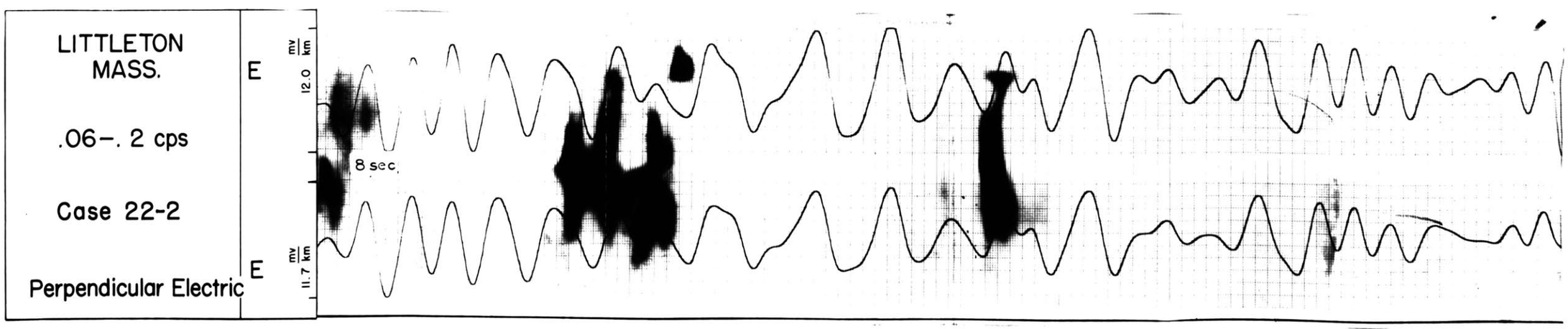

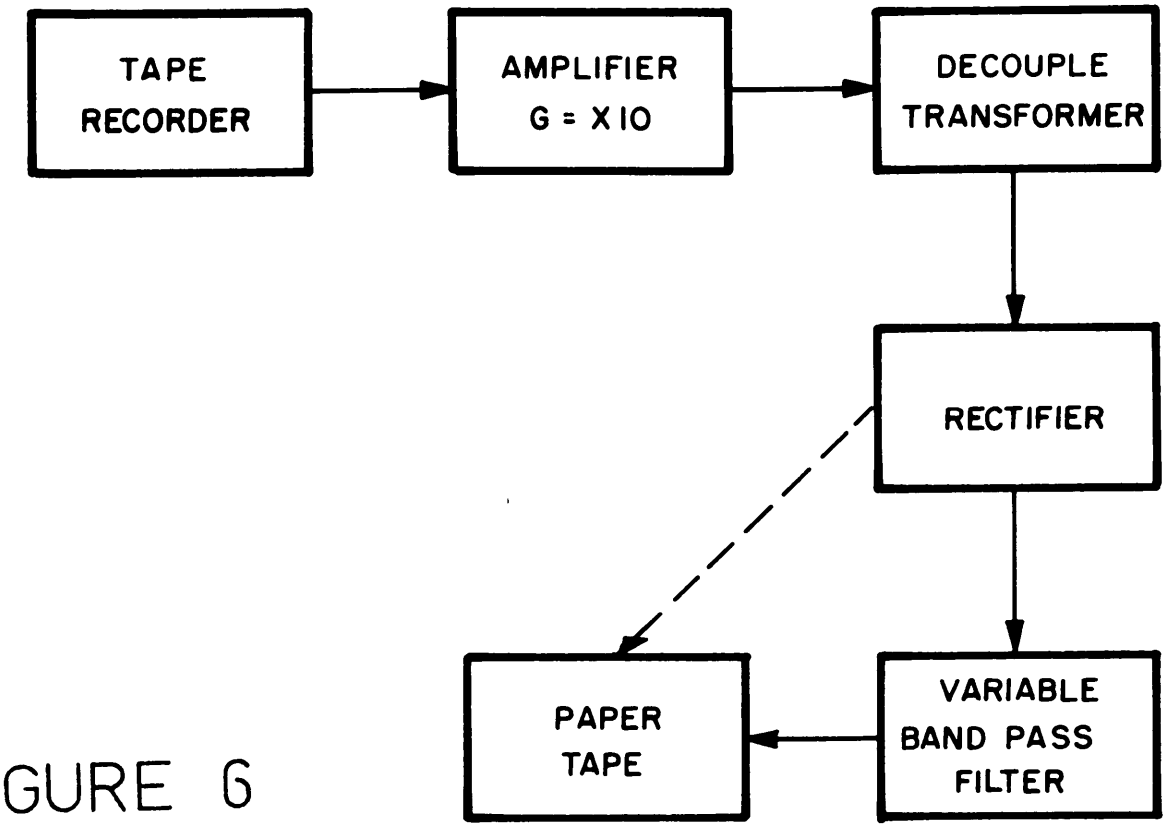

FIGURE 6

Laboratory Playback Instrumentation

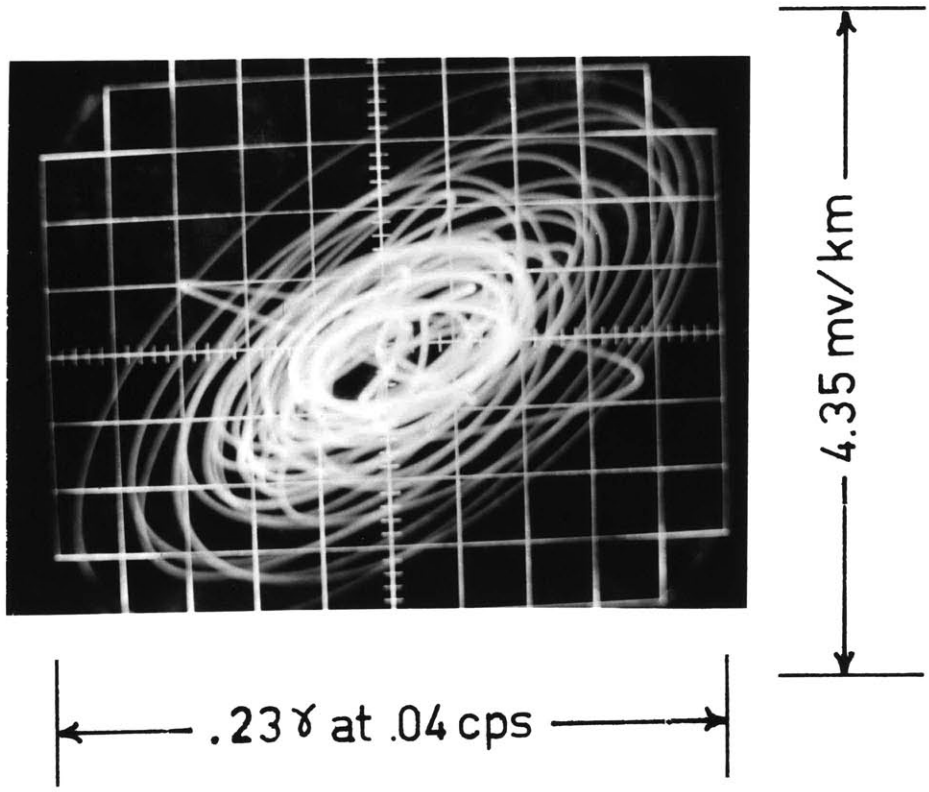

Oscilloscope Record
Case 12-12
.04-.05 cps

Blandford, Mass.
9/8/59

Figure 7

CHAPTER III

METHODS OF ANALYSIS OF RECORDS

General

In this section the methods of statistical analysis of the records are discussed. Second, error estimates are made and analyzed. Finally, the methods are presented for predicting the axes of the conductivity structure of the earth, given the field measurements on the earth's surface.

Most of the records used in this thesis were obtained at Littleton, Mass. on an unused portion of South Shaker Road. The approximate directions of the electric and magnetic pickups were E 10° N and N 10° W. This spot was chosen as a test site after earlier attempts to obtain records across New England had been abandoned until noise problems had been overcome. In these earlier attempts enough good records had been obtained to be encouraging, and Littleton was chosen as a development site.

The encouraging results were mostly obtained in the frequency band from .02 to .06 cps and examples are shown in Figure 9 of these early records. It was also evident that records taken over sedimentary sections as in the Connecticut River Valley gave resistivities an order of magnitude lower than those over igneous rocks.

The early calculations of apparent resistivity were done by examining the records, picking a coherent section, and taking the ratio of E to H at a point in that section. The scatter in the results was about a factor of ten. Some records had no apparent coherent sections and could not be used, so an investigation of available statistical techniques was begun with the hope that signals could be extracted from the records in this way.

Meanwhile instrumental techniques were improved so that more coherent records were obtained. Examples are shown in Figures 9 and 10.

For visual analysis very narrow band passing was necessary to get frequency resolution. An advantage of using statistical analysis is that these pass bands could be opened up. The actual choice of frequencies is arbitrary but consideration has to be given to the variation in field strengths throughout the band. The field strengths at 2 cps can be 20 times less than those at .02 cps, so band passing to keep this variation down to a factor of 5 to 10 throughout the pass band is done.

Without bandpassing, the analysis we have done could not have been accomplished. The amplifiers used before the band pass filters are linear over the total range of signal, and give no difficulty. After the filter, the magnetic tape recorder and the paper tape recorder both are limited in their linearity. Any attempt to record

the larger amplitude signals would place the smaller signals at or below the noise level of the instrumentation system. As mentioned in Chapter II, the band pass filtering contributed a great deal to the success of this investigation.

The final choice of pass bands was .005-.02, .02-.06, .06-.2 cps, .2-.6 cps, and .6-1 cps. Only one recording was made in the band from .005 to .02 cps because the special filter necessary to go this low in frequency were not delivered until late in November 1959. It was apparent in the summer of 1959 that frequencies as low as this and lower would be desirable, and the two layer model discussed in Chapter V will point this up.

All measurements done for this thesis were of only two field components. One suggestion for the early poor records was that the fields were elliptically polarized in some fashion, and the conductivity structure of the earth was anisotropic or two-dimensionally inhomogeneous. Attempts to follow up the suggestion led to investigation of these effects, and the results of these theoretical investigations are in the section on anisotropy and inhomogeneity.

In the field records obtained for this thesis, the two fields measured were one electric and one magnetic. The methods for handling the effects of anisotropy, inhomogeneity, and elliptic polarization assume measurement of the total horizontal fields; two electric and two magnetic components.

Statistical Analysis

Before presenting the method used to treat the data it is perhaps worthwhile to inquire into the nature of the records themselves. Although the sources of the magneto-telluric fields are not known, it can be assumed that signals are emitted at random times with random amplitudes. The records then will possess some of the properties of a stationary time series. In the absence of instrumental and transducer noise, the coherency between the electric and magnetic records should be good. In the presence of such instrumental noise, if the noise could be assumed to be associated with one signal, then an estimate of the coherency between two signals could be used to correct the noisy one. That is, if the coherency was only one-half, than half of the "noisy" signal was noise. Methods of treating stationary time series are available, and they allow estimates of the mean squared signal in narrow frequency bands.

These estimates are often called power spectral estimates and the essential idea is to make a Fourier analysis of the signal breaking it up into power within a narrow frequency band. In the limiting case, when the band width goes to zero, this is the power spectral density. The approach to obtaining the power spectra for stationary random processes is through the correlation functions. The correlation functions are convenient to obtain and once obtained, the Fourier transform of the correlation function yields the power spectra.

The use of correlation functions is to be preferred to a direct attack taking the Fourier spectra of the record directly. As Davenport and Root (1958) show, taking the Fourier spectra directly gives an estimate of the power spectra with the correct mean but it does not have zero variance even with infinite length records. Bendat (1958) suggests averaging over a number of records, but a number of questions are left unanswered. In contrast the use of correlation functions is a well-developed technique. In addition to those references cited, Blackman and Tukey (1958), Robinson (1954), and Simpson (1959) were found useful.

The advantages of using statistical techniques to estimate the power spectra are many. It is possible to use the coherency to estimate the amount of noise present, and if this noise can be assigned to one signal, the effect of the noise can be removed. Wider band recordings can be made and the statistical techniques relied upon to break the band into narrower frequency strips with estimates of the power in each strip. The data can be handled in an unbiased fashion and estimates of the errors involved in the statistical procedure made. Since we expect rather smooth changes in estimates of apparent resistivity, this can be used as a qualitative check on the procedure.

Before describing in detail the statistical procedure, the handling of the paper records will be discussed. The paper records were hand digitalized at equal spaced intervals.

This digital data was put through the computational operation on the IBM 704 at the M.I.T. Computation Center. The records had typical swings of 6 divisions and could be read to 0.1 division. Digitalization of a record of 150 points could be done in an hour.

The programming for the IBM 704 was done by T. R. Madden. The details of this general program will not be presented here. The program was set up to handle up to 500 points of data from each of two electric and two magnetic records. Auto and cross correlations for all combinations can be performed with up to 75 lags. Power spectra from the autocorrelations, and the coherency analysis are printed out. Examples of the printout format are in the data tables in Appendix I.

The computation was adapted with modifications from Tukey and Blackman (1958). Since this reference only covers autocorrelation, some of the cross correlation methods are from Robinson (1954) and Simpson (1959). T. R. Madden integrated these into the final program.

In this whole treatment of magnetotelluric records, they are assumed to represent a stationary time series. That is, the record has no time origin, and one stretch of record is as good a statistical sample as any other. The autocorrelation function is therefore dependent only on the lag. Now to the details of the analysis.

The autocorrelation function, R, is defined as

$$R(\tau) = \frac{1}{N_i - 1} \sum_i y_i(t)\, y_i(t-\tau)$$

where the y_i's are the values at the indicated times and τ is the lag. We do not normalize $R(\tau)$ as is sometimes done, and the unnormalized $R(\tau)$ is often called the auto-covariance function.

The digitalization interval, Δt, is set by the requirement of sampling the upper band-set frequency four times per cycle. This has the effect of placing the upper frequency limit at twice the upper band-set frequency. If we designate the upper frequency as f_{max}, then

$$f_{max} = \frac{1}{2\Delta t}$$

where Δt is in seconds and f in cps. The frequency range covered by the Fourier analysis runs from f = 0 to $f = f_{max}$ with the spectrum estimated at equi-spaced points at intervals

$$f = \frac{1}{2\, m\, \Delta t}$$

where m is the number of lags.

The calculation of the autocorrelation function

$$R(\tau) = \frac{1}{N_i - 1} \sum_i y_i(t)\, y_i(t-\tau)$$

is done assuming the mean y_i is zero. The data are read from the paper record taking one edge of the cross-hatched are as a zero reference. Thus all numbers are positive. The mean is subtracted from each point.

$$\text{Mean} = \frac{\sum_i Y_i}{N_i} = m$$

where Y_i represents the raw data points and N_i is the total number of points. Then,

$$y_i = Y_i - m$$

For cross correlation functions, $R_{xy}(\tau)$, the mean of each set, either x_i or y_i, is subtracted from the respective raw data. That is,

$$y_i = Y_i - m_y$$

$$x_i = X_i - m_x$$

$$R_{xy}(\tau) = \frac{1}{N_i - 1} \sum_i y_i(t)\, x_i(t-\tau)$$

After making the autocorrelation and cross correlation estimates, a raw power spectrum is computed as follows,

$$\Phi^*(w) = \Delta\tau \sum R(\tau) \cos w\tau$$

with $w_i = 0, 2\pi\Delta f, 4\pi\Delta f \cdots, 2\pi f$ max and $\Delta\tau$ the interval between lags. The raw $\Phi^*(\omega)$ is then smoothed, using the Hanning formula, to yield the final power spectrum,

$$\Phi(\omega_n) = \frac{1}{4}\Phi^*(\omega_{n-1}) + \frac{1}{2}\Phi^*(\omega) + \frac{1}{4}\Phi^*(\omega_{n+1})$$

The calculation of $\Phi^*(\omega)$ can be done as a matrix multiplication. The cosine matrix is post multiplied by a one column R matrix as follows:

$$\begin{bmatrix} \cos w_i \tau_j \end{bmatrix} \begin{bmatrix} R(\tau_0) \end{bmatrix} = \begin{bmatrix} \Phi^*(w_n) \end{bmatrix}$$

We need only consider the cosine transform for the autocorrelations as they are even functions.

The cross correlations generally are not even functions, so that both the sine and cosine transforms must be taken to determine the odd and even contributions. The method of doing this is similar to that described for the auto-correlations. The equations are

$$\Phi^*_{even}(\omega) = \Delta\tau \sum_{\tau} R^e_{xy}(\tau) \cos \omega\tau$$

$$\Phi^*_{odd}(\omega) = \Delta\tau \sum_{\tau} R^o_{xy}(\tau) \sin \omega\tau$$

$$R^e_{xy}(\tau) = \tfrac{1}{2}\left(R_{xy}(\tau) + R_{xy}(-\tau)\right)$$

$$R^o_{xy}(\tau) = \tfrac{1}{2}\left(R_{xy}(\tau) - R_{xy}(-\tau)\right)$$

Φ^*_{even} and Φ^*_{odd} are hanned using the previous formula to yield Φ_{even} and Φ_{odd}.

The table below illustrates the four frequency bands typically used, the Δt between lags, and the maximum frequency at which estimates would be made.

Table V Frequency Band and Digitalization Rate

Frequency Band	Δt	f_{max}
.02 - .06 cps	5 sec	.1 cps
.06 - .2	1	.50
.2 - .6	.5	1.0
.6 - 1.0	.2	2.5

The power spectra can then be used in a number of ways. A ratio of the cross spectra to the product of the auto spectra is used to test the coherency between E and H.

Robinson (1954) discusses this as the coefficient of coherency. It is defined as

$$Coh_{xy}(w) = \frac{\Phi_{xy}(w)}{\sqrt{\Phi_x(w)\ \Phi_y(w)}}$$

where Φ_{xy} is the cross correlation at w between x and y, and Φ_x and Φ_y are the autocorrelations of x and y respectively. The modulus of this coefficient represents the amount of linear coherency between E and H, and the argument is the phase lag of this coherency.

Finding the apparent resistivity can be done several ways. The most straightforward is to take

$$\frac{\Phi_E(w)}{\Phi_H(w)}\ K = \rho_a$$

where the constant takes account of amplifier gains, coil sensitivities, and the like. The above formula represents

$$\rho_a = .2\,T\,(E/H)^2$$

where E is in mv/.km, H in gammas, and T in seconds.

Another possible scheme is to take

$$\rho_a = K\ \frac{\Phi_E(w)}{\Phi_H(w)\ (coh_{EH}(w))^2}$$

where K is the same as before. This second formula assumes that the electric signal is noise-free. The magnetic signal is multiplied by the coherency squared so as to only use that part of the magnetic signal that is linearly coherent with the electric signal.

The justification for such a procedure is that our magnetic records seem to be more "noisy than the electric. This is illustrated in Figures 3 and 5 and in the coherency analysis for Cases 24-15 through 25-15 found in the Appendix I. These eight cases are all of the parallel magnetic field measured with two separate pickups, as discussed in Chapter II. Three have coherency less than .5 and five are better than this. Several are excellent. Although experimental techniques improved during these tests, the magnetic recordings still seem more noisy than the electric.

This justifies trying this second formula. In practice it was not used because attention was confined to records with coherency better than .7 and especially because application of this formula gave erratic results in resistivities. This wide spread in values of resistivity estimates and adjacent frequencies is not to be expected on physical grounds. Therefore, the first equation was used in calculations of apparent resistivity.

Error Analysis

Errors in the final estimate of apparent resistivity will be of two kinds; random errors and constant errors. The constant errors are those errors that would arise from inaccurate calibration of the equipment; for example a gain that was off by 25%. These constant errors will remain undetected by analysis of the spread in the results.

The random errors will cause a spread in the estimated values of ρ_a. A large error of this type in inherent in the statistical analysis, and will be estimated. A rough check of this random error can be made by observing the spread in values of apparent resistivity calculated from different records.

The constant errors will be small compared with the random errors. The amplification and attenuation instruments were checked by passing signals through the two channels including recording and playback and comparing the output. The outputs were identical within $\pm 2\%$. Since it is the ratio of the outputs that is important, the constant error introduced is $\pm 2\%$. The largest constant error of contribution is in the calibration of the magnetic coil. As was pointed out in Chapter II, two different methods gave differences of 25%. If it is assumed that this represents a miscalibration, then the error introduced in the apparent resistivity will be 25%.

The constant error will be taken as 25%. No further analysis of such things as length of electric line and electrode resistance will be done. This is justified only by the fact that the random errors introduced in the statistical analysis are so large that a few percent error in other factors is insignificant. With more and longer records, the errors introduced by the analysis may be reduced to an 80% range of 3 db. This is still large compared with errors in line length and resistance measurements.

The errors in the statistical analysis to determine the power spectra can be estimated. Tukey gives a formula for these errors assuming a standard Gaussian distribution of signal. As pointed out by Simpson (1959) the Tukey method of estimating the power spectra is the only standard procedure for estimating these errors. Blackman and Tukey (1958) give a formula for the calculation of the 80% range of estimates of the power spectra. Eighty percent of the estimates will fall in a range as given below.

$$\left(\begin{matrix}80\%\ \text{range} \\ \text{in db}\end{matrix}\right)^2 = \frac{125}{\left(\begin{matrix}\text{no. of record} \\ \text{pieces}\end{matrix}\right)\left\{\left(\begin{matrix}\text{length per} \\ \text{piece}\end{matrix}\right)\left(\begin{matrix}\text{resolution} \\ \text{in cps}\end{matrix}\right) - 1/3\right\} - 1/2}$$

This equation applies to digitally processed equi-spaced records, provided the spectrum is reasonably flat. Providing a flattening of the spectrum in handling the data is usually referred to as prewhitening. It has the effect of sharpening

up the spectral resolution so that large power at one frequency does not spill over into adjacent frequencies. The hanning procedure used smooths by averaging power at adjacent frequencies and power spectral peaks would give difficulties.

Prewhitening also has the effect of reducing the number of lags necessary to get the autocorrelation to drop to zero so that the spectral analysis will not be troubled by a sharp cutoff in the correlation function introduced by limiting the number of lags used.

In the pass-band our records were usually more or less white. Near the filter cut-offs trouble can be expected and generally our power spectral estimates do not cut off quite as sharply as the filters. In mid-band this does not seem to be a problem.

To estimate our errors several typical cases will be calculated using Tukey's formula. The observed spread in calculated values of resistivity will be calculated later.

Table VI Estimated Errors for Power Spectra

Frequency Range	Resolution in cps	Typical Record Length	80% Range
.02 - .06 cps	.005	750 sec	x 4.5
.06 - .2	.012	300	x 4.5
.2 - .6	.050	100	x 3.6
.6 - 2	.125	60	x 3.6

This table illustrates the large range within which 80% of the estimates will be found. The data being analyzed must come from a stationary Gaussian random process for this formula to hold.

The power spectra printed in the tables in Appendix I cannot be analyzed directly for their range because the signal changes from day to day. In effect, if we consider the signal to be formed by a wavelet arriving at random times with random amplitude, the treatment of the signal as a stationary time series is only justified if the wavelet does not change shape. Source strengths and spectral compositions very likely do change over a period of time, so comparison of spectral estimates between signals taken on different days is not possible. Figures 11 and 12 show this clearly, with Figure 12 showing a skewed spectral density and Figure 11 a flat one. The variations here are not due to errors in estimating, but reflect a difference in the power spectra of the magnetotelluric field.

Since comparisons and error estimates are not possible from case to case, the apparent resistivities will be examined for errors. The apparent resistivity is obtained by dividing two power spectral densities, so that the error estimate should take into account this division. A standard technique for handling the errors would treat them as Gaussian and independent. Then the standard deviation would be related to the individual standard deviations by

$$\left(\frac{\sigma_{pa}}{m_{pa}}\right)^2 = \left(\frac{\sigma_E}{m_E}\right)^2 + \left(\frac{\sigma_H}{m_H}\right)^2$$

This formula does not apply in the present case because its derivation assumes $\frac{\sigma_{pa}}{m_{pa}} << 1$ and likewise for the others. In the present case, $\frac{\sigma_{pa}}{m_{pa}} > 1$.

A simplification might be made if the E and H records were assumed perfectly coherent and white, but this is not a case of interest since non-whiteness is a property determined by the earth's conductivity properties. This is to say that the ratio of $(E)^2$ to $(H)^2$ is proportional to the earth's conductivity times the frequency of the measured wave, and it is unlikely that this ratio would dictate white signals even over our narrow frequency bands.

Without directly attacking the problem of estimating the errors in apparent resistivity, several observations will be made. The errors in estimating power spectra from finite length records of stationary time series are those of a statistical nature. We have available only a piece of record and we require estimation of power in narrow frequency bands. Even if the power spectra of H was considered known once an estimate of the E spectra was made, the error in apparent resistivity would be at least as great as that in estimating E. It is reasonable that the resistivity errors will be greater than those in E. The spread in resistivity estimates for our records can be seen in the

table below. The total range is used, so that multiplying the lowest value by the range encompasses all estimates.

Table VII Spread in Resistivity Estimates

Frequency Band	Records Used	Frequency	No. of Estimates	Total Range of Estimate
.02 - .06 cps	26-1	.020 cps	5	x3
	26-5	.030	4	x1.9
	26-6	.040	3	x5.8
	26-7	.050	3	x3
	27-5	.060	3	x2.2
.06 - .2	21-4	.070	2	x1.3
	27-3	.100	2	x2.7

The number of cases is small but the variation in estimates of ρ_a seems to fall within Tukey's range, considering Table VI.

For plotting the data, Tukey's 80% range will be shown as the variability for data. This range will be suitably calculated when several values are averaged. From comparing the ranges of estimates in Table VII with calculated estimates from Tukey's formula in Table VI, this appears to be an overestimate of the error.

Errors in period would arise through variations in the frequency of the voltage supplied to the tape recorder. A synchronous motor drives the tape transport. A frequency meter on the power supply showed a range of 58-62 cps which would be an error of 3.5%. This error is too small to be observed on the plots in the next chapter.

Anisotropy and Inhomogeneity

Some of the first records obtained were incoherent, and one possibility was that two effects not taken account of by Cagniard (1953) could be influencing the results. These effects were anisotropy or inhomogeneity in the earth and elliptic polarization of the magnetotelluric field.

In this section, consideration is given to the problems caused by such real earth effects. The problems are to first

detect the existence of the two-dimensionality and then to find the main axes of the two-dimensionality. Once this is done, the existing fields can be projected onto these axes, and as will be shown, measurements made along these main axes will be independent of each other.

An important point to emphasize is that the equations in this section are written for one frequency component. For example, when a field is described as one having constant phase between electric and magnetic signals, this means at a given frequency. The phase can vary with changing frequency.

This section assumes simultaneous measurement of two electric and two magnetic fields, enabling the calculation of the total horizontal magnetic field and the total horizontal electric field. It will further be assumed that the measurements will be along two axes at right angles to each other.

Although interpretation is not covered in this thesis, the purpose of finding the major axes is to enable interpretation to be accomplished. Neves (1957) considered two-dimensional inhomogeneities such as vertical contacts in detail. He broke up his treatment into two cases, that of magnetic field parallel to and electric field perpendicular to the contact, and that of electric field parallel to and magnetic field perpendicular to the contact. Final solution would be a superposition of the results from each of these two separate treatments.

Neves (1957) and Madden (1959) have shown that the effects of these two-dimensional inhomogeneities include modification of both the apparent resistivity and the phase relationships if magnetotelluric measurements are made within the influence range of the inhomogeneity. Figures 14 and 15 provide illustration of this point with the electric field perpendicular to the contact.

If the measured fields can be broken up into components along the major axes, meaning perpendicular to and parallel to the discontinuity for two-dimensional features, then two separate interpretations can be done. The interpretations can be combined for a final representation of the conductivity structure.

At this point definitions of the models of anisotropy and inhomogeneity are presented. Anisotropy refers to an earth conductivity that is homogeneous but anisotropic. It will be assumed that the anisotropy does not change with depth. The term inhomogeneity will be used to designate two-dimensional features such as contacts between rocks of differing electrical conductivities. For simplicity it will be assumed that the media on either side of the two-dimensional feature are homogeneous and isotropic, although this assumption is not essential to the treatment. The media could be horizontally layered, but the problem becomes more difficult to visualize and interpret.

The effect of these models is to make H_x dependent on

both E_y and E_x when x and y directions are not the axis of structure, whereas in the analysis of the present field data we assume H_x dependent on E_y only.

Some of the differences between the anisotropic model and the two-dimensional inhomogeneous model should be emphasized. In the anisotropic model the current in the ground does not parallel the electric field. The magnetic field is at right angles to the current sheet, but not perpendicular to the electric field. In the inhomogeneous model the current in the ground parallels the electric field. The magnetic field is not at right angles to the current sheet and the electric field because it is in part caused by currents flowing on the opposite side of the contact. These currents do not parallel those under the measuring station. These statements presume differential measurements of the fields so the problems of running an electric field measurement with one electrode on one side of a contact and one on the other are avoided.

A heuristic proof of these statements follows for the anisotropic model. The anisotropy in conductivity will have two major axes at right angles, along which the conductivity is different. An electric field can be decomposed along these axes. The current, j, will be related to the electric field by

$$\text{Axis 1} \qquad j_1 = \sigma_1 E_1$$

$$\text{Axis 2} \qquad j_2 = \sigma_2 E_2$$

Since $\sigma_1 \neq \sigma_2$, on forming the total j vector it will not parallel the electric field. Relating the magnetic field to the currents by $\vec{\nabla} \times \vec{H} = \vec{j}$, the magnetic field will be at right angles to $\vec{j}$ since in our model $\vec{j}$ is unidirectional in the earth.

For the inhomogeneous case, the electric field parallels the current flow because of the assumption of isotropy in the media on either side of the contact. However, to determine the magnetic field we would have to integrate over the currents as

$$\vec{H} = \frac{1}{4\pi} \vec{\nabla} \times \int \frac{\vec{j}}{r} \, dv$$

where r is the distance to the differential volume, dv. Within the influence of the currents on the opposite side of the contact, which may not parallel those on the measurement side, the magnetic field will not be perpendicular to the electric field.

The cases to be treated are as follows:

Case	Earth Conductivity Structure	Magnetotelluric Field
i	Horizontal Stratification	Elliptically polarized
ii	Anisotropic and Inhomogeneous	Linearly polarized
iii	Anisotropic and Inhomogeneous	Elliptically polarized

The cases get more difficult going down the list.

i) Elliptic polarization of the magnetotelluric field over a horizontally stratified earth adds no complications to the solution. If we label any two orthogonal axes, 1 and 2, then measurements along these axes, say E_1 and H_2, will give the correct resistivity. Also E_2 and H_1 will give the same result.

The simplest way to prove this is to consider the diagram below.

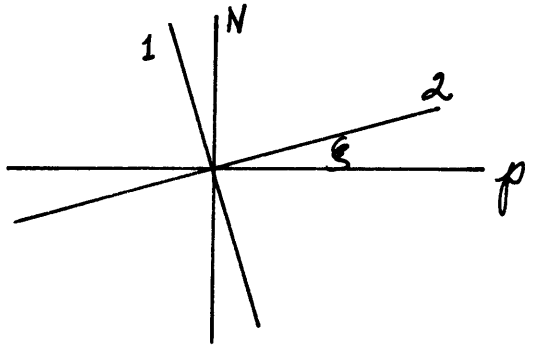

The electric field ellipse can be decomposed into linear fields along N and p, out of phase with each other. These two electric fields will give rise to two magnetic fields along p and N. The magnetic fields will be out of phase with each other by the same amount as the electric fields. Each magnetic field is out of phase with the electric field orthogonal to it by the same amount.

Superimposing these fields and making measurements along 1 and 2 gives

$$E_1 = +E_N \cos \xi - E_p \sin \xi$$
$$E_2 = +E_N \sin \xi + E_p \cos \xi$$
$$H_1 = H_N \cos \xi - H_p \sin \xi$$
$$H_2 = H_N \sin \xi + H_p \sin \xi$$

Also

$$H_N = -\alpha_{Np} E_p$$

$$H_p = \alpha_{pN} E_N$$

where $\alpha_{Np} = \alpha_{pN}$ and is complex representing a phase shift between E and H.

Substituting, we find

$$H_1 = -\alpha_{Np} E_2$$

$$H_2 = \alpha_{Np} E_1$$

Thus the apparent resistivities calculated from a measurement along any set of orthogonal axes will be the identical and the correct ones to use Cagniard's interpretative scheme.

Diagnostic features of this case are that the total fields remain at constant angles to each other and that the fields rotate.

ii) Anisotropic conductivity of the earth gives rise to further difficulties which can be resolved by multiple measurement.

To begin we derive a general tensor relationships for the magnetotelluric fields. Proceeding as in case i), consider the set of axes shown below.

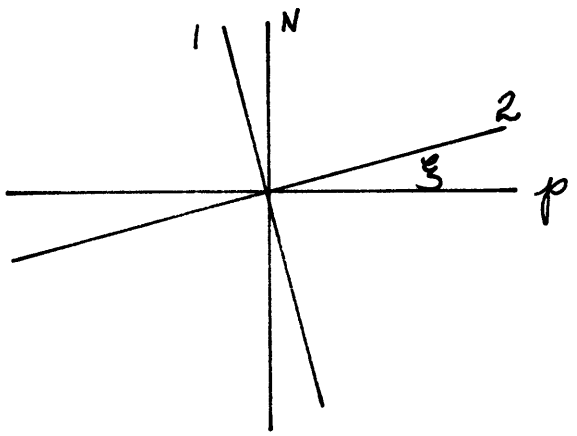

The axes N and p are major axes of the anisotropy and axes 1 and 2 are measuring axes. ξ is the unknown angle as shown.

Along the major axes the E-H relationships are

$$H_N = -\alpha_2 E_p$$

$$H_p = \alpha_1 E_N$$

where α_1 and α_2 are complex. Since the earth is homogeneous, the phase between H_N - E_p is the same as that between H_p - E_N, i.e. 45°.

We can write that

$$H_2 = H_p \cos\xi + H_N \sin\xi$$
$$H_1 = -H_p \sin\xi + H_N \cos\xi$$
$$E_N = E_2 \sin\xi + E_1 \cos\xi$$
$$E_p = E_2 \cos\xi - E_1 \sin\xi$$

Combining we find that

$$H_2 = \alpha_1 \{ E_2 \sin\xi\cos\xi + E_1 \cos^2\xi \} - \alpha_2 \{ E_2 \sin\xi\cos\xi - E_1 \sin^2\xi \}$$

$$H_1 = -\alpha_1 \{ E_2 \sin^2\xi + E_1 \cos\xi \sin\xi \} - \alpha_2 \{ E_2 \cos^2\xi - E_1 \cos\xi \sin\xi \}$$

and

$$H_2 = (\alpha_1 \cos^2\xi + \alpha_2 \sin^2\xi) E_1 + (\alpha_1 - \alpha_2) \sin\xi \cos\xi E_2$$

$$H_1 = -(\alpha_1 - \alpha_2) \cos\xi \sin\xi E_1 - (\alpha_1 \sin^2\xi + \alpha_2 \cos^2\xi) E_2$$

In tensor notation we have $H_i = \alpha_{ij}E_j$ and the tensor is neither symmetric nor antisymmetric. It can be broken up into symmetric and antisymmetric parts, as follows.

Symmetric

$$H_2^S = (\alpha_1 - \alpha_2)\sin\xi\cos\xi\, E_2 + \left(\frac{\alpha_1-\alpha_2}{2}\right)(\cos^2\xi - \sin^2\xi)\, E_1$$

$$H_1^S = \left(\frac{\alpha_1-\alpha_2}{2}\right)(\cos^2\xi - \sin^2\xi)E_2 - (\alpha_1-\alpha_2)\sin\xi\cos\xi\, E_1$$

Antisymmetric

$$H_2^A = -\left(\frac{\alpha_1+\alpha_2}{2}\right)E_1$$

$$H_1^A = \left(\frac{\alpha_1+\alpha_2}{2}\right)E_2$$

The reader should note that this mixed tensor results from the fact that the magnetic field is related to the electric field at right angles to it, in the absence of coupling.

The previous derivation is general enough to apply to the case of two-dimensional inhomogeneity as well as to anisotropy, provided we generalize α_1 and α_2 to include arbitrary phase between the electric and magnetic fields.

For anisotropy we have

$$H_2 = \alpha_{21}E_1 + \alpha_{22}E_2$$

$$H_1 = \alpha_{11}E_1 + \alpha_{12}E_2$$

and our measurements give us H_2, H_1, E_1, and E_2. The phase angles H_2-E_1, H_2-E_2, H_1-E_1, and H_1-E_2 will be identical, measured on noise-free records.

Noting that

$$\alpha_{21} = (\alpha_1 \cos^2\xi + \alpha_2 \sin^2\xi)$$

$$\alpha_{22} = (\alpha_1 - \alpha_2) \sin\xi \cos\xi$$

$$\alpha_{11} = -(\alpha_1 - \alpha_2) \sin\xi \cos\xi$$

$$\alpha_{12} = -(\alpha_1 \sin^2\xi + \alpha_2 \cos^2\xi)$$

we see that the unknowns α_1, α_2, and ξ are to be determined. With three unknowns and two equations per measurement, we require two measurements to solve for the unknowns.

The solution, details of which are in Appendix III, is given below where the superscripts I and II refer to the first and second measurement respectively.

$$\alpha_{11} = \frac{H_1^I E_2^{II} - H_1^{II} E_2^I}{E_1^I E_2^{II} - E_1^{II} E_2^I}$$

$$\alpha_{12} = \frac{H_1^I E_1^{II} - H_1^{II} E_1^I}{E_2^I E_1^{II} - E_2^{II} E_1^I}$$

$$\alpha_{21} = \frac{H_2^I E_2^{II} - H_2^{II} E_2^I}{E_1^I E_2^{II} - E_1^{II} E_2^I}$$

$$\alpha_{22} = \frac{H_2^I E_1^{II} - H_2^{II} E_1^I}{E_2^I E_1^{II} - E_2^{II} E_1^{II}}$$

We can avoid consideration here of the phase between electric and magnetic fields, since they are identical at all angles. Magnitudes only need be used, as gotten from

autocorrelation.

For inhomogeneity, the linearly polarized case has one linearly polarized field but the other is elliptically polarized. The case we will treat is linearly polarized electric field and elliptically polarized magnetic field.

Referring to the diagram below

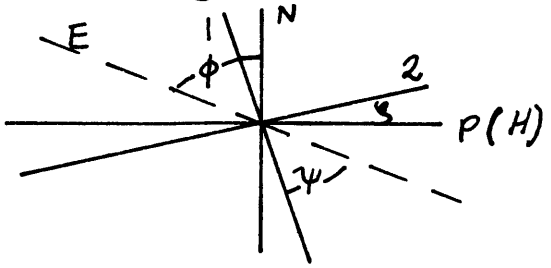

again

$$\left.\begin{aligned} H_H &= E_N \alpha_1 \\ H_N &= -E_H \alpha_2 \end{aligned}\right\} \quad \alpha\text{'s are complex}$$

The elliptic polarization is evident if we write

$$\begin{aligned} H_H &= E_N |\alpha_1| e^{i\phi_1} \\ H_N &= -E_H |\alpha_2| e^{i\phi_2} \end{aligned} \qquad \phi_1 \neq \phi_2$$

so that if the two electric fields are in phase, the magnetic fields will not be, resulting in elliptic polarization of the magnetic field.

The details of the derivation will be found in Appendix III. The method is to set up equations for H_2 and H_1 using first E_N and E_H and then substituting E_1 and E_2. Then put in the total electric field E and the angle ϕ that it makes with the unknown major axes, N and P.

The resulting equations are

$$H_2^I = E^I \left\{ \cos\phi\, \alpha_1 \cos\xi - \sin\phi\, \alpha_2 \sin\xi \right\}$$

$$H_1^I = - E^I \left\{ \cos\phi\, \alpha_1 \sin\xi + \sin\phi\, \alpha_2 \cos\xi \right\}$$

where the superscript I designates the measurement. Measured quantities are H_2^I, H_1^I, E^I and the phase angles between H_2^I-E^I and H_1^I-E^I. Also the angle $\phi^I = \psi^I + \xi$ where ψ^I is known.

If we let

$$\alpha_1 = |\alpha_1| e^{i\phi_1}$$

$$\alpha_2 = |\alpha_2| e^{i\phi_2}$$

and substitute, given the two equations for H_2^I and H_1^I we can solve for the real and imaginary parts of $|\alpha_1| e^{i\phi_1}$ in terms of functions of ξ, namely sines and cosines.

$$Im\,(\alpha_1 e^{i\phi_1}) = \alpha_1 \sin\phi_1 = \frac{F\,Im(H_1^I/E) + H\,Im(H_2^I/E)}{HE + FG}$$

$$Re\,(\alpha_1 e^{i\phi_1}) = \alpha_1 \cos\phi_1 = \frac{B\,Re(H_1^I/E) + D\,Re(H_2^{II}/E)}{AD + BC}$$

where A, B, C, D, E, F, G, and H are functions involving sin and cos ξ, as shown in Appendix III.

Equating these for two measurements we have two fourth order equations in sin ξ, one from the real and one from the imaginary part.

ξ is limited to 0 - 90° so sin ξ is limited to 0 - 1. There is no guarantee that only one root of the fourth order equation lies between 0 and 1. Two equations are available and they should have one identical root.

A rough numerical test was carried out making calculations

at 0°, 45°, and 90°. The equations from the real and imaginary parts had a solution between 0° and 45° as well as one between 45° and 90°. The method will be difficult to apply for analysis of field data because inaccuracies exist in the estimates of amplitudes and phase. The diagnostic test for this case is one linearly polarized field and one elliptically polarized one.

iii) When the field is elliptically polarized, and the conductivity structure is either anisotropic or two-dimensionally inhomogeneous, the diagnostic feature is that both fields are elliptically polarized. The general treatment to be given here and detailed in Appendix III will allow determination of the major axes. Separation of the anisotropic and inhomogeneous cases can be accomplished by determination of α_1 and α_2. For the anisotropic case α_1 and α_2 will have the same phase, while for the two-dimensional inhomogeneous case the phases will differ.

The method starts with the equations relating the electric and magnetic fields.

$$H_2 = \{E_1 \cos\xi + E_2 \sin\xi\}\alpha_1 \cos\xi + \{-E_1 \sin\xi + E_2 \cos\xi\}\alpha_2 \sin\xi$$

$$H_1 = -\{E_1 \cos\xi + E_2 \sin\xi\}\alpha_1 \sin\xi + \{-E_1 \sin\xi + E_2 \cos\xi\}\alpha_2 \cos\xi$$

The diagram for the axes is as in case ii) and α_1 and α_2 are complex.

As we have assumed all through this treatment, the records will be noise free and we can find by statistical techniques from our measurements the following information:

$$E_1 = H_2 \, e^{i\gamma_1} m_1$$
$$E_2 = H_2 \, e^{i\gamma_2} m_2$$
$$E_1 = H_1 \, e^{i\gamma_3} m_3$$
$$E_2 = H_2 \, e^{i\gamma_4} m_4$$

The amplitudes will be from autocorrelations and the phases from coherency analysis.

Substitution of these into the equations for H_2 and H_1 allows a solution of these two equations for either α_1 or α_2. A second measurement, independent of the first, also can be solved for α_1 or α_2. Equating these two again gives an equation fourth order in sin ξ. Appendix III has the details of this method.

It cannot be shown that this equation has only one root for ξ between 0 and 90°. It is a complex equation and both real and imaginary parts must vanish. Solutions will be complicated by errors in estimates of phase and power spectra.

It is evident that these complicating factors as covered in i), ii) and iii) do cause difficulties for field measurements. In case iii) the investigator may not be sure if his second measurement represents a different measurement until

he has returned from the field and put the records through some processing. The error spread in estimates of power spectra and phase may cause meaningless answers. Answers to these problems can come only with field experience.

A simple suggestion which will work in some cases is to observe the direction of the electric field or of the major axis of the electric field ellipse. This direction will be one of the major axes near a contact having a sharp step-up in conductivity. The same sort of observation applies to anisotropy. Application of such simple methods is unjustified unless some geologic information is available. As in most geophysical problems, there is no substitute for geologic control.

This chapter will close with a summary table for cases i, ii, and iii. In examining this table, it should be remembered that geographic coverage is essential to interpret two-dimensional conductivity structure and will offer another means for distinguishing anisotropy from inhomogeneity.

Table VIII - Summary of Anisotropy and Inhomogeneity Effects

Case	Conductivity Structure	Field Structure	Diagnostic Technique	Measurements Necessary
i	Horizontally Stratified	Elliptically Polarized	Constant phase E-H	1
ii	Anisotropic	Linearly Polarized	Both fields linear	2*
	Inhomogeneous	"Linearly" Polarized	One field linear, one elliptic	2
iii	Anisotropic	Elliptically Polarized	Solve equation, check phase of α_1 and α_2	2
	Inhomogeneous	Elliptically Polarized		2

* When two measurements are necessary they must be independent; that is, with different applied fields.

CHAPTER IV

RESULTS

General

In this chapter the results of the statistical analysis are presented and discussed. A figure of merit criteria is suggested to distinguish usable from useless records. This criterion is applied to the results. Based on the usable records plus near surface data from resistivity surveys by Hauck (1959) and Slichter (1934) a two-layer interpretation is made.

The geophysical implications of the two-layer interpretation will be discussed, and the existence of a resistivity discontinuity at a depth of 70 km postulated.

Results of statistical analysis

The machine results of the IBM 704 computations for the statistical analysis are in Appendix I. An examination of these tables shows a wide spread in coherency within the pass band. It was recognized that some of the records looked poor, and this low coherency is a quantitative measure of how bad they were. A figure of merit was assigned to each record, based on coherencies and phases. The figure of merit ran from 1 to 3 with the rules as stated below for determining the figure of merit for a given record.

A 1 was assigned to records having coherency better

than .7 in at least three adjacent frequency bands.

A 2 was assigned to records having coherency less than .7 but greater than .5 and consistent phases for greater than three adjacent frequency intervals.

A 3 was assigned to all other records.

Table VIII gives the case numbers and figures of merit for all cases in Appendix I where both electric and magnetic measurements were made.

Resistivities were calculated for records having merit figures of 1, and if needed, those with 2. The need was established by having none or one in a frequency range. The calculated resistivities are in Appendix II. The calculations were only done for those frequency bands that themselves met the requirements for merit figures of 1 or 2.

The resistivities in Appendix II were averaged. The cases averaged are listed in Table IX and the average resistivities presented in Table X.

No useful records for frequencies above .6 cps were obtained. With the measured resistivities of 8000 Ω-m or so, the skin depth is 65 km. This means that we are not getting detailed information from depths above this. However, two other sources of information were made available by A. Hauck (1959) who supplied results of his own resistivity survey and also his interpretation of data presented by Slichter (1934).

Hauck's resistivity survey used mile dipoles at up to

5 miles center-to-center spacings, allowing interpretations to depths of the order of 1 or 2 km. Slichter's data was taken by sending a current of 10-25 amperes through two electrodes 30 miles apart. One end of this dipole was near Boston and the other 30 miles to the west in Clinton, Mass. The resulting electric potentials were mapped over an area fifty miles in diameter centered on Clinton. The measurement was done using telephone circuits. These data have been interpreted by Hauck giving information on resistivities to depths of 5-10 km.

Three layer curves for resistivity soundings have been published by Compagnie Generale de Geophysique (1955). These curves are useful in this investigation since a rough picture of the earth's resistivity could be that it increases with depth until temperature effects cause a decrease. Examination of these curves shows that interpretations down to depths of .1 to .25 of the dipole spacing are possible. This fact was used in these previous estimates of depth of penetration.

Hauck's findings are that the apparent resistivity from his measurements at dipole separations of five miles are about 6000-10,000 ohm-meters. Slichter's data were interpreted to give apparent resistivities of 8000 ohm-meters measuring over distances of 40-55 kilometers.

This data is in good agreement with measurements at .6 cps, and gives an estimate of the resistivity of the

upper layers. We will use 8000 ohm-meters in the two-layer interpretation for apparent resistivity at frequencies greater than .6 cps.

The cases for which resistivities were calculated have the phase angles as shown in Table XI. The modified phase angles, obtained by changing the signs of the angles in Table XI and subtracting 90°, are shown in Table XII. The modification is required because the phase angles in Table XI are reversed in time, and the magnetic measurement takes the derivative of the field. The modified phase angles represent the phase between the electric and magnetic fields with a negative sign indicating the electric field leads the magnetic.

This phase angle comparison shows that the phase angles are not consistent within records and also vary greatly from record to record. There are several possible explanations for this behavior. Estimates of phase may vary widely. From examination of good magnetic records, $\pm$ 10° seems likely. This does not explain the huge derivations found on some records where phase shifts up to 180° are indicated, but this is caused in most cases by the program used to take the tangent. The tangent of -91° and 89° are the same, and since the program gives angles from -90 to +90, the 89° will be printed out. For 89°, our calculations would give a phase angle of -179° whereas the actual angle, -91°, corresponds to a phase of +1°. Examination of the records

in every case indicates that the phase should be close to 0° and not 180°.

Another explanation may be the effects of inhomogeneity. Examination of Figures 14 and 15 shows that with resistivity contrasts of 16, the apparent resistivity measured in the resistive media varies at most to twice the actual. The phase however gets up to 135°. Although only figures for the electric field perpendicular to the contact are available, it can also be postulated that other fields exist at right angles to the Figure 14-15 fields. Since we have not made measurements in the major axis system, both electric fields will influence the magnetic field measured.

Thus with different directions of fields, differing phase shifts may be expected. Experience at Littleton indicates that the electric field there is linearly polarized. The measurements of the magnetic field were inconclusive in this respect.

The phase shifts to be expected on the basis of the two-layer model run from -45° to -90°, based on the interpretation discussed in the next section. The phase shifts expected from Cagniard's curves are for f = .5 cps, ϕ = -45°; f = .2 cps, ϕ = -60°; f = .1 cps, ϕ = -75°; and f = .01 cps, ϕ = -90°. We can fit Littleton into Figures 14 and 15 on the resistive side by assuming the ocean to be two-dimensional. Littleton is at $kr \approx \frac{\sqrt{w}}{2}$. For f = .01 cps,

Littleton is at kr $\approx$.12, for f = 1 cps, it is at kr $\approx$ 1.2. Thus, at lower frequencies Littleton is "close" to the ocean. However, at these frequencies the ocean itself is less of a two-dimensional feature. The final analysis of the expected phase shifts at Littleton depends on obtaining results from analogue computer work, now underway in the Geophysics Laboratory.

One final observation on the phase shift is that it represents only a small fraction of the interval between digitalizations, perhaps 10-20%. Possibly this could give rise to errors in phase determination. At any rate, phase angles were not used in interpretation in this investigation.

A final error estimate of the apparent resistivities in Table X ismade in Table XIII. These errors were derived by using Tukey's formula as described in Chapter III.

Interpretation

Although data was collected only at Littleton, Massachusetts, an interpretation for this location will be attempted. This interpretation is based on Cagniard's two-layer master curves.

The data from Table X are plotted in Figure 16. The interpretation is accomplished by overlaying the two-layer master curves, Figure 13, with Figure 16. The data points are lined up to give the best fit to the master curves.

The mechanical procedure to get ρ_1, ρ_2, and h, the thickness of the upper layer is as follows. The resistivity of the upper layer, ρ_1, is found at the resistivity lining up with $\rho_a = 1\ \Omega\text{-}m$ on the master curve. The resistivity of the lower layer, ρ_2, is found by multiplying ρ_1 by the contrast, ρ_2/ρ_1, from the master curve giving the best fit to the data.

The thickness of the upper layer, h, is found by matching point A on the two-layer master curves with a period on the data plot. The thickness is found by taking this $(\text{period})^{\frac{1}{2}}$, X, and using it in the formula.

$$h = \frac{X}{8}\sqrt{10\,\rho_1}\ \text{km}$$

The author's interpretation, taking ρ_1 as 8000 ohm-meters, gives an h of 70 kilometers with a resistivity of the lower layer of less than 80 ohm-meters.

Figure 16 is found on a transparency in the pocket at the end of the thesis. Those wishing to check the above interpretation can use this in conjunction with Figure 13.

Before discussing the significance of this interpretation as regards temperature and conductivity in the earth, other possible interpretations should be discussed. A three-layer interpretation is not possible because the data do not indicate the presence of three layers. The error spread is too great at high frequencies to tell if multiple layering is present, and at lower frequencies a

two-layer interpretation fits the data extremely well.

It can be asked whether or not some other conductivity distribution would give rise to the same curve. This seems unlikely when data from Hauck (1959) is considered. The apparent resistivity as measured by Hauck and Slichter (1934) is quite constant at about 8000 ohm-meters down to 5-10 kilometers. At our highest frequency of .6 cps, again the apparent resistivity is about 8000 ohm-meters, making the skin depth 65 km. It is difficult to fit another resistivity-depth interpretation into the region down to 100 km or so in the light of this data.

Below the interpreted depth of 70 km any interpretation is within the data so long as the resistivity is below 80 ohm-meters. We do not have low enough frequencies to distinguish between 0 and 80 ohm-meters.

These comments point up the weak places in our magnetotelluric procedure. Better high frequency measurements will be necessary in places where measurements such as Slichter's do not exist. These high frequencies will serve to delineate the conductivity structure near-surface in more detail. Lower frequency measurements will be necessary to say anything about the interpretation below a conductivity discontinuity such as found.

The significance of this seeming conductivity discontinuity was at first obscure. The plot of resistivity versus depth shown in Figure 17, with the discontinuity

at 70 kilometers, illustrates the situation. Curves from McDonald (1957) and Lahiri and Price (1939) are also plotted, but with the full realization that interpretations done by these authors were not intended to be as detailed in the near-surface regions as our interpretations. However, the curves by McDonald and Lahiri and Price have been used by those interested in the temperature structure of the earth, and in some cases the values of electric conductivity from 0 to 200 km have been taken as representative. Our interpretation down to 125 km is radically different than either of the two curves plotted, and below this depth, could fit with Lahiri and Price's curve (d). This will be discussed later.

It must also be pointed out that Lahiri and Price have other curves with high resistivities extending to depths of greater than 500 kilometers. These do not fit with the interpretation of our magnetotelluric data.

The temperature structure of the earth has recently been reviewed by MacDonald (1959). A typical temperature distribution was taken from his work. Conductivities as measured by Hughes (1953) for diopside, olivine, and enstatite were calculated for the temperature distribution chosen. The temperature distribution was MacDonald's Model 8 and is shown in Table 14 along with the calculated resistivities.

The conductivities calculated were the ionic con-

ductivities using the formula

$$\sigma_{ionic} = \sigma_2 \, e^{-E_2/k_o T}$$

with k_o Boltzmann's constant and T in ^{o}K. The values of the parameters used were

	Olivine	Enstatite	Diopside
E_2	3 ev	2.8 ev	4.0 ev
σ_2	$5 \times 10^{8}\ \Omega^{-1}\text{-m}^{-1}$	$10^{6}\ \Omega^{-1}\text{-m}^{-1}$	$10^{12}\ \Omega^{-1}\text{-m}^{-1}$

The ionic resistivity alone was plotted, although electronic conductivity also takes place and may be contributing as much as one-half according to Tozer (1959) at temperatures of 1600 ^{o}K. Hughes (1959) suggests that above 1400 ^{o}K conduction is mainly ionic.

For our purposes the ionic resistivity is plotted in Figure 17 for the three materials, olivine, diopside, and enstatite. An explanation for the conductivity "discontinuity" can now be proposed. Above roughly 70 km the conductivity is determined by pore fluids, with probably some ionic conductivity beginning as the pore fluid conductivity is "squeezed out." At about this critical depth, the temperature effects begin to take over, and from there on the ionic conductivity dominates. This conductivity discontinuity is to be expected on the basis of the other temperature distributions. The Model 8 temperature distribution has low values; MacDonald's other models run up to plus $500^{o}K$ higher at depths of 120 km but at 30 km

the variation is only plus 100°K. Calculations based on Model 7 of MacDonald are plotted for olivine and enstatite, and the calculated data is shown in Table XV.

A general picture emerges that many of the materials proposed for the upper mantle region could fit the conductivity profile found. The temperature profile is indeterminate enough to allow many choices.

Since the data do not indicate a value for the resistivity in the lower layer, only an upper limit, it is very difficult to make definitive statements. It is clear that this will remain a limitation of the magnetotelluric method for determining conductivity in the mantle. With the longest periods measured being 200 seconds, we will be limited to only a depth determination of this resistivity discontinuity. This applies as long as the upper layer has an apparent resistivity of 8000 ohm meters, and even with an apparent resistivity as low as 2000 ohm meters we would need to have data at 2000 second periods to determine the lower layer resistivity. For the case of an upper layer resistivity of 8000 ohm meters, examination of Figure 13 shows that we would need roughly 10,000 second period measurements to begin to interpret the lower layer resistivity.

The determination of the depth to this discontinuity is influenced by the slope of the line through the points on Figure 16 and by the ρ_1 of the upper layer. A possible

interpretation might be that this line continues upward, since Slichter's resistivity data only goes to 10 km deep. The author does not feel this is a valid interpretation, but even if it is, and the material from 10 to 70 km had a resistivity of 100,000 ohm-meters the depth to the discontinuity does not change. This is due to the inter-relationship of h and ρ_1 .

One further statement about the depth to this resistivity discontinuity is in order. By stretching the interpretation, we can fit a depth of 100 km into the data. The spread in depth from 70-100 km allows most of the materials and the temperature profiles to fit the magnetotelluric data. This emphasizes the problems of further interpretation, and indicates the need for accuracy in the measurements.

Conclusions

The magnetotelluric data indicate a sharp resistivity change at depths around 70 km. This change fits in well with current temperature profiles in the earth, and with conductivity data.

As best we know this change, shown as a discontinuity from our data, has not been described before. It is suggested that it be called the OHMO rather than the 70 kilometer resistivity discontinuity, for convenience.

Table VIII Case Frequencies and Merit Numbers

Case No.	Frequency	Merit No.
20-8	.02 - .04 cps	2
21-3	.04 - .06	2
21-4	.06 - .1	1
24-5	.02 - .06	3
24-6	.06 - .2	2
26-1	.02 - .06	1
26-2	.2 - .6	3
26-3	.08 - .2	2
26-4	.06 - .08	2
26-5	.02 - .04	1
26-6	.02 - .06	1
26-7	.02 - .06	1
27-1	.6 - 1.0	3
27-2	.2 - .6	2
27-3	.06 - .2	1
27-4	.005 - .02	2
27-5	.02 - .06	1

Table IX Cases Averaged

Frequency	Cases Averaged
.005 - .02 cps	27-4
.02 - .06	26-1
	26-5
	26-6
	26-7
	27-5
.06 - .2	21-4
	27-3
.2 - .6	27-2
.6 - 1	*none

*Data from deep resistivity survey used.

Table X Average Resistivities

f	ρ_a	T
.006 cps	310 Ω-m	167 sec^{-1}
.009	430	111
.012	810	84
.016	550	62
.019	530	53
.020	1190	50
.030	1520	33
.040	3700	25
.050	3200	20
.060	3300	17
.062	3400	16
.075	2900	13.5
.087	2200	11.5
.100	4800	10.0
.150	12000	6.7
.20	9800	5
.30	8300	3.3
.40	6200	2.5
.50	7200	2.0
.60	4900	1.7

Table XI Phase Angles

f(cps)	27-4				
.006	-12°				
.009	0				
.012	-86				
.016	-20				
.019	-46				
	26-1	26-5	26-6	26-7	27-5
.020	-83°	-87°	-68°	-40°	-18°
.030	83	-78	-19	-76	-26
.040	-42	77	-79	39	-42
.050	-49	90	-66	-27	-32
.060	-44	-74	86	48	-30
	21-4	27-3			
.062	-53°				
.075	-45	-13°			
.087	-33				
.100	-34	-16			
.150		-19			
	27-2				
.20	-14°				
.30	-26				
.40	-8				
.50	-15				
.60	-30				

Table XII Modified Phase Angles*

f(cps)	27-4				
.006	-78°				
.009	-90				
.012	-4				
.016	-70				
.019	-44				
	26-1	26-5	26-6	26-7	27-5
.020	-7°	-3°	-22°	-50°	-72°
.030	-173	-12	-71	-14	-64
.040	-48	-177	-11	-129	-48
.050	-41	-180	-24	-63	-58
.060	-46	-16	-176	-138	-60
	21-4	72-3			
.062	-37°	-			
.075	-45	-77°			
.087	-57	-			
.100	-56	-74			
.150		-71			
	27-2				
.20	-76°				
.30	-64				
.40	-82				
.50	-75				
.60	-60				

*Negative Sign means electric leading magnetic

Table XIII Error Analysis

Case No.	f cps	Δf cps	l sec	error db	error range
27-4	.005-.020	.003	1200	5.8	x1.95
26-1	.020-.060	.010	535		
26-5	↓	↓	965		
26-6			475	for l = 600	
26-7			495	4.9 (1 pc.)	x1.80
27-5			830	2.1 (5 pc.)	x1.29
21-4	.060-.2	.013	482	4.8	x1.74
27-3	↓	.050	166	4.25	x1.63
27-2	.2-.6	.100	75	4.35	x1.65

Table XIV Temperature and Resistivity at Depth

Model 8

Olivine

Depth	Temperature	Resistivity
30 km	670° K	6×10^{13} Ω-m
50	900	2×10^{8}
70	1200	8×10^{3}
100	1500	20
200	1900	1.2×10^{-1}

Diopside

Depth	Temperature	Resistivity
30 km	670° K	10^{18} Ω-m
50	900	3×10^{10}
70	1200	10^{5}
100	1500	30
200	1900	5×10^{-2}

Enstatite

Depth	Temperature	Resistivity
30 km	670° K	10^{15} Ω-m
50	900	10^{10}
70	1200	10^{6}
100	1500	2×10^{3}
200	1900	20

Table XV Temperature and Resistivity at Depth

Model 7

Olivine

Depth	Temperature	Resistivity
30 km	690° K	8×10^{13} Ω-m
50	980	10^{7}
70	1270	10^{3}
100	2000	5×10^{-2}
200	2370	6.5×10^{-3}

Enstatite

Depth	Temperature	Resistivity
30 km	670° K	5×10^{14} Ω-m
50	980	3×10^{8}
70	1270	6×10^{4}
100	2000	10
200	2370	1.7

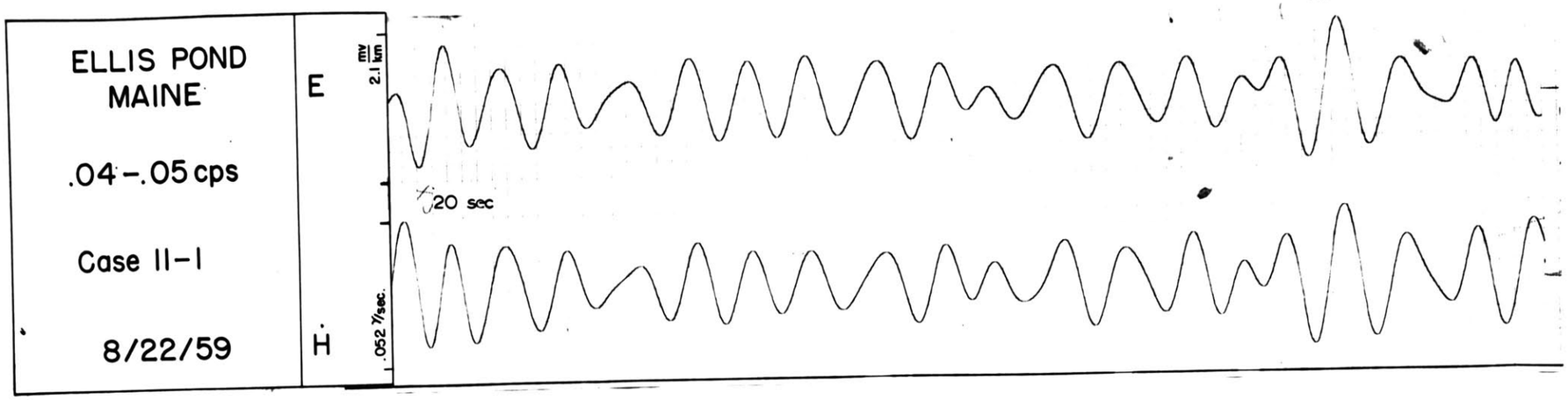

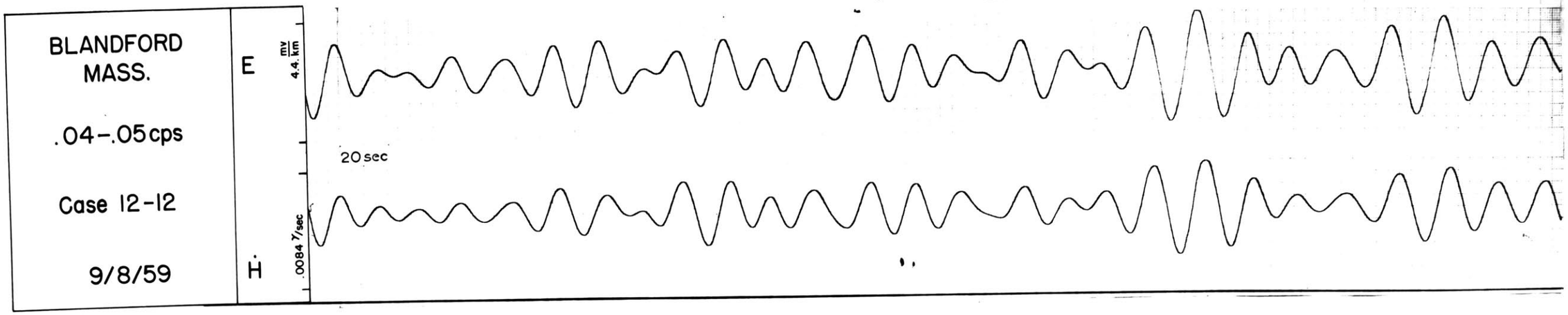

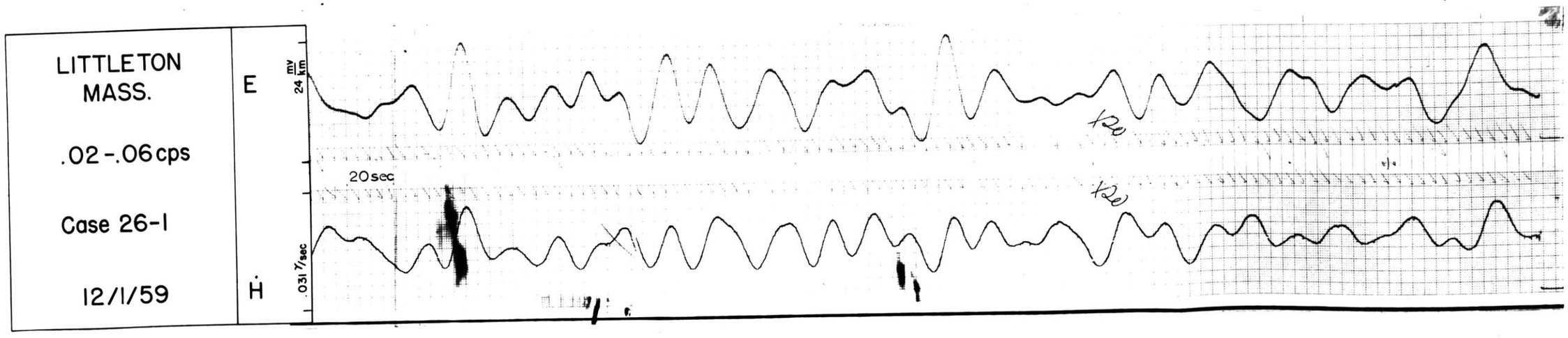

FIGURE 9 ELECTRIC-MAGNETIC RECORDS

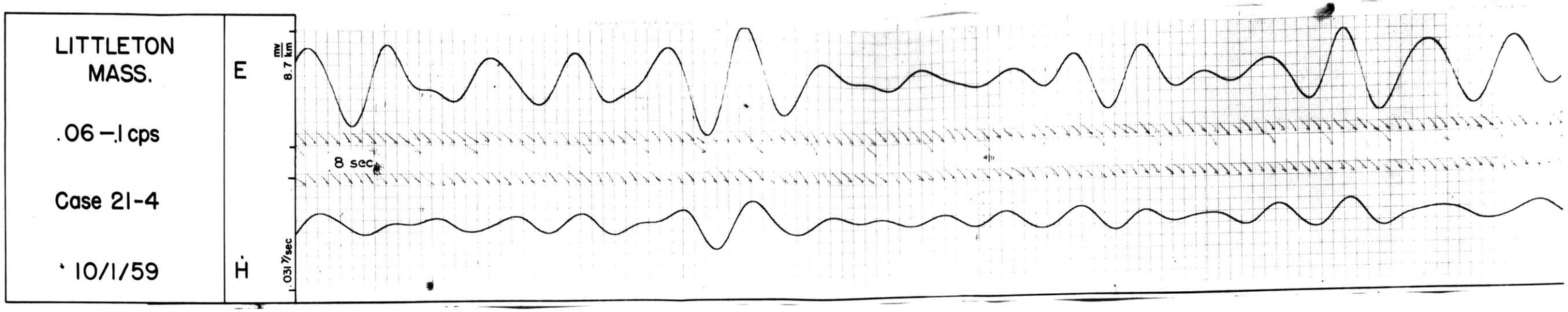

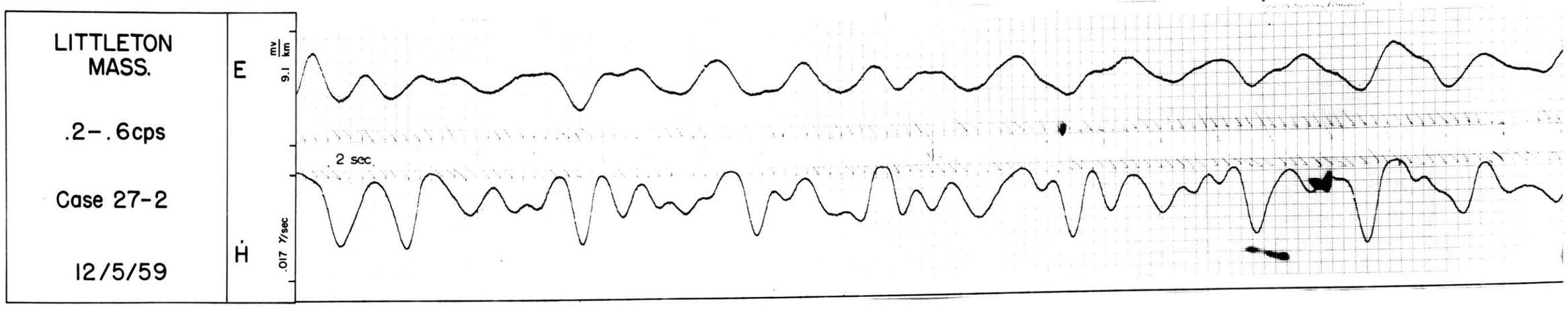

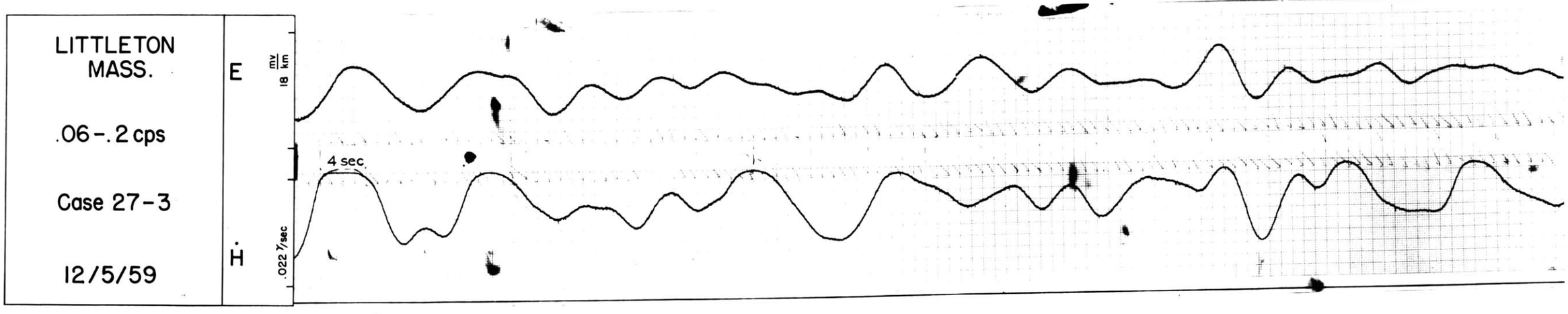

FIGURE 10 ELECTRIC-MAGNETIC RECORDS

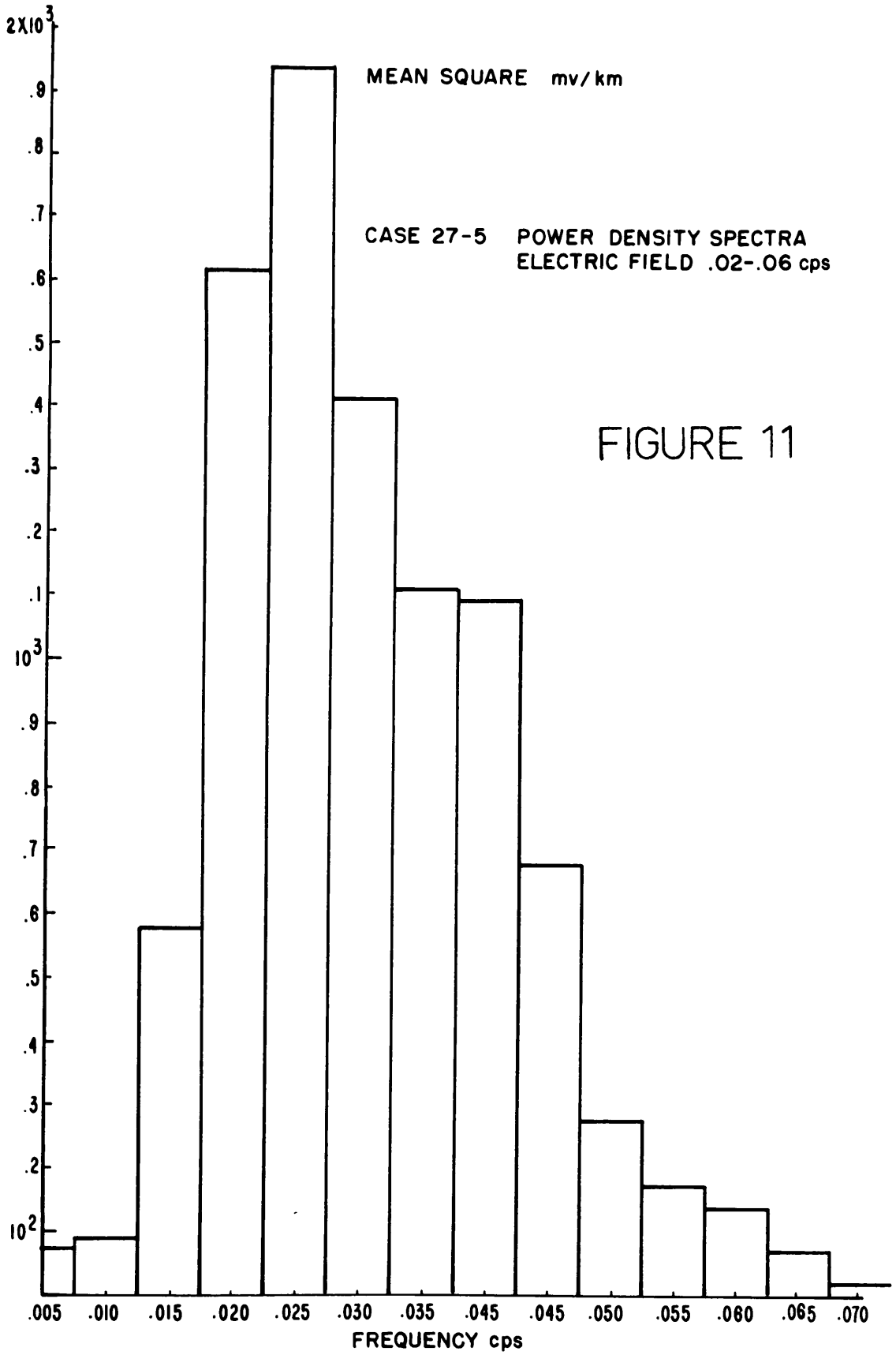
MEAN SQUARE mv/km
CASE 27-5 POWER DENSITY SPECTRA
ELECTRIC FIELD .02-.06 cps
2X10^3
.9
.8
.7
.6
.5
.4
.3
.2
.1
10^3
.9
.8
.7
.6
.5
.4
.3
.2
10^2
.005 .010 .015 .020 .025 .030 .035 .045 .045 .050 .055 .060 .065 .070
FREQUENCY cps

FIGURE 11

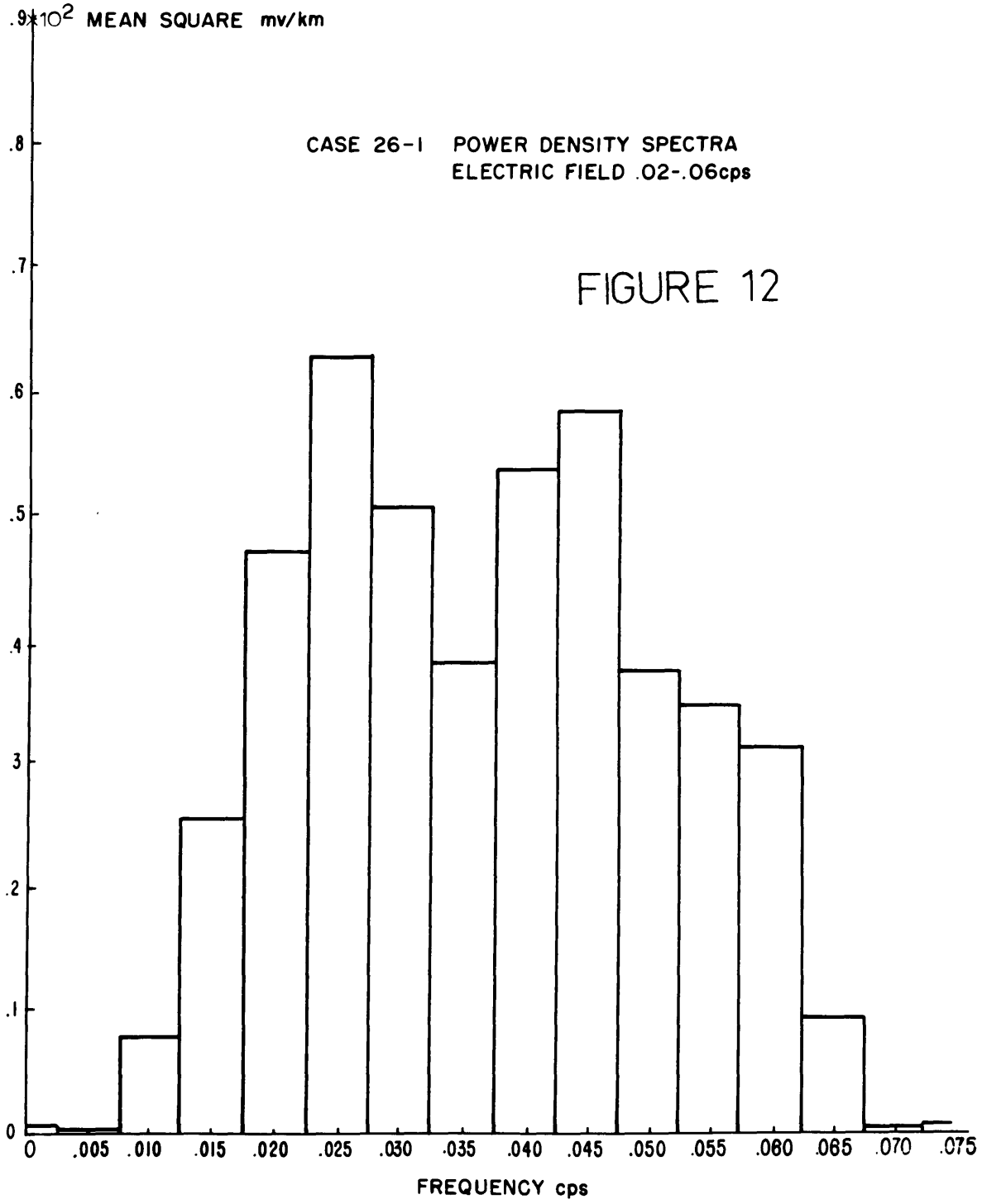
.9*10^2 MEAN SQUARE mv/km
CASE 26-1 POWER DENSITY SPECTRA
ELECTRIC FIELD .02-.06cps
.8
.7
.6
.5
.4
3
.2
.1
0
0 .005 .010 .015 .020 .025 .030 .035 .040 .045 .050 .055 .060 .065 .070 .075
FREQUENCY cps

FIGURE 12

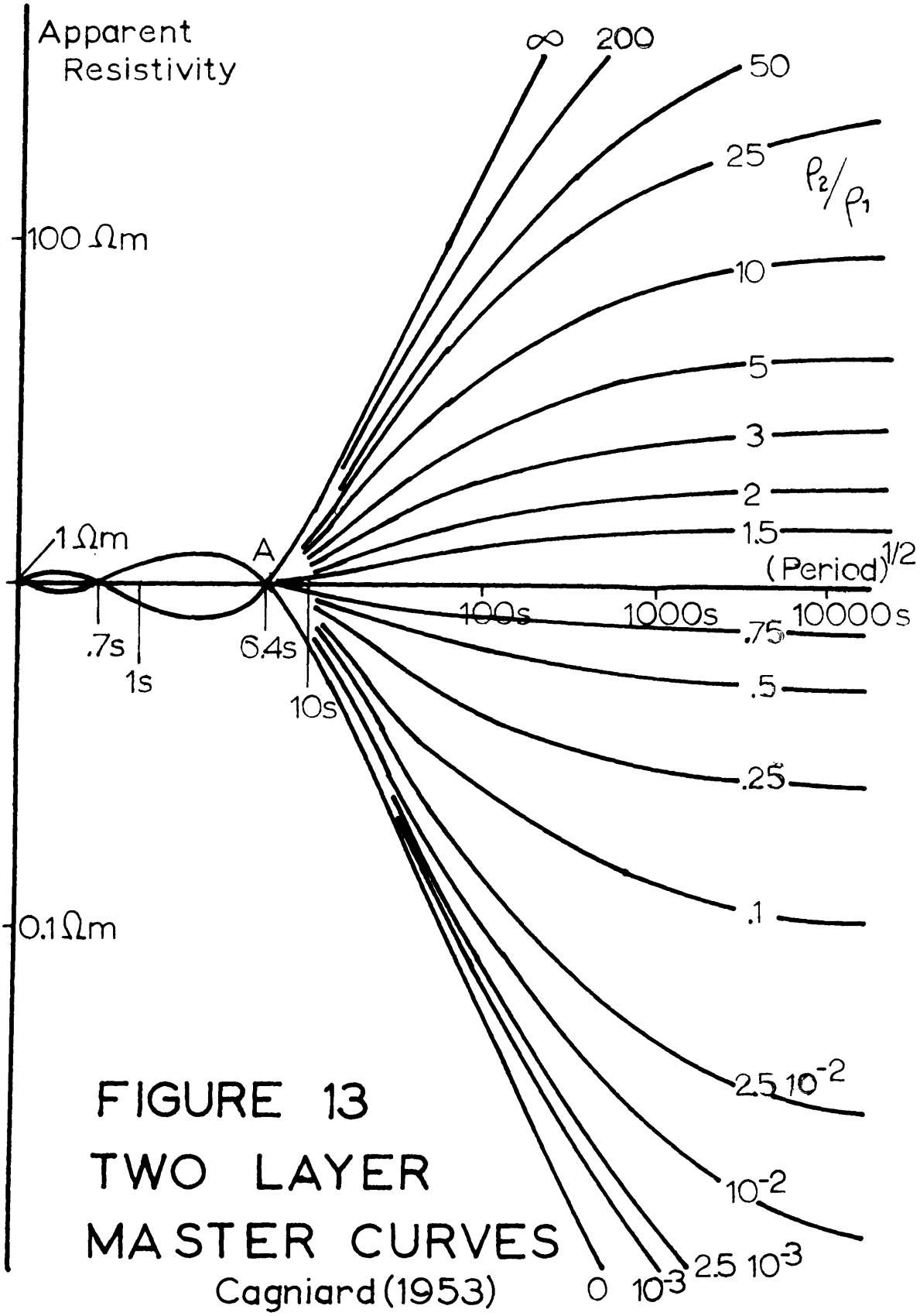

FIGURE 13
TWO LAYER
MASTER CURVES
Cagniard (1953)

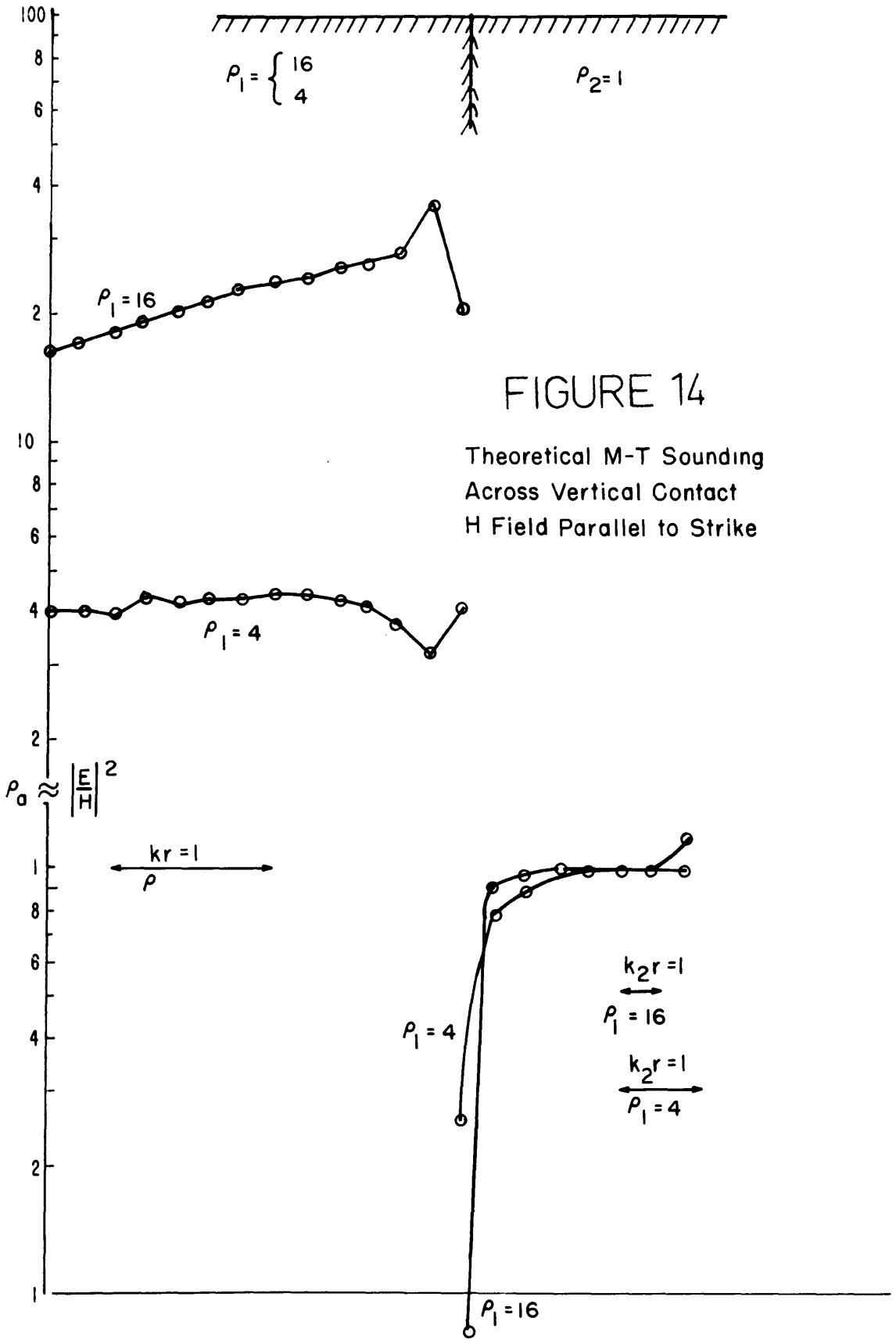

FIGURE 14

Theoretical M-T Sounding
Across Vertical Contact
H Field Parallel to Strike

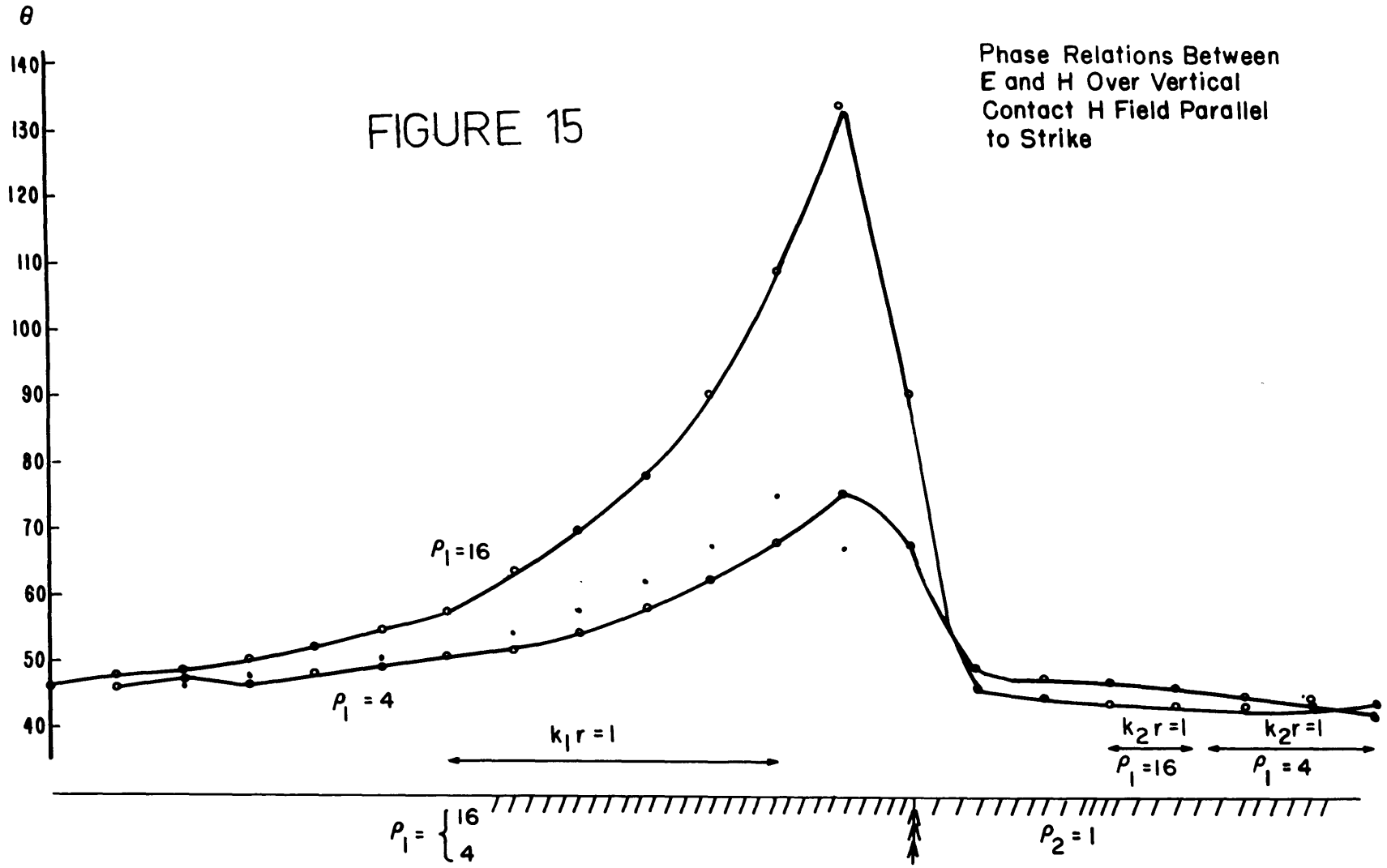
θ
140
130
120
110
100
90
80
70
60
50
40
FIGURE 15
Phase Relations Between
E and H Over Vertical
Contact H Field Parallel
to Strike
ρ1 = 16
ρ1 = 4
k1r = 1
k2r = 1
ρ1 = 16
k2r = 1
ρ1 = 4
ρ1 = { 16 / 4
ρ2 = 1

FIGURE 16

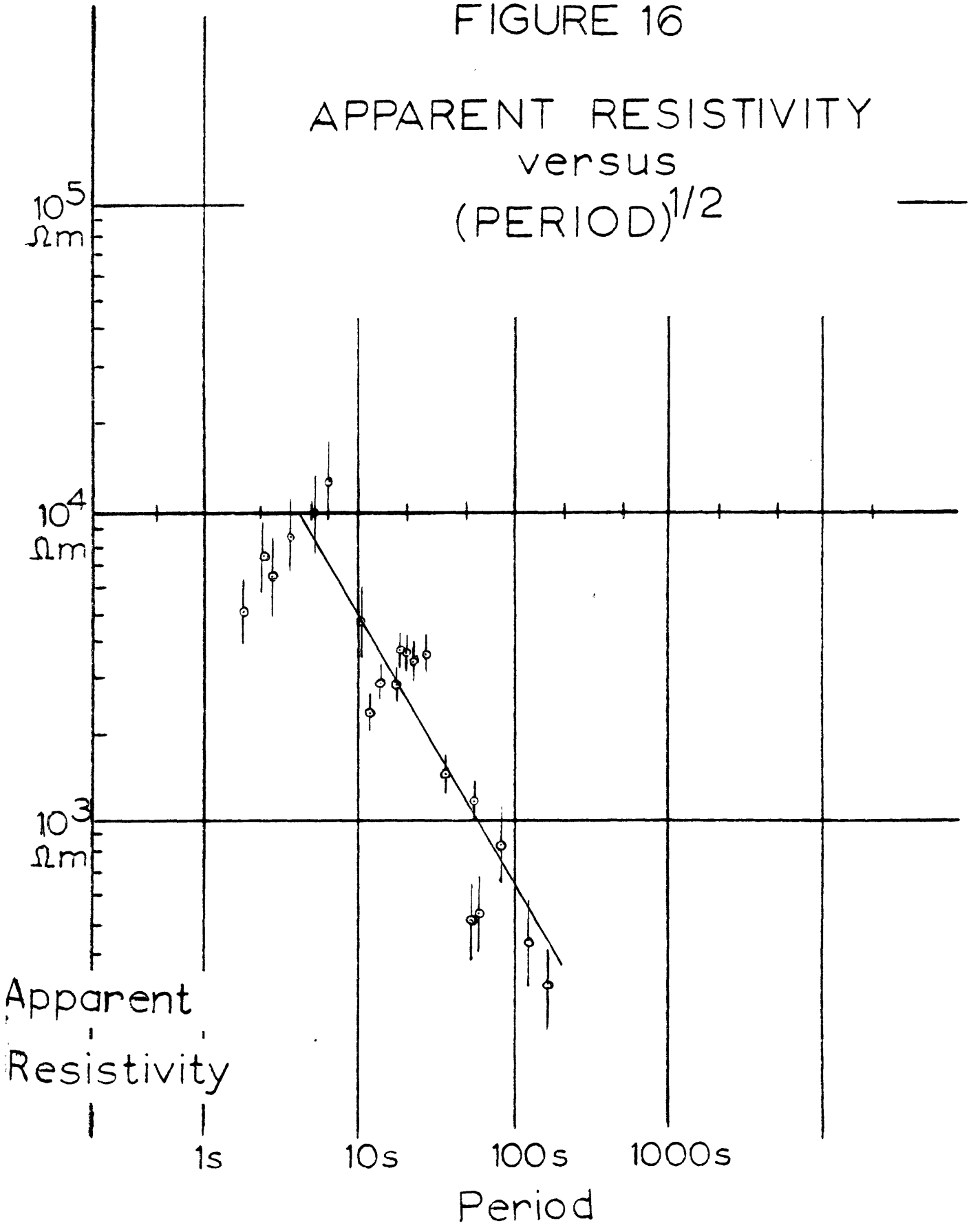
APPARENT RESISTIVITY
versus
(PERIOD)^1/2
10^5 Ωm
10^4 Ωm
10^3 Ωm
Apparent
Resistivity
1s
10s
100s
1000s
Period

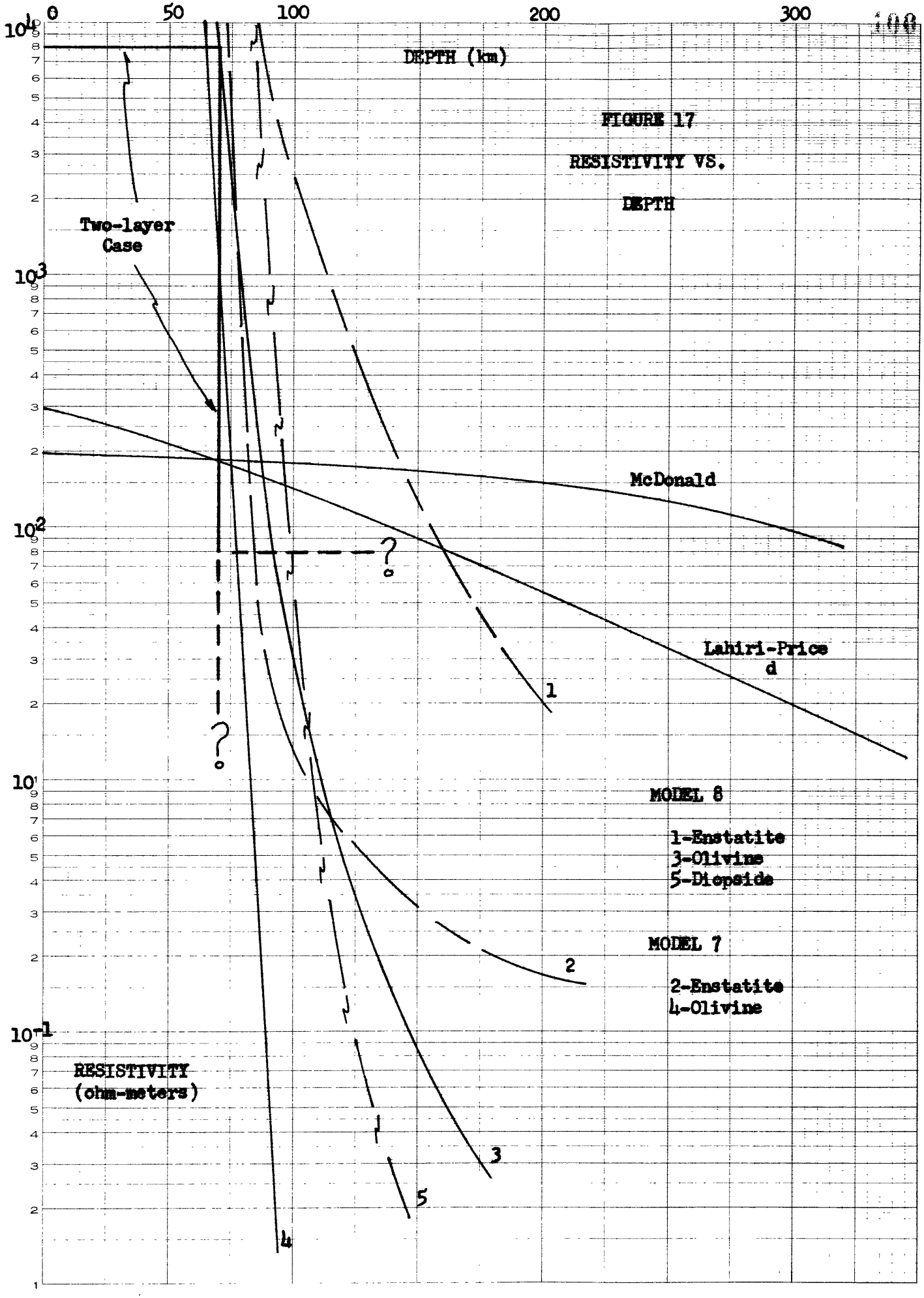
0
50
100
200
300
DEPTH (km)
FIGURE 17
RESISTIVITY VS.
DEPTH
Two-layer
Case
McDonald
Lahiri-Price
d
MODEL 8
1-Enstatite
3-Olivine
5-Diopside
MODEL 7
2-Enstatite
4-Olivine
RESISTIVITY
(ohm-meters)
1
2
3
4
5
?
?

CHAPTER V

FURTHER WORK

The purpose of this chapter is to outline recommended further work.

Equipment modifications

Total field measurements should be made to enable the determination of the real earth effects described in Chapter III.

This means that two additional field components must be measured, one electric and one magnetic. This can be done by duplicating the amplifiers, filters, and choppers presently used and time sharing the signal on the magnetic tape. A timing mark would be very helpful also to aid in digitalizing the records and to improve timing accuracy.

Eventually it might be desirable to automatically digitalize the records as the data is taken or from the magnetic tape.

It might also prove advantageous to use the Sandborn recorder directly in the field.

Crustal exploration

After the equipment modifications have been made, a crustal exploration should be undertaken. Massachusetts is convenient and a magnetotelluric survey across the State

should take no more than eight stations. After this, tests over various geologic sections should be undertaken.

In making these tests checks for two-dimensional and anisotropic effects would be made.

Theoretical work

There is a continuing need for work on the general problem of low frequency electromagnetic wave propagation over an inhomogeneous earth.

Beyond this, a study of the means for performing correlations and the errors in the methods would be welcome. The whole problem of the statistical analysis of magneto-telluric records is recommended for future study.

Sources of the magnetotelluric field

Investigation of the sources of the geomagnetic variations, be they magnetohydrodynamic or what, is another, closely allied, field of investigation. It might be possible to work with an already existing magnetic observatory to supplement rapid run magnetic records taken in the field and study these geomagnetic variations.

Error reduction

Error reduction can be accomplished in part by taking longer records. An interesting experiment would be to record for long enough in each frequency band so that 500 points of data were available for correlation. It would then be possible to test the effect of longer runs and the

stationarity of the data time series. Lengths of runs to accomplish this are shown below.

Table XVI Length of Record to Give 500 Data Points

Frequency Band	Digitalization Interval	Record Time
.005 - .02 cps	10 secs	5000 secs
.02 - .06	5	2500
.06 - .2	1	500
.2 - .6	.5	250
.6 -1.0	.2	100

Continental OHMO investigation

If the magnetotelluric survey of Massachusetts picks out the resistivity discontinuity, or OHMO, at depth, a continental investigation should be undertaken as soon as possible. The results of such an investigation will be interesting, and provided better high frequency (7.6 cps) data can be obtained, a more detailed picture of crustal conductivity structure will be obtained.

General

The recommendations for further work contained here deal primarily with the magnetotelluric field and its interpretation. This work ties in with many other fields of geophysics; for example, electrical conductivity measurements of rocks, temperature conditions at depth, and general

crustal structure. It is to be hoped that magnetotellurics will also prove of use in these fields.

APPENDIX I

STATISTICAL ANALYSIS RESULTS

In this appendix are the machine results of the IBM 704 computations discussed in Chapters III and IV.

Each case starts on a new page with the case number, location, date and frequency band on the first line. The second line begins with DEC and has twelve numbers following this. The numbers represent

1 - Number of data points for H 1
2 - Number of data points for H 2
3 - Number of data points for E 1
4 - Number of data points for E 2
5 - Number of lags calculated
6 - Time interval between lags in seconds
7 - 12 - These numbers are either 1 or 0 and direct the calculation of cross correlations. The correlations are HE 12, HE 11, HH 12, HE 21, HE 22, EE 12. A 1 means compute and a 0 means no computation.

In the tables, the first is the power density spectra and the second the results of coherency analysis. The power density spectra are in mean square gammas for the magnetic field and mean square millivolts per kilometer for the electric. The amplitude and phase of the coherency analysis are presented.

CASE 20-8 LITTLETON MASS 9/26/59 .02-.04 CPS
DEC 190,0,0,190,20,5.,1,0,0,0,0,0
PG 44,1F CANTWELL H1 E2 ONLY

POWER DENSITY SPECTRA

FREQ	H1	H2	E1	E2
	MS GAMMAS		MS MV/KM	
.002	.165E-02	.	.	.972E-02
.005	.322E-02	.	.	.250E-01
.010	.431E-03	.	.	.325E-00
.015	.330E-02	.	.	.166E 01
.020	.637E-02	.	.	.130E 02
.025	.139E-01	.	.	.304E 02
.030	.192E-01	.	.	.302E 02
.035	.113E-01	.	.	.185E 02
.040	.235E-02	.	.	.103E 02
.045	.395E-03	.	.	.389E 01
.050	.223E-03	.	.	.699E 00
.055	.679E-04	.	.	.298E-00
.060	.363E-04	.	.	.156E-00
.065	.124E-04	.	.	.898E-02
.070	.674E-05	.	.	.408E-01
.075	.180E-05	.	.	.476E-01
.080	.310E-05	.	.	.450E-01
.085	.276E-06	.	.	.371E-01
.090	.628E-07	.	.	.379E-01
.095	.237E-06	.	.	.384E-01
.100	.662E-06	.	.	.407E-01

COHERENCY ANALYSIS

FREQ	(H1,E2)		(H1,E1)		(H1,H2)		(H2,E1)		(H2,E2)		(E1,E2)	
	AMP	PHASE	AMP	PHASE	AMP	PHASE	AMP	PHASE	AMP	PHASE	AMP	PHASE
.002	8.71	90.	0.	0.	0.	0.	0.	0.	0.	0.	0.	0.
.005	0.48	72.	0.	0.	0.	0.	0.	0.	0.	0.	0.	0.
.010	0.22	-59.	0.	0.	0.	0.	0.	0.	0.	0.	0.	0.
.015	0.43	-61.	0.	0.	0.	0.	0.	0.	0.	0.	0.	0.
.020	0.44	-48.	0.	0.	0.	0.	0.	0.	0.	0.	0.	0.
.025	0.46	-41.	0.	0.	0.	0.	0.	0.	0.	0.	0.	0.
.030	0.52	-49.	0.	0.	0.	0.	0.	0.	0.	0.	0.	0.
.035	0.53	-59.	0.	0.	0.	0.	0.	0.	0.	0.	0.	0.
.040	0.34	-66.	0.	0.	0.	0.	0.	0.	0.	0.	0.	0.
.045	0.17	22.	0.	0.	0.	0.	0.	0.	0.	0.	0.	0.
.050	0.39	6.	0.	0.	0.	0.	0.	0.	0.	0.	0.	0.
.055	0.33	-80.	0.	0.	0.	0.	0.	0.	0.	0.	0.	0.
.060	0.06	-55.	0.	0.	0.	0.	0.	0.	0.	0.	0.	0.
.065	0.53	12.	0.	0.	0.	0.	0.	0.	0.	0.	0.	0.
.070	0.17	40.	0.	0.	0.	0.	0.	0.	0.	0.	0.	0.
.075	0.55	-46.	0.	0.	0.	0.	0.	0.	0.	0.	0.	0.
.080	0.32	-32.	0.	0.	0.	0.	0.	0.	0.	0.	0.	0.
.085	0.99	-56.	0.	0.	0.	0.	0.	0.	0.	0.	0.	0.
.090	1.36	-4.	0.	0.	0.	0.	0.	0.	0.	0.	0.	0.
.095	0.68	21.	0.	0.	0.	0.	0.	0.	0.	0.	0.	0.
.100	2.03	77.	0.	0.	0.	0.	0.	0.	0.	0.	0.	0.

0 0 1758.3

CASE 21-3 LITTLETON MASS 10/1/59 .04-.06 CPS
DEC 151,0,0,151,20,5.,1,0,0,0,0,0
PG 47,1F CANTWELL GEOPHYSICS LAB H1 E2 ONLY

POWER DENSITY SPECTRA

FREQ	H1	H2	E1	E2
	MS GAMMAS		MS MV/KM	
.002	.371E-01	.	.	.991E-01
.005	.109E-01	.	.	.971E-01
.010	.178E-02	.	.	.110E-00
.015	.107E-02	.	.	.978E-01
.020	.820E-03	.	.	.916E-01
.025	.122E-02	.	.	.207E-00
.030	.627E-02	.	.	.793E 00
.035	.159E-01	.	.	.598E 01
.040	.227E-01	.	.	.168E 02
.045	.236E-01	.	.	.213E 02
.050	.273E-01	.	.	.160E 02
.055	.226E-01	.	.	.110E 02
.060	.819E-02	.	.	.655E 01
.065	.158E-02	.	.	.217E 01
.070	.110E-02	.	.	.651E 00
.075	.551E-03	.	.	.369E-00
.080	.196E-03	.	.	.225E-00
.085	.830E-04	.	.	.173E-00
.090	.777E-04	.	.	.118E-00
.095	.455E-04	.	.	.151E-00
.100	.433E-04	.	.	.200E-00

COHERENCY ANALYSIS

FREQ	(H1,E2)		(H1,E1)		(H1,H2)		(H2,E1)		(H2,E2)		(E1,E2)	
	AMP	PHASE	AMP	PHASE	AMP	PHASE	AMP	PHASE	AMP	PHASE	AMP	PHASE
.002	0.72	25.	0.	0.	0.	0.	0.	0.	0.	0.	0.	0.
.005	0.42	16.	0.	0.	0.	0.	0.	0.	0.	0.	0.	0.
.010	0.26	12.	0.	0.	0.	0.	0.	0.	0.	0.	0.	0.
.015	0.16	2.	0.	0.	0.	0.	0.	0.	0.	0.	0.	0.
.020	0.37	-4.	0.	0.	0.	0.	0.	0.	0.	0.	0.	0.
.025	0.56	-79.	0.	0.	0.	0.	0.	0.	0.	0.	0.	0.
.030	0.33	-19.	0.	0.	0.	0.	0.	0.	0.	0.	0.	0.
.035	0.38	-12.	0.	0.	0.	0.	0.	0.	0.	0.	0.	0.
.040	0.44	-38.	0.	0.	0.	0.	0.	0.	0.	0.	0.	0.
.045	0.50	-42.	0.	0.	0.	0.	0.	0.	0.	0.	0.	0.
.050	0.52	-24.	0.	0.	0.	0.	0.	0.	0.	0.	0.	0.
.055	0.62	-17.	0.	0.	0.	0.	0.	0.	0.	0.	0.	0.
.060	0.70	-24.	0.	0.	0.	0.	0.	0.	0.	0.	0.	0.
.065	0.56	-45.	0.	0.	0.	0.	0.	0.	0.	0.	0.	0.
.070	0.45	-57.	0.	0.	0.	0.	0.	0.	0.	0.	0.	0.
.075	0.64	-33.	0.	0.	0.	0.	0.	0.	0.	0.	0.	0.
.080	0.54	-44.	0.	0.	0.	0.	0.	0.	0.	0.	0.	0.
.085	0.72	-38.	0.	0.	0.	0.	0.	0.	0.	0.	0.	0.
.090	0.82	-11.	0.	0.	0.	0.	0.	0.	0.	0.	0.	0.
.095	0.49	11.	0.	0.	0.	0.	0.	0.	0.	0.	0.	0.
.100	0.21	41.	0.	0.	0.	0.	0.	0.	0.	0.	0.	0.

0 0 1758.5

CASE 21-4 LITTLETON MASS 10/1/59 .06-.1 CPS
DEC 241,0,0,241,20,2.,1,0,0,0,0,0
PG 47,1F CANTWELL H1 E2 ONLY

POWER DENSITY SPECTRA

FREQ	H1	H2	E1	E2
	MS GAMMAS		MS MV/KM	
.006	.939E-02	.	.	.123E-00
.012	.375E-02	.	.	.940E-01
.025	.266E-03	.	.	.199E-00
.037	.338E-02	.	.	.129E 01
.050	.167E-01	.	.	.123E 02
.062	.214E-01	.	.	.258E 02
.075	.157E-01	.	.	.200E 02
.087	.926E-02	.	.	.751E 01
.100	.390E-02	.	.	.284E 01
.112	.922E-03	.	.	.961E 00
.125	.178E-03	.	.	.364E-00
.137	.495E-04	.	.	.212E-00
.150	.245E-04	.	.	.142E-00
.162	.108E-04	.	.	.130E-00
.175	.708E-05	.	.	.113E-00
.187	.334E-05	.	.	.132E-00
.200	.194E-05	.	.	.148E-00
.212	.581E-06	.	.	.153E-00
.225	.238E-06	.	.	.137E-00
.237	.386E-06	.	.	.118E-00
.250	.366E-06	.	.	.106E-00

COHERENCY ANALYSIS

FREQ	(H1,E2)		(H1,E1)		(H1,H2)		(H2,E1)		(H2,E2)		(E1,E2)	
	AMP	PHASE	AMP	PHASE	AMP	PHASE	AMP	PHASE	AMP	PHASE	AMP	PHASE
.006	0.25	17.	0.	0.	0.	0.	0.	0.	0.	0.	0.	0.
.012	0.16	59.	0.	0.	0.	0.	0.	0.	0.	0.	0.	0.
.025	0.26	64.	0.	0.	0.	0.	0.	0.	0.	0.	0.	0.
.037	0.69	-48.	0.	0.	0.	0.	0.	0.	0.	0.	0.	0.
.050	0.86	-55.	0.	0.	0.	0.	0.	0.	0.	0.	0.	0.
.062	0.85	-53.	0.	0.	0.	0.	0.	0.	0.	0.	0.	0.
.075	0.78	-45.	0.	0.	0.	0.	0.	0.	0.	0.	0.	0.
.087	0.73	-33.	0.	0.	0.	0.	0.	0.	0.	0.	0.	0.
.100	0.56	-34.	0.	0.	0.	0.	0.	0.	0.	0.	0.	0.
.112	0.13	-60.	0.	0.	0.	0.	0.	0.	0.	0.	0.	0.
.125	0.18	56.	0.	0.	0.	0.	0.	0.	0.	0.	0.	0.
.137	0.35	53.	0.	0.	0.	0.	0.	0.	0.	0.	0.	0.
.150	0.08	-38.	0.	0.	0.	0.	0.	0.	0.	0.	0.	0.
.162	0.20	-30.	0.	0.	0.	0.	0.	0.	0.	0.	0.	0.
.175	0.24	-15.	0.	0.	0.	0.	0.	0.	0.	0.	0.	0.
.187	0.35	-10.	0.	0.	0.	0.	0.	0.	0.	0.	0.	0.
.200	0.36	-37.	0.	0.	0.	0.	0.	0.	0.	0.	0.	0.
.212	0.55	-35.	0.	0.	0.	0.	0.	0.	0.	0.	0.	0.
.225	0.46	-11.	0.	0.	0.	0.	0.	0.	0.	0.	0.	0.
.237	0.37	14.	0.	0.	0.	0.	0.	0.	0.	0.	0.	0.
.250	0.48	-18.	0.	0.	0.	0.	0.	0.	0.	0.	0.	0.

0 0 1758.8

CASE 24-5 LITTLETON MASS 10/29/59 .02-.06CPS
DEC 189,0,0,189,20,5.,1,0,0,0,0,0
PG 52 1F CANTWELL H1 E2 ONLY

POWER DENSITY SPECTRA

FREQ	H1	H2	E1	E2
	MS GAMMAS		MS MV/KM	
.002	.197E 01	.	.	.295E-00
.005	.558E 00	.	.	.195E-00
.010	.153E-00	.	.	.215E-00
.015	.115E-00	.	.	.196E 01
.020	.155E-00	.	.	.560E 01
.025	.158E-00	.	.	.965E 01
.030	.150E-00	.	.	.124E 02
.035	.140E-00	.	.	.116E 02
.040	.111E-00	.	.	.822E 01
.045	.703E-01	.	.	.498E 01
.050	.323E-01	.	.	.331E 01
.055	.132E-01	.	.	.226E 01
.060	.657E-02	.	.	.114E 01
.065	.359E-02	.	.	.426E-00
.070	.327E-02	.	.	.180E-00
.075	.299E-02	.	.	.115E-00
.080	.236E-02	.	.	.526E-01
.085	.184E-02	.	.	.184E-01
.090	.149E-02	.	.	.994E-02
.095	.123E-02	.	.	.513E-03
.100	.107E-02	.	.	.147E-02

COHERENCY ANALYSIS

FREQ	(H1,E2)		(H1,E1)		(H1,H2)		(H2,E1)		(H2,E2)		(E1,E2)	
	AMP	PHASE	AMP	PHASE	AMP	PHASE	AMP	PHASE	AMP	PHASE	AMP	PHASE
.002	0.36	-17.	0.	0.	0.	0.	0.	0.	0.	0.	0.	0.
.005	0.61	-30.	0.	0.	0.	0.	0.	0.	0.	0.	0.	0.
.010	0.48	-36.	0.	0.	0.	0.	0.	0.	0.	0.	0.	0.
.015	0.21	78.	0.	0.	0.	0.	0.	0.	0.	0.	0.	0.
.020	0.13	41.	0.	0.	0.	0.	0.	0.	0.	0.	0.	0.
.025	0.25	-3.	0.	0.	0.	0.	0.	0.	0.	0.	0.	0.
.030	0.47	10.	0.	0.	0.	0.	0.	0.	0.	0.	0.	0.
.035	0.60	25.	0.	0.	0.	0.	0.	0.	0.	0.	0.	0.
.040	0.52	24.	0.	0.	0.	0.	0.	0.	0.	0.	0.	0.
.045	0.33	-5.	0.	0.	0.	0.	0.	0.	0.	0.	0.	0.
.050	0.20	7.	0.	0.	0.	0.	0.	0.	0.	0.	0.	0.
.055	0.24	45.	0.	0.	0.	0.	0.	0.	0.	0.	0.	0.
.060	0.25	18.	0.	0.	0.	0.	0.	0.	0.	0.	0.	0.
.065	0.34	34.	0.	0.	0.	0.	0.	0.	0.	0.	0.	0.
.070	0.20	78.	0.	0.	0.	0.	0.	0.	0.	0.	0.	0.
.075	0.35	25.	0.	0.	0.	0.	0.	0.	0.	0.	0.	0.
.080	0.32	-43.	0.	0.	0.	0.	0.	0.	0.	0.	0.	0.
.085	0.33	90.	0.	0.	0.	0.	0.	0.	0.	0.	0.	0.
.090	0.37	62.	0.	0.	0.	0.	0.	0.	0.	0.	0.	0.
.095	1.20	33.	0.	0.	0.	0.	0.	0.	0.	0.	0.	0.
.100	0.61	11.	0.	0.	0.	0.	0.	0.	0.	0.	0.	0.

0 0 1759.0

CASE 24-6 LITTLETON,MASS 10/29/59 .06-.2 CPS
DEC 185,0,0,185,20,2,,1,0,0,0,0,0
PG 52,1F CANTWELL H1 E2 ONLY

POWER DENSITY SPECTRA

FREQ	H1	H2	E1	E2
	MS GAMMAS		MS MV/KM	
.006	.550E-02	.	.	.603E-01
.012	.112E-02	.	.	.514E-01
.025	.537E-03	.	.	.834E-01
.037	.274E-03	.	.	.531E 00
.050	.155E-02	.	.	.411E 01
.062	.288E-02	.	.	.988E 01
.075	.206E-02	.	.	.134E 02
.087	.882E-03	.	.	.117E 02
.100	.570E-03	.	.	.644E 01
.112	.472E-03	.	.	.460E 01
.125	.352E-03	.	.	.518E 01
.137	.220E-03	.	.	.397E 01
.150	.150E-03	.	.	.230E 01
.162	.123E-03	.	.	.111E 01
.175	.725E-04	.	.	.783E 00
.187	.403E-04	.	.	.650E 00
.200	.320E-04	.	.	.468E-00
.212	.220E-04	.	.	.364E-00
.225	.119E-04	.	.	.212E-00
.237	.666E-05	.	.	.133E-00
.250	.475E-05	.	.	.126E-00

COHERENCY ANALYSIS

FREQ	(H1,E2)		(H1,E1)		(H1,H2)		(H2,E1)		(H2,E2)		(E1,E2)	
	AMP	PHASE	AMP	PHASE	AMP	PHASE	AMP	PHASE	AMP	PHASE	AMP	PHASE
.006	0.38	-70.	0.	0.	0.	0.	0.	0.	0.	0.	0.	0.
.012	0.18	-84.	0.	0.	0.	0.	0.	0.	0.	0.	0.	0.
.025	0.73	6.	0.	0.	0.	0.	0.	0.	0.	0.	0.	0.
.037	0.42	1.	0.	0.	0.	0.	0.	0.	0.	0.	0.	0.
.050	0.54	-46.	0.	0.	0.	0.	0.	0.	0.	0.	0.	0.
.062	0.59	-46.	0.	0.	0.	0.	0.	0.	0.	0.	0.	0.
.075	0.51	-39.	0.	0.	0.	0.	0.	0.	0.	0.	0.	0.
.087	0.44	-15.	0.	0.	0.	0.	0.	0.	0.	0.	0.	0.
.100	0.41	-16.	0.	0.	0.	0.	0.	0.	0.	0.	0.	0.
.112	0.30	-89.	0.	0.	0.	0.	0.	0.	0.	0.	0.	0.
.125	0.28	41.	0.	0.	0.	0.	0.	0.	0.	0.	0.	0.
.137	0.02	10.	0.	0.	0.	0.	0.	0.	0.	0.	0.	0.
.150	0.39	12.	0.	0.	0.	0.	0.	0.	0.	0.	0.	0.
.162	0.42	-1.	0.	0.	0.	0.	0.	0.	0.	0.	0.	0.
.175	0.38	-5.	0.	0.	0.	0.	0.	0.	0.	0.	0.	0.
.187	0.38	6.	0.	0.	0.	0.	0.	0.	0.	0.	0.	0.
.200	0.58	-3.	0.	0.	0.	0.	0.	0.	0.	0.	0.	0.
.212	0.77	-7.	0.	0.	0.	0.	0.	0.	0.	0.	0.	0.
.225	0.63	0.	0.	0.	0.	0.	0.	0.	0.	0.	0.	0.
.237	0.47	12.	0.	0.	0.	0.	0.	0.	0.	0.	0.	0.
.250	0.48	2.	0.	0.	0.	0.	0.	0.	0.	0.	0.	0.

0 0 1759.3

CASE 24-15 LITTLETON MASS 10/29/59 .06-.2 CPS
DEC 105,105,0,0,20,2.,0,0,1,0,0,0
PG 52 1F CANTWELL H1 H2 ONLY PARALLEL

POWER DENSITY SPECTRA

FREQ	H1	H2	E1	E2
	MS GAMMAS		MS MV/KM	
.006	.175E-01	.396E-02	.	.
.012	.522E-02	.975E-03	.	.
.025	.141E-02	.322E-03	.	.
.037	.208E-02	.211E-03	.	.
.050	.466E-02	.555E-03	.	.
.062	.579E-02	.843E-03	.	.
.075	.603E-02	.591E-03	.	.
.087	.592E-02	.254E-03	.	.
.100	.419E-02	.166E-03	.	.
.112	.318E-02	.164E-03	.	.
.125	.367E-02	.122E-03	.	.
.137	.276E-02	.642E-04	.	.
.150	.147E-02	.264E-04	.	.
.162	.120E-02	.130E-04	.	.
.175	.766E-03	.149E-04	.	.
.187	.308E-03	.186E-04	.	.
.200	.143E-03	.155E-04	.	.
.212	.455E-04	.758E-05	.	.
.225	.294E-04	.353E-05	.	.
.237	.324E-04	.325E-05	.	.
.250	.252E-04	.325E-05	.	.

COHERENCY ANALYSIS

FREQ	(H1,E2)		(H1,E1)		(H1,H2)		(H2,E1)		(H2,E2)		(E1,E2)	
	AMP	PHASE	AMP	PHASE	AMP	PHASE	AMP	PHASE	AMP	PHASE	AMP	PHASE
.006	0.	0.	0.	0.	1.00	1.	0.	0.	0.	0.	0.	0.
.012	0.	0.	0.	0.	0.90	4.	0.	0.	0.	0.	0.	0.
.025	0.	0.	0.	0.	0.90	2.	0.	0.	0.	0.	0.	0.
.037	0.	0.	0.	0.	0.51	-30.	0.	0.	0.	0.	0.	0.
.050	0.	0.	0.	0.	0.71	-72.	0.	0.	0.	0.	0.	0.
.062	0.	0.	0.	0.	0.48	-82.	0.	0.	0.	0.	0.	0.
.075	0.	0.	0.	0.	0.17	32.	0.	0.	0.	0.	0.	0.
.087	0.	0.	0.	0.	0.31	-46.	0.	0.	0.	0.	0.	0.
.100	0.	0.	0.	0.	0.39	-73.	0.	0.	0.	0.	0.	0.
.112	0.	0.	0.	0.	0.13	-22.	0.	0.	0.	0.	0.	0.
.125	0.	0.	0.	0.	0.23	77.	0.	0.	0.	0.	0.	0.
.137	0.	0.	0.	0.	0.20	-24.	0.	0.	0.	0.	0.	0.
.150	0.	0.	0.	0.	0.19	27.	0.	0.	0.	0.	0.	0.
.162	0.	0.	0.	0.	0.44	4.	0.	0.	0.	0.	0.	0.
.175	0.	0.	0.	0.	0.35	-1.	0.	0.	0.	0.	0.	0.
.187	0.	0.	0.	0.	0.15	-53.	0.	0.	0.	0.	0.	0.
.200	0.	0.	0.	0.	0.27	-87.	0.	0.	0.	0.	0.	0.
.212	0.	0.	0.	0.	0.35	49.	0.	0.	0.	0.	0.	0.
.225	0.	0.	0.	0.	0.74	1.	0.	0.	0.	0.	0.	0.
.237	0.	0.	0.	0.	0.71	26.	0.	0.	0.	0.	0.	0.
.250	0.	0.	0.	0.	0.67	48.	0.	0.	0.	0.	0.	0.

0 0 1759.4

CASE24-16 LITTLETON MASS 10/29/59 .06-.2 CPS
DEC 178,178,0,0,20,2,,0,0,1,0,0,0
PG52 1F CANTWELL H1 H2 ONLY PARALLEL
POWER DENSITY SPECTRA

FREQ	H1	H2	E1	E2
	MS GAMMAS		MS MV/KM	
.006	.717E-05	.127E-03	.	.
.012	.185E-02	.996E-04	.	.
.025	.692E-04	.160E-04	.	.
.037	.269E-02	.160E-03	.	.
.050	.903E-02	.539E-03	.	.
.062	.165E-01	.984E-03	.	.
.075	.191E-01	.115E-02	.	.
.087	.207E-01	.855E-03	.	.
.100	.205E-01	.484E-03	.	.
.112	.135E-01	.241E-03	.	.
.125	.664E-02	.105E-03	.	.
.137	.370E-02	.659E-04	.	.
.150	.199E-02	.378E-04	.	.
.162	.948E-03	.193E-04	.	.
.175	.604E-03	.127E-04	.	.
.187	.454E-03	.486E-05	.	.
.200	.185E-03	.222E-05	.	.
.212	.565E-04	.151E-05	.	.
.225	.429E-04	.119E-05	.	.
.237	.153E-04	.104E-05	.	.
.250	.482E-05	.107E-05	.	.

COHERENCY ANALYSIS

FREQ	(H1,E2)		(H1,E1)		(H1,H2)		(H2,E1)		(H2,E2)		(E1,E2)	
	AMP	PHASE	AMP	PHASE	AMP	PHASE	AMP	PHASE	AMP	PHASE	AMP	PHASE
.006	0.	0.	0.	0.	4.10	-79.	0.	0.	0.	0.	0.	0.
.012	0.	0.	0.	0.	0.50	-12.	0.	0.	0.	0.	0.	0.
.025	0.	0.	0.	0.	7.47	16.	0.	0.	0.	0.	0.	0.
.037	0.	0.	0.	0.	0.29	-6.	0.	0.	0.	0.	0.	0.
.050	0.	0.	0.	0.	0.41	63.	0.	0.	0.	0.	0.	0.
.062	0.	0.	0.	0.	0.25	-23.	0.	0.	0.	0.	0.	0.
.075	0.	0.	0.	0.	0.29	17.	0.	0.	0.	0.	0.	0.
.087	0.	0.	0.	0.	0.03	77.	0.	0.	0.	0.	0.	0.
.100	0.	0.	0.	0.	0.35	-0.	0.	0.	0.	0.	0.	0.
.112	0.	0.	0.	0.	0.52	-28.	0.	0.	0.	0.	0.	0.
.125	0.	0.	0.	0.	0.38	-63.	0.	0.	0.	0.	0.	0.
.137	0.	0.	0.	0.	0.41	68.	0.	0.	0.	0.	0.	0.
.150	0.	0.	0.	0.	0.46	69.	0.	0.	0.	0.	0.	0.
.162	0.	0.	0.	0.	0.23	56.	0.	0.	0.	0.	0.	0.
.175	0.	0.	0.	0.	0.05	-6.	0.	0.	0.	0.	0.	0.
.187	0.	0.	0.	0.	0.12	56.	0.	0.	0.	0.	0.	0.
.200	0.	0.	0.	0.	0.23	-5.	0.	0.	0.	0.	0.	0.
.212	0.	0.	0.	0.	0.36	-79.	0.	0.	0.	0.	0.	0.
.225	0.	0.	0.	0.	0.61	-63.	0.	0.	0.	0.	0.	0.
.237	0.	0.	0.	0.	0.26	-23.	0.	0.	0.	0.	0.	0.
.250	0.	0.	0.	0.	0.78	-88.	0.	0.	0.	0.	0.	0.

0 0 1759.7

CASE 24-11 LITTLETON MASS 10/29/59 .02-.06 CPS
DEC 96,96,0,0,20,5,,0,0,1,0,0,0
PG 52 1F CANTWELL H1 H2 ONLY PARALLEL

POWER DENSITY SPECTRA

FREQ	H1	H2	E1	E2
	MS GAMMAS		MS MV/KM	
.002	.285E-01	.478E-01	.	.
.005	.204E-01	.196E-01	.	.
.010	.238E-01	.574E-02	.	.
.015	.532E-01	.127E-01	.	.
.020	.769E-01	.144E-01	.	.
.025	.572E-01	.239E-01	.	.
.030	.452E-01	.343E-01	.	.
.035	.526E-01	.200E-01	.	.
.040	.416E-01	.505E-02	.	.
.045	.204E-01	.261E-02	.	.
.050	.802E-02	.116E-02	.	.
.055	.404E-02	.227E-03	.	.
.060	.219E-02	.173E-03	.	.
.065	.960E-03	.761E-04	.	.
.070	.840E-03	.343E-04	.	.
.075	.512E-03	.285E-04	.	.
.080	.128E-03	.396E-04	.	.
.085	.910E-05	.312E-04	.	.
.090	.441E-06	.324E-04	.	.
.095	.154E-05	.355E-04	.	.
.100	.302E-05	.368E-04	.	.

COHERENCY ANALYSIS

FREQ	(H1,E2)		(H1,E1)		(H1,H2)		(H2,E1)		(H2,E2)		(E1,E2)	
	AMP	PHASE	AMP	PHASE	AMP	PHASE	AMP	PHASE	AMP	PHASE	AMP	PHASE
.002	0.	0.	0.	0.	2.09	-28.	0.	0.	0.	0.	0.	0.
.005	0.	0.	0.	0.	0.72	26.	0.	0.	0.	0.	0.	0.
.010	0.	0.	0.	0.	1.16	-14.	0.	0.	0.	0.	0.	0.
.015	0.	0.	0.	0.	0.45	10.	0.	0.	0.	0.	0.	0.
.020	0.	0.	0.	0.	0.38	65.	0.	0.	0.	0.	0.	0.
.025	0.	0.	0.	0.	0.23	-15.	0.	0.	0.	0.	0.	0.
.030	0.	0.	0.	0.	0.43	15.	0.	0.	0.	0.	0.	0.
.035	0.	0.	0.	0.	0.24	28.	0.	0.	0.	0.	0.	0.
.040	0.	0.	0.	0.	0.33	-87.	0.	0.	0.	0.	0.	0.
.045	0.	0.	0.	0.	0.40	80.	0.	0.	0.	0.	0.	0.
.050	0.	0.	0.	0.	0.17	79.	0.	0.	0.	0.	0.	0.
.055	0.	0.	0.	0.	0.45	-60.	0.	0.	0.	0.	0.	0.
.060	0.	0.	0.	0.	0.42	76.	0.	0.	0.	0.	0.	0.
.065	0.	0.	0.	0.	0.20	-34.	0.	0.	0.	0.	0.	0.
.070	0.	0.	0.	0.	0.65	86.	0.	0.	0.	0.	0.	0.
.075	0.	0.	0.	0.	0.16	-74.	0.	0.	0.	0.	0.	0.
.080	0.	0.	0.	0.	0.25	-21.	0.	0.	0.	0.	0.	0.
.085	0.	0.	0.	0.	2.29	9.	0.	0.	0.	0.	0.	0.
.090	0.	0.	0.	0.	3.63	1.	0.	0.	0.	0.	0.	0.
.095	0.	0.	0.	0.	1.73	13.	0.	0.	0.	0.	0.	0.
.100	0.	0.	0.	0.	2.14	24.	0.	0.	0.	0.	0.	0.

0 0 1759.8

CASE 24-19 LITTLETON MASS 10/29/59 .02-.06 CPS
DEC 186,186,0,0,20,5,,0,0,1,0,0,0
PG 52 1F CANTWELL H1 H2 PARALLEL ONLY

POWER DENSITY SPECTRA

FREQ	H1	H2	E1	E2
	MS GAMMAS		MS MV/KM	
.002	.518E 00	.103E-00	.	.
.005	.165E-00	.320E-01	.	.
.010	.326E-01	.798E-02	.	.
.015	.932E-01	.477E-01	.	.
.020	.229E-00	.773E-01	.	.
.025	.395E-00	.131E-00	.	.
.030	.513E 00	.173E-00	.	.
.035	.536E 00	.169E-00	.	.
.040	.392E-00	.125E-00	.	.
.045	.158E-00	.539E-01	.	.
.050	.356E-01	.106E-01	.	.
.055	.191E-01	.209E-02	.	.
.060	.167E-01	.943E-03	.	.
.065	.820E-02	.769E-03	.	.
.070	.170E-02	.351E-03	.	.
.075	.640E-03	.748E-04	.	.
.080	.453E-03	.668E-05	.	.
.085	.189E-03	.211E-04	.	.
.090	.257E-04	.218E-04	.	.
.095	.189E-05	.209E-04	.	.
.100	.867E-05	.213E-04	.	.

COHERENCY ANALYSIS

FREQ	(H1,E2)		(H1,E1)		(H1,H2)		(H2,E1)		(H2,E2)		(E1,E2)	
	AMP	PHASE	AMP	PHASE	AMP	PHASE	AMP	PHASE	AMP	PHASE	AMP	PHASE
.002	0.	0.	0.	0.	0.84	-2.	0.	0.	0.	0.	0.	0.
.005	0.	0.	0.	0.	0.53	24.	0.	0.	0.	0.	0.	0.
.010	0.	0.	0.	0.	0.73	-3.	0.	0.	0.	0.	0.	0.
.015	0.	0.	0.	0.	0.43	15.	0.	0.	0.	0.	0.	0.
.020	0.	0.	0.	0.	0.36	-1.	0.	0.	0.	0.	0.	0.
.025	0.	0.	0.	0.	0.51	-8.	0.	0.	0.	0.	0.	0.
.030	0.	0.	0.	0.	0.60	4.	0.	0.	0.	0.	0.	0.
.035	0.	0.	0.	0.	0.71	10.	0.	0.	0.	0.	0.	0.
.040	0.	0.	0.	0.	0.81	4.	0.	0.	0.	0.	0.	0.
.045	0.	0.	0.	0.	0.84	-5.	0.	0.	0.	0.	0.	0.
.050	0.	0.	0.	0.	0.61	-15.	0.	0.	0.	0.	0.	0.
.055	0.	0.	0.	0.	0.35	20.	0.	0.	0.	0.	0.	0.
.060	0.	0.	0.	0.	0.54	78.	0.	0.	0.	0.	0.	0.
.065	0.	0.	0.	0.	0.51	-84.	0.	0.	0.	0.	0.	0.
.070	0.	0.	0.	0.	0.34	-24.	0.	0.	0.	0.	0.	0.
.075	0.	0.	0.	0.	1.44	28.	0.	0.	0.	0.	0.	0.
.080	0.	0.	0.	0.	4.27	18.	0.	0.	0.	0.	0.	0.
.085	0.	0.	0.	0.	2.38	8.	0.	0.	0.	0.	0.	0.
.090	0.	0.	0.	0.	4.76	7.	0.	0.	0.	0.	0.	0.
.095	0.	0.	0.	0.	4.87	5.	0.	0.	0.	0.	0.	0.
.100	0.	0.	0.	0.	6.07	13.	0.	0.	0.	0.	0.	0.

0 0 1800.1

CASE 25-3 LITTLETON MASS 11/15/59 .02-.06 CPS
DEC 147,147,0,0,20,5.,0,0,1,0,0,0
PG 64 1F CANTWELL H1 H2 ONLY

POWER DENSITY SPECTRA

FREQ	H1	H2	E1	E2
	MS GAMMAS		MS MV/KM	
.002	.831E-01	.136E-01	.	.
.005	.414E-01	.685E-02	.	.
.010	.523E-02	.287E-02	.	.
.015	.422E-01	.288E-01	.	.
.020	.109E-00	.441E-01	.	.
.025	.145E-00	.408E-01	.	.
.030	.146E-00	.397E-01	.	.
.035	.123E-00	.451E-01	.	.
.040	.103E-00	.543E-01	.	.
.045	.718E-01	.441E-01	.	.
.050	.265E-01	.176E-01	.	.
.055	.404E-02	.322E-02	.	.
.060	.194E-02	.637E-03	.	.
.065	.117E-02	.162E-03	.	.
.070	.327E-03	.597E-04	.	.
.075	.820E-04	.919E-05	.	.
.080	.926E-04	.591E-05	.	.
.085	.541E-04	.140E-04	.	.
.090	.202E-04	.795E-05	.	.
.095	.264E-04	.129E-04	.	.
.100	.264E-04	.124E-04	.	.

COHERENCY ANALYSIS

FREQ	(H1,E2)		(H1,E1)		(H1,H2)		(H2,E1)		(H2,E2)		(E1,E2)	
	AMP	PHASE	AMP	PHASE	AMP	PHASE	AMP	PHASE	AMP	PHASE	AMP	PHASE
.002	0.	0.	0.	0.	1.34	81.	0.	0.	0.	0.	0.	0.
.005	0.	0.	0.	0.	0.93	-4.	0.	0.	0.	0.	0.	0.
.010	0.	0.	0.	0.	1.70	-80.	0.	0.	0.	0.	0.	0.
.015	0.	0.	0.	0.	0.71	-8.	0.	0.	0.	0.	0.	0.
.020	0.	0.	0.	0.	0.69	-2.	0.	0.	0.	0.	0.	0.
.025	0.	0.	0.	0.	0.74	20.	0.	0.	0.	0.	0.	0.
.030	0.	0.	0.	0.	0.83	28.	0.	0.	0.	0.	0.	0.
.035	0.	0.	0.	0.	0.78	19.	0.	0.	0.	0.	0.	0.
.040	0.	0.	0.	0.	0.82	7.	0.	0.	0.	0.	0.	0.
.045	0.	0.	0.	0.	0.86	5.	0.	0.	0.	0.	0.	0.
.050	0.	0.	0.	0.	0.73	3.	0.	0.	0.	0.	0.	0.
.055	0.	0.	0.	0.	0.29	-18.	0.	0.	0.	0.	0.	0.
.060	0.	0.	0.	0.	0.41	11.	0.	0.	0.	0.	0.	0.
.065	0.	0.	0.	0.	0.52	-27.	0.	0.	0.	0.	0.	0.
.070	0.	0.	0.	0.	0.47	-60.	0.	0.	0.	0.	0.	0.
.075	0.	0.	0.	0.	0.92	-16.	0.	0.	0.	0.	0.	0.
.080	0.	0.	0.	0.	1.55	-20.	0.	0.	0.	0.	0.	0.
.085	0.	0.	0.	0.	1.75	0.	0.	0.	0.	0.	0.	0.
.090	0.	0.	0.	0.	3.27	5.	0.	0.	0.	0.	0.	0.
.095	0.	0.	0.	0.	1.53	10.	0.	0.	0.	0.	0.	0.
.100	0.	0.	0.	0.	1.10	10.	0.	0.	0.	0.	0.	0.

0 0 1800.3

CASE 25-11 LITTLETON MASS 11/14/59 .06-.2 CPS
DEC 143,143,0,0,20,2.,0,0,1,0,0,0
PG 62 1F CANTWELL H1 H2 ONLY

POWER DENSITY SPECTRA

FREQ	H1	H2	E1	E2
	MS GAMMAS		MS MV/KM	
.006	.544E-01	.177E-02	.	.
.012	.139E-01	.348E-04	.	.
.025	.537E-02	.227E-03	.	.
.037	.268E-02	.437E-05	.	.
.050	.633E-02	.112E-02	.	.
.062	.100E-01	.233E-02	.	.
.075	.693E-02	.186E-02	.	.
.087	.387E-02	.958E-03	.	.
.100	.267E-02	.602E-03	.	.
.112	.149E-02	.605E-03	.	.
.125	.127E-02	.647E-03	.	.
.137	.981E-03	.533E-03	.	.
.150	.413E-03	.296E-03	.	.
.162	.354E-03	.128E-03	.	.
.175	.377E-03	.833E-04	.	.
.187	.229E-03	.541E-04	.	.
.200	.155E-03	.274E-04	.	.
.212	.139E-03	.134E-04	.	.
.225	.973E-04	.538E-05	.	.
.237	.662E-04	.318E-05	.	.
.250	.582E-04	.281E-05	.	.

COHERENCY ANALYSIS

FREQ	(H1,E2)		(H1,E1)		(H1,H2)		(H2,E1)		(H2,E2)		(E1,E2)	
	AMP	PHASE	AMP	PHASE	AMP	PHASE	AMP	PHASE	AMP	PHASE	AMP	PHASE
.006	0.	0.	0.	0.	0.45	33.	0.	0.	0.	0.	0.	0.
.012	0.	0.	0.	0.	0.49	-7.	0.	0.	0.	0.	0.	0.
.025	0.	0.	0.	0.	0.49	-33.	0.	0.	0.	0.	0.	0.
.037	0.	0.	0.	0.	0.97	89.	0.	0.	0.	0.	0.	0.
.050	0.	0.	0.	0.	0.88	13.	0.	0.	0.	0.	0.	0.
.062	0.	0.	0.	0.	0.91	7.	0.	0.	0.	0.	0.	0.
.075	0.	0.	0.	0.	0.85	-1.	0.	0.	0.	0.	0.	0.
.087	0.	0.	0.	0.	0.76	-11.	0.	0.	0.	0.	0.	0.
.100	0.	0.	0.	0.	0.62	-13.	0.	0.	0.	0.	0.	0.
.112	0.	0.	0.	0.	0.54	6.	0.	0.	0.	0.	0.	0.
.125	0.	0.	0.	0.	0.77	19.	0.	0.	0.	0.	0.	0.
.137	0.	0.	0.	0.	0.80	13.	0.	0.	0.	0.	0.	0.
.150	0.	0.	0.	0.	0.66	-2.	0.	0.	0.	0.	0.	0.
.162	0.	0.	0.	0.	0.52	-20.	0.	0.	0.	0.	0.	0.
.175	0.	0.	0.	0.	0.52	-18.	0.	0.	0.	0.	0.	0.
.187	0.	0.	0.	0.	0.47	-19.	0.	0.	0.	0.	0.	0.
.200	0.	0.	0.	0.	0.52	-10.	0.	0.	0.	0.	0.	0.
.212	0.	0.	0.	0.	0.57	7.	0.	0.	0.	0.	0.	0.
.225	0.	0.	0.	0.	0.60	28.	0.	0.	0.	0.	0.	0.
.237	0.	0.	0.	0.	0.65	38.	0.	0.	0.	0.	0.	0.
.250	0.	0.	0.	0.	0.69	34.	0.	0.	0.	0.	0.	0.

0 0 1800.5

CASE 25-14 LITTLETON MASS 11/14/59 .06-.2 CPS
DEC 151,151,0,0,20,2.,0,0,1,0,0,0
PG 62 1F CANTWELL H1 H2 ONLY

POWER DENSITY SPECTRA

FREQ	H1	H2	E1	E2
	MS GAMMAS		MS MV/KM	
.006	.500E-02	.125E-03	.	.
.012	.223E-02	.256E-03	.	.
.025	.403E-03	.113E-04	.	.
.037	.301E-02	.669E-03	.	.
.050	.793E-02	.171E-02	.	.
.062	.758E-02	.151E-02	.	.
.075	.348E-02	.634E-03	.	.
.087	.153E-02	.252E-03	.	.
.100	.125E-02	.220E-03	.	.
.112	.890E-03	.160E-03	.	.
.125	.619E-03	.844E-04	.	.
.137	.412E-03	.465E-04	.	.
.150	.232E-03	.224E-04	.	.
.162	.163E-03	.123E-04	.	.
.175	.103E-03	.108E-04	.	.
.187	.533E-04	.952E-05	.	.
.200	.301E-04	.776E-05	.	.
.212	.160E-04	.379E-05	.	.
.225	.122E-04	.167E-05	.	.
.237	.114E-04	.118E-05	.	.
.250	.108E-04	.918E-06	.	.

COHERENCY ANALYSIS

FREQ	(H1,E2)		(H1,E1)		(H1,H2)		(H2,E1)		(H2,E2)		(E1,E2)	
	AMP	PHASE	AMP	PHASE	AMP	PHASE	AMP	PHASE	AMP	PHASE	AMP	PHASE
.006	0.	0.	0.	0.	0.23	9.	0.	0.	0.	0.	0.	0.
.012	0.	0.	0.	0.	0.63	18.	0.	0.	0.	0.	0.	0.
.025	0.	0.	0.	0.	0.64	-5.	0.	0.	0.	0.	0.	0.
.037	0.	0.	0.	0.	0.95	11.	0.	0.	0.	0.	0.	0.
.050	0.	0.	0.	0.	0.97	9.	0.	0.	0.	0.	0.	0.
.062	0.	0.	0.	0.	0.96	5.	0.	0.	0.	0.	0.	0.
.075	0.	0.	0.	0.	0.94	-2.	0.	0.	0.	0.	0.	0.
.087	0.	0.	0.	0.	0.87	1.	0.	0.	0.	0.	0.	0.
.100	0.	0.	0.	0.	0.86	14.	0.	0.	0.	0.	0.	0.
.112	0.	0.	0.	0.	0.82	10.	0.	0.	0.	0.	0.	0.
.125	0.	0.	0.	0.	0.79	2.	0.	0.	0.	0.	0.	0.
.137	0.	0.	0.	0.	0.86	4.	0.	0.	0.	0.	0.	0.
.150	0.	0.	0.	0.	0.87	14.	0.	0.	0.	0.	0.	0.
.162	0.	0.	0.	0.	0.84	24.	0.	0.	0.	0.	0.	0.
.175	0.	0.	0.	0.	0.74	14.	0.	0.	0.	0.	0.	0.
.187	0.	0.	0.	0.	0.71	-10.	0.	0.	0.	0.	0.	0.
.200	0.	0.	0.	0.	0.69	6.	0.	0.	0.	0.	0.	0.
.212	0.	0.	0.	0.	0.71	38.	0.	0.	0.	0.	0.	0.
.225	0.	0.	0.	0.	0.66	12.	0.	0.	0.	0.	0.	0.
.237	0.	0.	0.	0.	0.62	-11.	0.	0.	0.	0.	0.	0.
.250	0.	0.	0.	0.	0.42	-13.	0.	0.	0.	0.	0.	0.

0 0 1800.7

CASE 25-15 LITTLETON MASS 11/14/59 .02-.06 CPS
DEC 103,103,0,0,20,5.,0,0,1,0,0,0
PG 62-1F CANTWELL H1 H2 ONLY

POWER DENSITY SPECTRA

FREQ	H1	H2	E1	E2
	MS GAMMAS		MS MV/KM	
.002	.303E-00	.293E-01	.	.
.005	.426E-01	.167E-02	.	.
.010	.223E-01	.357E-02	.	.
.015	.169E-01	.577E-02	.	.
.020	.348E-01	.112E-01	.	.
.025	.707E-01	.205E-01	.	.
.030	.161E-00	.471E-01	.	.
.035	.250E-00	.707E-01	.	.
.040	.241E-00	.644E-01	.	.
.045	.168E-00	.458E-01	.	.
.050	.823E-01	.252E-01	.	.
.055	.224E-01	.781E-02	.	.
.060	.400E-02	.134E-02	.	.
.065	.106E-02	.257E-03	.	.
.070	.866E-03	.106E-03	.	.
.075	.600E-03	.323E-04	.	.
.080	.916E-04	.542E-04	.	.
.085	.806E-04	.346E-04	.	.
.090	.122E-03	.143E-04	.	.
.095	.150E-03	.300E-07	.	.
.100	.139E-03	.502E-06	.	.

COHERENCY ANALYSIS

FREQ	(H1,E2)		(H1,E1)		(H1,H2)		(H2,E1)		(H2,E2)		(E1,E2)	
	AMP	PHASE	AMP	PHASE	AMP	PHASE	AMP	PHASE	AMP	PHASE	AMP	PHASE
.002	0.	0.	0.	0.	0.74	-21.	0.	0.	0.	0.	0.	0.
.005	0.	0.	0.	0.	1.15	75.	0.	0.	0.	0.	0.	0.
.010	0.	0.	0.	0.	0.61	1.	0.	0.	0.	0.	0.	0.
.015	0.	0.	0.	0.	0.78	30.	0.	0.	0.	0.	0.	0.
.020	0.	0.	0.	0.	0.73	24.	0.	0.	0.	0.	0.	0.
.025	0.	0.	0.	0.	0.83	10.	0.	0.	0.	0.	0.	0.
.030	0.	0.	0.	0.	0.96	5.	0.	0.	0.	0.	0.	0.
.035	0.	0.	0.	0.	0.99	6.	0.	0.	0.	0.	0.	0.
.040	0.	0.	0.	0.	0.99	8.	0.	0.	0.	0.	0.	0.
.045	0.	0.	0.	0.	0.98	9.	0.	0.	0.	0.	0.	0.
.050	0.	0.	0.	0.	0.98	6.	0.	0.	0.	0.	0.	0.
.055	0.	0.	0.	0.	0.96	6.	0.	0.	0.	0.	0.	0.
.060	0.	0.	0.	0.	0.80	13.	0.	0.	0.	0.	0.	0.
.065	0.	0.	0.	0.	0.41	-1.	0.	0.	0.	0.	0.	0.
.070	0.	0.	0.	0.	0.44	-12.	0.	0.	0.	0.	0.	0.
.075	0.	0.	0.	0.	0.32	-26.	0.	0.	0.	0.	0.	0.
.080	0.	0.	0.	0.	1.63	5.	0.	0.	0.	0.	0.	0.
.085	0.	0.	0.	0.	1.26	14.	0.	0.	0.	0.	0.	0.
.090	0.	0.	0.	0.	0.72	4.	0.	0.	0.	0.	0.	0.
.095	0.	0.	0.	0.	4.11	-47.	0.	0.	0.	0.	0.	0.
.100	0.	0.	0.	0.	0.81	-52.	0.	0.	0.	0.	0.	0.

0 0 1800.9

CASE 26-1 LITTLETON MASS 12/1/59 .02-.06 CPS
DEC 107,0,0,107,20,5.,1,0,0,0,0,0
PG 67 1F CANTWELL H1 E2 ONLY

POWER DENSITY SPECTRA

FREQ	H1	H2	E1	E2
	MS GAMMAS		MS MV/KM	
.002	.826E 00	.	.	.170E 01
.005	.152E-00	.	.	.106E 01
.010	.114E-00	.	.	.802E 01
.015	.182E-00	.	.	.257E 02
.020	.183E-00	.	.	.473E 02
.025	.147E-00	.	.	.626E 02
.030	.814E-01	.	.	.512E 02
.035	.324E-01	.	.	.382E 02
.040	.333E-01	.	.	.544E 02
.045	.368E-01	.	.	.584E 02
.050	.260E-01	.	.	.375E 02
.055	.212E-01	.	.	.349E 02
.060	.159E-01	.	.	.315E 02
.065	.604E-02	.	.	.999E 01
.070	.174E-02	.	.	.129E 01
.075	.119E-02	.	.	.135E 01
.080	.616E-03	.	.	.362E-00
.085	.219E-03	.	.	.292E-00
.090	.833E-04	.	.	.193E-00
.095	.792E-04	.	.	.416E-02
.100	.512E-04	.	.	.262E-00

COHERENCY ANALYSIS

FREQ	(H1,E2)		(H1,E1)		(H1,H2)		(H2,E1)		(H2,E2)		(E1,E2)	
	AMP	PHASE	AMP	PHASE	AMP	PHASE	AMP	PHASE	AMP	PHASE	AMP	PHASE
.002	0.73	-84.	0.	0.	0.	0.	0.	0.	0.	0.	0.	0.
.005	0.57	46.	0.	0.	0.	0.	0.	0.	0.	0.	0.	0.
.010	0.65	-69.	0.	0.	0.	0.	0.	0.	0.	0.	0.	0.
.015	0.77	-73.	0.	0.	0.	0.	0.	0.	0.	0.	0.	0.
.020	0.61	-83.	0.	0.	0.	0.	0.	0.	0.	0.	0.	0.
.025	0.65	81.	0.	0.	0.	0.	0.	0.	0.	0.	0.	0.
.030	0.67	83.	0.	0.	0.	0.	0.	0.	0.	0.	0.	0.
.035	0.51	-57.	0.	0.	0.	0.	0.	0.	0.	0.	0.	0.
.040	0.76	-42.	0.	0.	0.	0.	0.	0.	0.	0.	0.	0.
.045	0.82	-45.	0.	0.	0.	0.	0.	0.	0.	0.	0.	0.
.050	0.75	-49.	0.	0.	0.	0.	0.	0.	0.	0.	0.	0.
.055	0.82	-47.	0.	0.	0.	0.	0.	0.	0.	0.	0.	0.
.060	0.91	-44.	0.	0.	0.	0.	0.	0.	0.	0.	0.	0.
.065	0.95	-48.	0.	0.	0.	0.	0.	0.	0.	0.	0.	0.
.070	0.93	-52.	0.	0.	0.	0.	0.	0.	0.	0.	0.	0.
.075	0.69	-20.	0.	0.	0.	0.	0.	0.	0.	0.	0.	0.
.080	0.79	-7.	0.	0.	0.	0.	0.	0.	0.	0.	0.	0.
.085	0.60	-46.	0.	0.	0.	0.	0.	0.	0.	0.	0.	0.
.090	0.79	47.	0.	0.	0.	0.	0.	0.	0.	0.	0.	0.
.095	4.70	49.	0.	0.	0.	0.	0.	0.	0.	0.	0.	0.
.100	1.86	-87.	0.	0.	0.	0.	0.	0.	0.	0.	0.	0.

0 0 1801.1

CASE 26-2 LITTLETON MASS 12/1/59 .2-.6 CPS
DEC 154,0,0,154,20,,5,1,0,0,0,0,0
PG 67 1F CANTWELL H1 E2 ONLY

POWER DENSITY SPECTRA

FREQ	H1	H2	E1	E2
	MS GAMMAS		MS MV/KM	
.025	.290E-02	.	.	.790E 00
.050	.466E-03	.	.	.422E-00
.100	.482E-04	.	.	.873E-01
.150	.316E-04	.	.	.352E-00
.200	.522E-04	.	.	.762E 00
.250	.623E-04	.	.	.953E 00
.300	.450E-04	.	.	.923E 00
.350	.311E-04	.	.	.768E 00
.400	.238E-04	.	.	.564E 00
.450	.138E-04	.	.	.361E-00
.500	.936E-05	.	.	.150E-00
.550	.807E-05	.	.	.723E-01
.600	.568E-05	.	.	.947E-01
.650	.365E-05	.	.	.657E-01
.700	.238E-05	.	.	.322E-01
.750	.173E-05	.	.	.256E-01
.800	.104E-05	.	.	.183E-01
.850	.368E-06	.	.	.105E-01
.900	.101E-06	.	.	.403E-02
.950	.103E-06	.	.	.215E-02
.000	.121E-06	.	.	.376E-02

COHERENCY ANALYSIS

FREQ	(H1,E2)		(H1,E1)		(H1,H2)		(H2,E1)		(H2,E2)		(E1,E2)	
	AMP	PHASE	AMP	PHASE	AMP	PHASE	AMP	PHASE	AMP	PHASE	AMP	PHASE
.025	0.86	1.	0.	0.	0.	0.	0.	0.	0.	0.	0.	0.
.050	0.78	1.	0.	0.	0.	0.	0.	0.	0.	0.	0.	0.
.100	0.23	-53.	0.	0.	0.	0.	0.	0.	0.	0.	0.	0.
.150	0.37	62.	0.	0.	0.	0.	0.	0.	0.	0.	0.	0.
.200	0.55	80.	0.	0.	0.	0.	0.	0.	0.	0.	0.	0.
.250	0.50	-83.	0.	0.	0.	0.	0.	0.	0.	0.	0.	0.
.300	0.33	-53.	0.	0.	0.	0.	0.	0.	0.	0.	0.	0.
.350	0.26	-67.	0.	0.	0.	0.	0.	0.	0.	0.	0.	0.
.400	0.36	62.	0.	0.	0.	0.	0.	0.	0.	0.	0.	0.
.450	0.27	53.	0.	0.	0.	0.	0.	0.	0.	0.	0.	0.
.500	0.14	-21.	0.	0.	0.	0.	0.	0.	0.	0.	0.	0.
.550	0.15	-0.	0.	0.	0.	0.	0.	0.	0.	0.	0.	0.
.600	0.35	85.	0.	0.	0.	0.	0.	0.	0.	0.	0.	0.
.650	0.46	85.	0.	0.	0.	0.	0.	0.	0.	0.	0.	0.
.700	0.34	-43.	0.	0.	0.	0.	0.	0.	0.	0.	0.	0.
.750	0.55	-18.	0.	0.	0.	0.	0.	0.	0.	0.	0.	0.
.800	0.48	-7.	0.	0.	0.	0.	0.	0.	0.	0.	0.	0.
.850	0.53	50.	0.	0.	0.	0.	0.	0.	0.	0.	0.	0.
.900	0.92	61.	0.	0.	0.	0.	0.	0.	0.	0.	0.	0.
.950	0.37	12.	0.	0.	0.	0.	0.	0.	0.	0.	0.	0.
.000	0.44	50.	0.	0.	0.	0.	0.	0.	0.	0.	0.	0.

0 0 1801.3

CASE 26-3 LITTLETON MASS 12/1/59 .08-.2 CPS
DEC 175,0,0,175,20,1.,1,0,0,0,0,0
PG 67 1F CANTWELL H1 E2 ONLY

POWER DENSITY SPECTRA

FREQ	H1	H2	E1	E2
	MS GAMMAS		MS MV/KM	
.012	.614E-01	.	.	.266E 01
.025	.917E-02	.	.	.159E 01
.050	.114E-02	.	.	.104E 01
.075	.889E-03	.	.	.230E 01
.100	.558E-03	.	.	.302E 01
.125	.327E-03	.	.	.250E 01
.150	.234E-03	.	.	.161E 01
.175	.147E-03	.	.	.120E 01
.200	.778E-04	.	.	.105E 01
.225	.322E-04	.	.	.560E 00
.250	.966E-05	.	.	.143E-00
.275	.544E-05	.	.	.678E-01
.300	.198E-05	.	.	.249E-01
.325	.595E-06	.	.	.717E-03
.350	.580E-06	.	.	.171E-02
.375	.200E-06	.	.	.321E-03
.400	.945E-08	.	.	.301E-02
.425	.341E-07	.	.	.290E-02
.450	.260E-07	.	.	.114E-02
.475	.414E-07	.	.	.180E-02
.500	.394E-07	.	.	.278E-02

COHERENCY ANALYSIS

FREQ	(H1,E2)		(H1,E1)		(H1,H2)		(H2,E1)		(H2,E2)		(E1,E2)	
	AMP	PHASE	AMP	PHASE	AMP	PHASE	AMP	PHASE	AMP	PHASE	AMP	PHASE
.012	1.00	2.	0.	0.	0.	0.	0.	0.	0.	0.	0.	0.
.025	0.96	-0.	0.	0.	0.	0.	0.	0.	0.	0.	0.	0.
.050	0.44	-27.	0.	0.	0.	0.	0.	0.	0.	0.	0.	0.
.075	0.14	-53.	0.	0.	0.	0.	0.	0.	0.	0.	0.	0.
.100	0.21	-72.	0.	0.	0.	0.	0.	0.	0.	0.	0.	0.
.125	0.54	-68.	0.	0.	0.	0.	0.	0.	0.	0.	0.	0.
.150	0.68	-63.	0.	0.	0.	0.	0.	0.	0.	0.	0.	0.
.175	0.54	-57.	0.	0.	0.	0.	0.	0.	0.	0.	0.	0.
.200	0.49	-70.	0.	0.	0.	0.	0.	0.	0.	0.	0.	0.
.225	0.51	-76.	0.	0.	0.	0.	0.	0.	0.	0.	0.	0.
.250	0.38	-36.	0.	0.	0.	0.	0.	0.	0.	0.	0.	0.
.275	0.37	-35.	0.	0.	0.	0.	0.	0.	0.	0.	0.	0.
.300	0.41	-55.	0.	0.	0.	0.	0.	0.	0.	0.	0.	0.
.325	0.43	-90.	0.	0.	0.	0.	0.	0.	0.	0.	0.	0.
.350	1.26	-25.	0.	0.	0.	0.	0.	0.	0.	0.	0.	0.
.375	2.44	-47.	0.	0.	0.	0.	0.	0.	0.	0.	0.	0.
.400	0.99	-61.	0.	0.	0.	0.	0.	0.	0.	0.	0.	0.
.425	0.45	14.	0.	0.	0.	0.	0.	0.	0.	0.	0.	0.
.450	1.04	-9.	0.	0.	0.	0.	0.	0.	0.	0.	0.	0.
.475	0.50	86.	0.	0.	0.	0.	0.	0.	0.	0.	0.	0.
.500	1.04	77.	0.	0.	0.	0.	0.	0.	0.	0.	0.	0.

0 0 1801.5

CASE 26-4 LITTLETON MASS 12/1/59 .06-.08 CPS
DEC 149,0,0,149,20,2.,1,0,0,0,0,0
PG 67 1F CANTWELL H1 E2 ONLY

POWER DENSITY SPECTRA

FREQ	H1	H2	E1	E2
	MS GAMMAS		MS MV/KM	
.006	.550E-02	.	.	.775E-01
.012	.244E-03	.	.	.404E-01
.025	.284E-02	.	.	.851E 00
.037	.463E-02	.	.	.366E 01
.050	.334E-02	.	.	.527E 01
.062	.174E-02	.	.	.498E 01
.075	.773E-03	.	.	.427E 01
.087	.176E-03	.	.	.292E 01
.100	.517E-04	.	.	.141E 01
.112	.395E-04	.	.	.323E-00
.125	.941E-05	.	.	.395E-01
.137	.338E-05	.	.	.269E-01
.150	.215E-05	.	.	.201E-02
.162	.215E-05	.	.	.939E-02
.175	.134E-05	.	.	.130E-02
.187	.339E-06	.	.	.429E-03
.200	.182E-06	.	.	.709E-02
.212	.492E-07	.	.	.690E-02
.225	.278E-06	.	.	.745E-02
.237	.359E-06	.	.	.548E-02
.250	.289E-06	.	.	.734E-02

COHERENCY ANALYSIS

FREQ	(H1,E2)		(H1,E1)		(H1,H2)		(H2,E1)		(H2,E2)		(E1,E2)	
	AMP	PHASE	AMP	PHASE	AMP	PHASE	AMP	PHASE	AMP	PHASE	AMP	PHASE
.006	1.01	-72.	0.	0.	0.	0.	0.	0.	0.	0.	0.	0.
.012	2.30	39.	0.	0.	0.	0.	0.	0.	0.	0.	0.	0.
.025	0.51	-84.	0.	0.	0.	0.	0.	0.	0.	0.	0.	0.
.037	0.50	-90.	0.	0.	0.	0.	0.	0.	0.	0.	0.	0.
.050	0.41	-60.	0.	0.	0.	0.	0.	0.	0.	0.	0.	0.
.062	0.68	-12.	0.	0.	0.	0.	0.	0.	0.	0.	0.	0.
.075	0.77	-3.	0.	0.	0.	0.	0.	0.	0.	0.	0.	0.
.087	0.40	8.	0.	0.	0.	0.	0.	0.	0.	0.	0.	0.
.100	0.11	31.	0.	0.	0.	0.	0.	0.	0.	0.	0.	0.
.112	0.26	-69.	0.	0.	0.	0.	0.	0.	0.	0.	0.	0.
.125	1.07	23.	0.	0.	0.	0.	0.	0.	0.	0.	0.	0.
.137	0.88	14.	0.	0.	0.	0.	0.	0.	0.	0.	0.	0.
.150	2.59	-4.	0.	0.	0.	0.	0.	0.	0.	0.	0.	0.
.162	0.93	-22.	0.	0.	0.	0.	0.	0.	0.	0.	0.	0.
.175	2.56	-42.	0.	0.	0.	0.	0.	0.	0.	0.	0.	0.
.187	3.71	-70.	0.	0.	0.	0.	0.	0.	0.	0.	0.	0.
.200	0.54	-46.	0.	0.	0.	0.	0.	0.	0.	0.	0.	0.
.212	1.23	60.	0.	0.	0.	0.	0.	0.	0.	0.	0.	0.
.225	1.10	41.	0.	0.	0.	0.	0.	0.	0.	0.	0.	0.
.237	1.48	24.	0.	0.	0.	0.	0.	0.	0.	0.	0.	0.
.250	1.70	-22.	0.	0.	0.	0.	0.	0.	0.	0.	0.	0.

0 0 1801.8

CASE 26-5 LITTLETON MASS 12/1/59 .02-.04 CPS
DEC 193,0,0,193,20,5.,1,0,0,0,0,0
PG 67 1F CANTWELL H1 E2 ONLY

POWER DENSITY SPECTRA

FREQ	H1	H2	E1	E2
	MS GAMMAS		MS MV/KM	
.002	.125E 01	.	.	.279E 01
.005	.422E-01	.	.	.676E-01
.010	.378E-00	.	.	.141E 02
.015	.103E 01	.	.	.936E 02
.020	.102E 01	.	.	.147E 03
.025	.509E 00	.	.	.958E 02
.030	.175E-00	.	.	.493E 02
.035	.854E-01	.	.	.368E 02
.040	.370E-01	.	.	.217E 02
.045	.884E-02	.	.	.963E 01
.050	.441E-02	.	.	.372E 01
.055	.199E-02	.	.	.240E 01
.060	.583E-03	.	.	.132E 01
.065	.286E-03	.	.	.798E 00
.070	.108E-03	.	.	.103E 01
.075	.411E-05	.	.	.120E 01
.080	.565E-04	.	.	.127E 01
.085	.492E-04	.	.	.118E 01
.090	.416E-04	.	.	.102E 01
.095	.364E-04	.	.	.866E 00
.100	.365E-04	.	.	.767E 00

COHERENCY ANALYSIS

FREQ	(H1,E2)		(H1,E1)		(H1,H2)		(H2,E1)		(H2,E2)		(E1,E2)	
	AMP	PHASE	AMP	PHASE	AMP	PHASE	AMP	PHASE	AMP	PHASE	AMP	PHASE
.002	1.26	-66.	0.	0.	0.	0.	0.	0.	0.	0.	0.	0.
.005	4.94	47.	0.	0.	0.	0.	0.	0.	0.	0.	0.	0.
.010	0.88	-75.	0.	0.	0.	0.	0.	0.	0.	0.	0.	0.
.015	0.92	-85.	0.	0.	0.	0.	0.	0.	0.	0.	0.	0.
.020	0.91	-87.	0.	0.	0.	0.	0.	0.	0.	0.	0.	0.
.025	0.79	-85.	0.	0.	0.	0.	0.	0.	0.	0.	0.	0.
.030	0.32	-78.	0.	0.	0.	0.	0.	0.	0.	0.	0.	0.
.035	0.18	64.	0.	0.	0.	0.	0.	0.	0.	0.	0.	0.
.040	0.48	77.	0.	0.	0.	0.	0.	0.	0.	0.	0.	0.
.045	0.56	88.	0.	0.	0.	0.	0.	0.	0.	0.	0.	0.
.050	0.40	90.	0.	0.	0.	0.	0.	0.	0.	0.	0.	0.
.055	0.47	83.	0.	0.	0.	0.	0.	0.	0.	0.	0.	0.
.060	0.14	-74.	0.	0.	0.	0.	0.	0.	0.	0.	0.	0.
.065	0.19	44.	0.	0.	0.	0.	0.	0.	0.	0.	0.	0.
.070	0.53	58.	0.	0.	0.	0.	0.	0.	0.	0.	0.	0.
.075	0.92	51.	0.	0.	0.	0.	0.	0.	0.	0.	0.	0.
.080	0.11	7.	0.	0.	0.	0.	0.	0.	0.	0.	0.	0.
.085	0.14	47.	0.	0.	0.	0.	0.	0.	0.	0.	0.	0.
.090	0.21	66.	0.	0.	0.	0.	0.	0.	0.	0.	0.	0.
.095	0.13	47.	0.	0.	0.	0.	0.	0.	0.	0.	0.	0.
.100	0.75	83.	0.	0.	0.	0.	0.	0.	0.	0.	0.	0.

0 0 1802.0

CASE 26-6 LITTLETON MASS 12/1/59 .02-.06 CPS
DEC 95,0,0,95,20,5,,1,0,0,0,0,0
PG 67 1F CANTWELL H1 E2 ONLY

POWER DENSITY SPECTRA

FREQ	H1	H2	E1	E2
	MS GAMMAS		MS MV/KM	
.002	.265E 01	.	.	.290E 01
.005	.363E-00	.	.	.148E 01
.010	.359E-00	.	.	.124E 02
.015	.728E 00	.	.	.436E 02
.020	.643E 00	.	.	.553E 02
.025	.317E-00	.	.	.391E 02
.030	.132E-00	.	.	.270E 02
.035	.812E-01	.	.	.281E 02
.040	.870E-01	.	.	.415E 02
.045	.827E-01	.	.	.469E 02
.050	.492E-01	.	.	.339E 02
.055	.254E-01	.	.	.210E 02
.060	.105E-01	.	.	.949E 01
.065	.129E-02	.	.	.891E 00
.070	.382E-03	.	.	.389E-00
.075	.606E-03	.	.	.110E 01
.080	.321E-03	.	.	.109E 01
.085	.466E-04	.	.	.497E-00
.090	.332E-04	.	.	.205E-00
.095	.357E-04	.	.	.214E-00
.100	.150E-04	.	.	.176E-00

COHERENCY ANALYSIS

FREQ	(H1,E2)		(H1,E1)		(H1,H2)		(H2,E1)		(H2,E2)		(E1,E2)	
	AMP	PHASE	AMP	PHASE	AMP	PHASE	AMP	PHASE	AMP	PHASE	AMP	PHASE
.002	0.74	-53.	0.	0.	0.	0.	0.	0.	0.	0.	0.	0.
.005	0.22	14.	0.	0.	0.	0.	0.	0.	0.	0.	0.	0.
.010	0.82	-79.	0.	0.	0.	0.	0.	0.	0.	0.	0.	0.
.015	0.81	-72.	0.	0.	0.	0.	0.	0.	0.	0.	0.	0.
.020	0.69	-68.	0.	0.	0.	0.	0.	0.	0.	0.	0.	0.
.025	0.59	-50.	0.	0.	0.	0.	0.	0.	0.	0.	0.	0.
.030	0.49	-19.	0.	0.	0.	0.	0.	0.	0.	0.	0.	0.
.035	0.16	-49.	0.	0.	0.	0.	0.	0.	0.	0.	0.	0.
.040	0.59	-79.	0.	0.	0.	0.	0.	0.	0.	0.	0.	0.
.045	0.83	-69.	0.	0.	0.	0.	0.	0.	0.	0.	0.	0.
.050	0.83	-66.	0.	0.	0.	0.	0.	0.	0.	0.	0.	0.
.055	0.77	-84.	0.	0.	0.	0.	0.	0.	0.	0.	0.	0.
.060	0.76	86.	0.	0.	0.	0.	0.	0.	0.	0.	0.	0.
.065	0.60	-1.	0.	0.	0.	0.	0.	0.	0.	0.	0.	0.
.070	0.31	72.	0.	0.	0.	0.	0.	0.	0.	0.	0.	0.
.075	0.52	-66.	0.	0.	0.	0.	0.	0.	0.	0.	0.	0.
.080	0.38	-33.	0.	0.	0.	0.	0.	0.	0.	0.	0.	0.
.085	0.59	-44.	0.	0.	0.	0.	0.	0.	0.	0.	0.	0.
.090	1.16	-10.	0.	0.	0.	0.	0.	0.	0.	0.	0.	0.
.095	0.89	12.	0.	0.	0.	0.	0.	0.	0.	0.	0.	0.
.100	2.71	-44.	0.	0.	0.	0.	0.	0.	0.	0.	0.	0.

0 0 1802.2

CASE 26-7 LITTLETON MASS 12/1/59 .02-.06CPS
DEC 99,0,0,99,20,5.,1,0,0,0,0
PG 67 1F CANTWELL H1 E2 ONLY

POWER DENSITY SPECTRA

FREQ	H1	H2	E1	E2
	MS GAMMAS		MS MV/KM	
.002	.185E 01	.	.	.528E 01
.005	.564E 00	.	.	.616E 01
.010	.412E-00	.	.	.172E 02
.015	.724E 00	.	.	.652E 02
.020	.704E 00	.	.	.108E 03
.025	.380E-00	.	.	.794E 02
.030	.232E-00	.	.	.396E 02
.035	.191E-00	.	.	.279E 02
.040	.101E-00	.	.	.202E 02
.045	.464E-01	.	.	.182E 02
.050	.293E-01	.	.	.117E 02
.055	.145E-01	.	.	.363E 01
.060	.621E-02	.	.	.226E 01
.065	.238E-02	.	.	.276E 01
.070	.609E-03	.	.	.213E 01
.075	.177E-03	.	.	.766E 00
.080	.996E-04	.	.	.154E-00
.085	.890E-04	.	.	.367E-01
.090	.174E-04	.	.	.162E-00
.095	.322E-04	.	.	.110E-00
.100	.460E-04	.	.	.468E-01

COHERENCY ANALYSIS

FREQ	(H1,E2)		(H1,E1)		(H1,H2)		(H2,E1)		(H2,E2)		(E1,E2)	
	AMP	PHASE	AMP	PHASE	AMP	PHASE	AMP	PHASE	AMP	PHASE	AMP	PHASE
.002	0.40	11.	0.	0.	0.	0.	0.	0.	0.	0.	0.	0.
.005	0.70	-4.	0.	0.	0.	0.	0.	0.	0.	0.	0.	0.
.010	0.62	-36.	0.	0.	0.	0.	0.	0.	0.	0.	0.	0.
.015	0.83	-44.	0.	0.	0.	0.	0.	0.	0.	0.	0.	0.
.020	0.92	-40.	0.	0.	0.	0.	0.	0.	0.	0.	0.	0.
.025	0.86	-39.	0.	0.	0.	0.	0.	0.	0.	0.	0.	0.
.030	0.50	-76.	0.	0.	0.	0.	0.	0.	0.	0.	0.	0.
.035	0.55	48.	0.	0.	0.	0.	0.	0.	0.	0.	0.	0.
.040	0.40	39.	0.	0.	0.	0.	0.	0.	0.	0.	0.	0.
.045	0.40	-58.	0.	0.	0.	0.	0.	0.	0.	0.	0.	0.
.050	0.54	-27.	0.	0.	0.	0.	0.	0.	0.	0.	0.	0.
.055	0.53	20.	0.	0.	0.	0.	0.	0.	0.	0.	0.	0.
.060	0.12	48.	0.	0.	0.	0.	0.	0.	0.	0.	0.	0.
.065	0.43	-77.	0.	0.	0.	0.	0.	0.	0.	0.	0.	0.
.070	0.96	-62.	0.	0.	0.	0.	0.	0.	0.	0.	0.	0.
.075	0.72	-72.	0.	0.	0.	0.	0.	0.	0.	0.	0.	0.
.080	2.11	27.	0.	0.	0.	0.	0.	0.	0.	0.	0.	0.
.085	3.64	27.	0.	0.	0.	0.	0.	0.	0.	0.	0.	0.
.090	1.91	39.	0.	0.	0.	0.	0.	0.	0.	0.	0.	0.
.095	1.84	5.	0.	0.	0.	0.	0.	0.	0.	0.	0.	0.
.100	3.53	34.	0.	0.	0.	0.	0.	0.	0.	0.	0.	0.

0 0 1802.4
DPR M277 DATA OUTPUT IS FINISHED, THANK YOU

CASE 27-1 LITTLETON MASS 12/5/59 .6-1 CPS
DEC 166,0,0,166,20,.2,1,0,0,0,0,0
PG 0000000000000000000000000000000000000000000000000000000000000000

POWER DENSITY SPECTRA

FREQ	H1	H2	E1	E2
	MS GAMMAS		MS MV/KM	
.062	.403E-05	.	.	.234E-03
.125	.124E-05	.	.	.515E-03
.250	.418E-06	.	.	.208E-02
.375	.120E-05	.	.	.617E-02
.500	.361E-05	.	.	.112E-01
.625	.479E-05	.	.	.146E-01
.750	.339E-05	.	.	.163E-01
.875	.148E-05	.	.	.127E-01
.000	.445E-06	.	.	.650E-02
.125	.103E-06	.	.	.389E-02
.250	.346E-07	.	.	.210E-02
.375	.146E-07	.	.	.756E-03
.500	.449E-08	.	.	.432E-03
.625	.229E-08	.	.	.272E-03
.750	.132E-08	.	.	.145E-03
.875	.121E-08	.	.	.697E-04
.000	.126E-08	.	.	.438E-04
.125	.952E-09	.	.	.748E-05
.250	.770E-09	.	.	.438E-05
.375	.780E-09	.	.	.635E-05
.500	.782E-09	.	.	.428E-05

COHERENCY ANALYSIS

FREQ	(H1,E2)		(H1,E1)		(H1,H2)		(H2,E1)		(H2,E2)		(E1,E2)	
	AMP	PHASE	AMP	PHASE	AMP	PHASE	AMP	PHASE	AMP	PHASE	AMP	PHASE
.062	0.56	-31.	0.	0.	0.	0.	0.	0.	0.	0.	0.	0.
.125	0.36	-65.	0.	0.	0.	0.	0.	0.	0.	0.	0.	0.
.250	0.56	26.	0.	0.	0.	0.	0.	0.	0.	0.	0.	0.
.375	0.44	-80.	0.	0.	0.	0.	0.	0.	0.	0.	0.	0.
.500	0.63	-68.	0.	0.	0.	0.	0.	0.	0.	0.	0.	0.
.625	0.55	-69.	0.	0.	0.	0.	0.	0.	0.	0.	0.	0.
.750	0.43	-40.	0.	0.	0.	0.	0.	0.	0.	0.	0.	0.
.875	0.47	2.	0.	0.	0.	0.	0.	0.	0.	0.	0.	0.
.000	0.50	55.	0.	0.	0.	0.	0.	0.	0.	0.	0.	0.
.125	0.48	65.	0.	0.	0.	0.	0.	0.	0.	0.	0.	0.
.250	0.27	-5.	0.	0.	0.	0.	0.	0.	0.	0.	0.	0.
.375	0.26	-67.	0.	0.	0.	0.	0.	0.	0.	0.	0.	0.
.500	0.35	-50.	0.	0.	0.	0.	0.	0.	0.	0.	0.	0.
.625	0.68	-4.	0.	0.	0.	0.	0.	0.	0.	0.	0.	0.
.750	0.21	-1.	0.	0.	0.	0.	0.	0.	0.	0.	0.	0.
.875	0.13	-14.	0.	0.	0.	0.	0.	0.	0.	0.	0.	0.
.000	0.40	10.	0.	0.	0.	0.	0.	0.	0.	0.	0.	0.
.125	0.56	16.	0.	0.	0.	0.	0.	0.	0.	0.	0.	0.
.250	0.84	-42.	0.	0.	0.	0.	0.	0.	0.	0.	0.	0.
.375	1.30	24.	0.	0.	0.	0.	0.	0.	0.	0.	0.	0.
.500	2.39	37.	0.	0.	0.	0.	0.	0.	0.	0.	0.	0.

0 0 328.8

CASE 27-2 LITTLETON MASS 12/5/59 .2-.6 CPS
DEC 150,0,0,150,20,.5,1,0,0,0,0,0
PG 000000000000000000000000000000000000000000000000000000000000000000

POWER DENSITY SPECTRA

FREQ	H1	H2	E1	E2
	MS GAMMAS		MS MV/KM	
.025	.218E-03	.	.	.195E-01
.050	.517E-04	.	.	.208E-01
.100	.459E-04	.	.	.424E-01
.150	.660E-04	.	.	.165E-00
.200	.746E-04	.	.	.592E 00
.250	.590E-04	.	.	.868E 00
.300	.388E-04	.	.	.539E 00
.350	.318E-04	.	.	.224E-00
.400	.221E-04	.	.	.223E-00
.450	.116E-04	.	.	.245E-00
.500	.804E-05	.	.	.156E-00
.550	.524E-05	.	.	.683E-01
.600	.411E-05	.	.	.617E-01
.650	.368E-05	.	.	.551E-01
.700	.160E-05	.	.	.249E-01
.750	.589E-06	.	.	.623E-02
.800	.442E-06	.	.	.389E-02
.850	.162E-06	.	.	.171E-02
.900	.120E-06	.	.	.789E-03
.950	.119E-06	.	.	.169E-03
.000	.962E-07	.	.	.112E-03

COHERENCY ANALYSIS

FREQ	(H1,E2)		(H1,E1)		(H1,H2)		(H2,E1)		(H2,E2)		(E1,E2)	
	AMP	PHASE	AMP	PHASE	AMP	PHASE	AMP	PHASE	AMP	PHASE	AMP	PHASE
.025	0.49	-16.	0.	0.	0.	0.	0.	0.	0.	0.	0.	0.
.050	0.55	0.	0.	0.	0.	0.	0.	0.	0.	0.	0.	0.
.100	0.63	-40.	0.	0.	0.	0.	0.	0.	0.	0.	0.	0.
.150	0.72	-27.	0.	0.	0.	0.	0.	0.	0.	0.	0.	0.
.200	0.77	-14.	0.	0.	0.	0.	0.	0.	0.	0.	0.	0.
.250	0.79	-18.	0.	0.	0.	0.	0.	0.	0.	0.	0.	0.
.300	0.72	-26.	0.	0.	0.	0.	0.	0.	0.	0.	0.	0.
.350	0.61	-18.	0.	0.	0.	0.	0.	0.	0.	0.	0.	0.
.400	0.51	-8.	0.	0.	0.	0.	0.	0.	0.	0.	0.	0.
.450	0.38	-14.	0.	0.	0.	0.	0.	0.	0.	0.	0.	0.
.500	0.38	-15.	0.	0.	0.	0.	0.	0.	0.	0.	0.	0.
.550	0.65	-27.	0.	0.	0.	0.	0.	0.	0.	0.	0.	0.
.600	0.81	-30.	0.	0.	0.	0.	0.	0.	0.	0.	0.	0.
.650	0.70	-22.	0.	0.	0.	0.	0.	0.	0.	0.	0.	0.
.700	0.36	-16.	0.	0.	0.	0.	0.	0.	0.	0.	0.	0.
.750	0.19	-11.	0.	0.	0.	0.	0.	0.	0.	0.	0.	0.
.800	0.37	-30.	0.	0.	0.	0.	0.	0.	0.	0.	0.	0.
.850	0.24	-48.	0.	0.	0.	0.	0.	0.	0.	0.	0.	0.
.900	0.16	23.	0.	0.	0.	0.	0.	0.	0.	0.	0.	0.
.950	0.94	5.	0.	0.	0.	0.	0.	0.	0.	0.	0.	0.
.000	1.35	7.	0.	0.	0.	0.	0.	0.	0.	0.	0.	0.

0 0 329.0

CASE 27-3 LITTLETON MASS 12/5/59 .06-.2 CPS
DEC 166,0,0,166,20,1.,1,0,0,0,0,0
PG 0000000000000000000000000000000000000000000000000000000000000000

POWER DENSITY SPECTRA

FREQ	H1	H2	E1	E2
	MS GAMMAS		MS MV/KM	
.012	.350E-02	.	.	.391E-00
.025	.899E-02	.	.	.131E 01
.050	.134E-01	.	.	.650E 01
.075	.111E-01	.	.	.117E 02
.100	.452E-02	.	.	.882E 01
.125	.837E-03	.	.	.402E 01
.150	.229E-03	.	.	.280E 01
.175	.153E-03	.	.	.178E 01
.200	.751E-04	.	.	.812E 00
.225	.322E-04	.	.	.316E-00
.250	.118E-04	.	.	.579E-01
.275	.473E-05	.	.	.203E-01
.300	.164E-05	.	.	.116E-01
.325	.784E-06	.	.	.343E-05
.350	.273E-06	.	.	.289E-02
.375	.192E-06	.	.	.155E-02
.400	.473E-07	.	.	.109E-02
.425	.432E-07	.	.	.400E-02
.450	.134E-07	.	.	.152E-02
.475	.451E-07	.	.	.387E-02
.500	.882E-07	.	.	.455E-02

COHERENCY ANALYSIS

FREQ	(H1,E2)		(H1,E1)		(H1,H2)		(H2,E1)		(H2,E2)		(E1,E2)	
	AMP	PHASE	AMP	PHASE	AMP	PHASE	AMP	PHASE	AMP	PHASE	AMP	PHASE
.012	1.08	22.	0.	0.	0.	0.	0.	0.	0.	0.	0.	0.
.025	0.35	-15.	0.	0.	0.	0.	0.	0.	0.	0.	0.	0.
.050	0.60	-13.	0.	0.	0.	0.	0.	0.	0.	0.	0.	0.
.075	0.71	-13.	0.	0.	0.	0.	0.	0.	0.	0.	0.	0.
.100	0.71	-16.	0.	0.	0.	0.	0.	0.	0.	0.	0.	0.
.125	0.61	-24.	0.	0.	0.	0.	0.	0.	0.	0.	0.	0.
.150	0.67	-19.	0.	0.	0.	0.	0.	0.	0.	0.	0.	0.
.175	0.63	-24.	0.	0.	0.	0.	0.	0.	0.	0.	0.	0.
.200	0.57	-40.	0.	0.	0.	0.	0.	0.	0.	0.	0.	0.
.225	0.53	-38.	0.	0.	0.	0.	0.	0.	0.	0.	0.	0.
.250	0.40	3.	0.	0.	0.	0.	0.	0.	0.	0.	0.	0.
.275	0.23	-56.	0.	0.	0.	0.	0.	0.	0.	0.	0.	0.
.300	0.22	-5.	0.	0.	0.	0.	0.	0.	0.	0.	0.	0.
.325	5.67	64.	0.	0.	0.	0.	0.	0.	0.	0.	0.	0.
.350	2.00	81.	0.	0.	0.	0.	0.	0.	0.	0.	0.	0.
.375	3.48	-81.	0.	0.	0.	0.	0.	0.	0.	0.	0.	0.
.400	5.51	59.	0.	0.	0.	0.	0.	0.	0.	0.	0.	0.
.425	2.46	24.	0.	0.	0.	0.	0.	0.	0.	0.	0.	0.
.450	7.88	29.	0.	0.	0.	0.	0.	0.	0.	0.	0.	0.
.475	2.82	37.	0.	0.	0.	0.	0.	0.	0.	0.	0.	0.
.500	1.88	30.	0.	0.	0.	0.	0.	0.	0.	0.	0.	0.

0 0 329.2

CASE 27-4 LITTLETON MASS 12/5/59 .005-.02 CPS
DEC 120,0,0,120,20,10,,1,0,0,0,0
PG 0000000000000000000000000000000000000000000000000000000000000000

POWER DENSITY SPECTRA

FREQ	H1	H2	E1	E2
	MS GAMMAS		MS MV/KM	
.001	.413E 03	.	.	.729E 02
.002	.304E 03	.	.	.210E 03
.005	.305E 03	.	.	.174E 04
.007	.285E 03	.	.	.391E 04
.010	.146E 03	.	.	.380E 04
.012	.298E 02	.	.	.154E 04
.015	.304E 01	.	.	.227E 03
.017	.360E 01	.	.	.130E 03
.020	.194E 01	.	.	.124E 03
.022	.965E 00	.	.	.127E 03
.025	.445E-00	.	.	.973E 02
.027	.274E-00	.	.	.520E 02
.030	.134E-00	.	.	.165E 02
.032	.457E-01	.	.	.103E 02
.035	.640E-02	.	.	.809E 01
.037	.688E-02	.	.	.789E 00
.040	.107E-03	.	.	.405E 01
.042	.336E-02	.	.	.482E 01
.045	.327E-03	.	.	.311E 01
.047	.383E-02	.	.	.198E 01
.050	.696E-02	.	.	.214E 01

COHERENCY ANALYSIS

FREQ	(H1,E2)		(H1,E1)		(H1,H2)		(H2,E1)		(H2,E2)		(E1,E2)	
	AMP	PHASE	AMP	PHASE	AMP	PHASE	AMP	PHASE	AMP	PHASE	AMP	PHASE
.001	0.57	-26.	0.	0.	0.	0.	0.	0.	0.	0.	0.	0.
.002	0.60	16.	0.	0.	0.	0.	0.	0.	0.	0.	0.	0.
.005	0.80	-7.	0.	0.	0.	0.	0.	0.	0.	0.	0.	0.
.007	0.87	-6.	0.	0.	0.	0.	0.	0.	0.	0.	0.	0.
.010	0.89	-2.	0.	0.	0.	0.	0.	0.	0.	0.	0.	0.
.012	0.82	-3.	0.	0.	0.	0.	0.	0.	0.	0.	0.	0.
.015	0.63	-70.	0.	0.	0.	0.	0.	0.	0.	0.	0.	0.
.017	0.76	-36.	0.	0.	0.	0.	0.	0.	0.	0.	0.	0.
.020	0.84	-31.	0.	0.	0.	0.	0.	0.	0.	0.	0.	0.
.022	0.80	-19.	0.	0.	0.	0.	0.	0.	0.	0.	0.	0.
.025	0.67	-41.	0.	0.	0.	0.	0.	0.	0.	0.	0.	0.
.027	0.81	-81.	0.	0.	0.	0.	0.	0.	0.	0.	0.	0.
.030	1.00	-83.	0.	0.	0.	0.	0.	0.	0.	0.	0.	0.
.032	1.08	-57.	0.	0.	0.	0.	0.	0.	0.	0.	0.	0.
.035	1.09	88.	0.	0.	0.	0.	0.	0.	0.	0.	0.	0.
.037	3.57	2.	0.	0.	0.	0.	0.	0.	0.	0.	0.	0.
.040	5.64	7.	0.	0.	0.	0.	0.	0.	0.	0.	0.	0.
.042	2.40	-2.	0.	0.	0.	0.	0.	0.	0.	0.	0.	0.
.045	5.97	-20.	0.	0.	0.	0.	0.	0.	0.	0.	0.	0.
.047	1.39	-17.	0.	0.	0.	0.	0.	0.	0.	0.	0.	0.
.050	1.32	19.	0.	0.	0.	0.	0.	0.	0.	0.	0.	0.

0 0 329.4

Note:

In Case 27-5 the E2 power spectra must be divided by 11 because the gain was put in the machine as 300 when it should have been 1000.

CASE 27-5 LITTLETON MASS 12/5/59 .02-.06 CPS
DEC 166,0,0,166,20,5,,1,0,0,0,0,0
PG 000000000000000000000000000000000000000000000000000000000000

POWER DENSITY SPECTRA

FREQ	H1	H2	E1	E2
	MS GAMMAS		MS MV/KM	
.002	.727E 00	.	.	.535E 02
.005	.353E-00	.	.	.628E 02
.010	.362E-00	.	.	.872E 02
.015	.130E 01	.	.	.582E 03
.020	.170E 01	.	.	.162E 04
.025	.993E 00	.	.	.194E 04
.030	.454E-00	.	.	.141E 04
.035	.419E-00	.	.	.112E 04
.040	.321E-00	.	.	.100E 04
.045	.148E-00	.	.	.637E 03
.050	.604E-01	.	.	.287E 03
.055	.283E-01	.	.	.177E 03
.060	.157E-01	.	.	.144E 03
.065	.884E-02	.	.	.731E 02
.070	.278E-02	.	.	.152E 02
.075	.101E-02	.	.	.592E 01
.080	.775E-03	.	.	.123E 02
.085	.348E-03	.	.	.164E 02
.090	.186E-03	.	.	.200E 02
.095	.187E-03	.	.	.243E 02
.100	.211E-03	.	.	.257E 02

COHERENCY ANALYSIS

FREQ	(H1,E2)		(H1,E1)		(H1,H2)		(H2,E1)		(H2,E2)		(E1,E2)	
	AMP	PHASE	AMP	PHASE	AMP	PHASE	AMP	PHASE	AMP	PHASE	AMP	PHASE
.002	0.07	69.	0.	0.	0.	0.	0.	0.	0.	0.	0.	0.
.005	0.40	-21.	0.	0.	0.	0.	0.	0.	0.	0.	0.	0.
.010	0.61	-11.	0.	0.	0.	0.	0.	0.	0.	0.	0.	0.
.015	0.87	-18.	0.	0.	0.	0.	0.	0.	0.	0.	0.	0.
.020	0.91	-18.	0.	0.	0.	0.	0.	0.	0.	0.	0.	0.
.025	0.87	-19.	0.	0.	0.	0.	0.	0.	0.	0.	0.	0.
.030	0.81	-26.	0.	0.	0.	0.	0.	0.	0.	0.	0.	0.
.035	0.86	-36.	0.	0.	0.	0.	0.	0.	0.	0.	0.	0.
.040	0.91	-42.	0.	0.	0.	0.	0.	0.	0.	0.	0.	0.
.045	0.87	-38.	0.	0.	0.	0.	0.	0.	0.	0.	0.	0.
.050	0.82	-32.	0.	0.	0.	0.	0.	0.	0.	0.	0.	0.
.055	0.83	-45.	0.	0.	0.	0.	0.	0.	0.	0.	0.	0.
.060	0.78	-30.	0.	0.	0.	0.	0.	0.	0.	0.	0.	0.
.065	0.67	-10.	0.	0.	0.	0.	0.	0.	0.	0.	0.	0.
.070	0.51	25.	0.	0.	0.	0.	0.	0.	0.	0.	0.	0.
.075	0.48	38.	0.	0.	0.	0.	0.	0.	0.	0.	0.	0.
.080	0.44	14.	0.	0.	0.	0.	0.	0.	0.	0.	0.	0.
.085	0.22	23.	0.	0.	0.	0.	0.	0.	0.	0.	0.	0.
.090	0.31	-57.	0.	0.	0.	0.	0.	0.	0.	0.	0.	0.
.095	0.46	-62.	0.	0.	0.	0.	0.	0.	0.	0.	0.	0.
.100	0.45	-66.	0.	0.	0.	0.	0.	0.	0.	0.	0.	0.

0 0 329.6

CASE 27-1 LITTLETON MASS 12/5/59 .6-1 CPS
DEC 166.0.0.166.40..2.1.0.0.0.0.0
PG 000000000000000000000000000000000000000000000000000000000000000000

POWER DENSITY SPECTRA

FREQ	H1	H2	E1	E2
	MS GAMMAS		MS MV/KM	
.031	.648E-05	.	.	.294E-03
.062	.368E-05	.	.	.291E-03
.125	.172E-05	.	.	.315E-03
.187	.693E-06	.	.	.476E-03
.250	.325E-06	.	.	.112E-02
.312	.126E-06	.	.	.367E-02
.375	.661E-06	.	.	.697E-02
.437	.112E-05	.	.	.675E-02
.500	.263E-05	.	.	.109E-01
.562	.482E-05	.	.	.184E-01
.625	.574E-05	.	.	.134E-01
.687	.521E-05	.	.	.991E-02
.750	.354E-05	.	.	.207E-01
.812	.223E-05	.	.	.223E-01
.875	.155E-05	.	.	.105E-01
.937	.748E-06	.	.	.584E-02
.000	.295E-06	.	.	.668E-02
.062	.184E-06	.	.	.482E-02
.125	.703E-07	.	.	.390E-02
.187	.330E-07	.	.	.341E-02
.250	.388E-07	.	.	.162E-02
.312	.291E-07	.	.	.930E-03
.375	.134E-07	.	.	.686E-03
.437	.174E-08	.	.	.346E-03
.500	.314E-08	.	.	.448E-03
.562	.461E-08	.	.	.445E-03
.625	.286E-08	.	.	.250E-03
.687	.937E-09	.	.	.158E-03
.750	.806E-09	.	.	.138E-03
.812	.111E-08	.	.	.786E-04
.875	.142E-08	.	.	.762E-04
.937	.132E-08	.	.	.584E-04
.000	.139E-08	.	.	.395E-04
.062	.118E-08	.	.	.214E-04
.125	.871E-09	.	.	.998E-05
.187	.766E-09	.	.	.444E-05
.250	.762E-09	.	.	.112E-04
.312	.739E-09	.	.	.147E-04
.375	.722E-09	.	.	.490E-05
.437	.813E-09	.	.	.465E-05
.500	.919E-09	.	.	.631E-05

COHERENCY ANALYSIS

FREQ	(H1,E2)		(H1,E1)		(H1,H2)		(H2,E1)		(H2,E2)		(E1,E2)	
	AMP	PHASE	AMP	PHASE	AMP	PHASE	AMP	PHASE	AMP	PHASE	AMP	PHASE
.031	0.73	75.	0.	0.	0.	0.	0.	0.	0.	0.	0.	0.
.062	0.46	80.	0.	0.	0.	0.	0.	0.	0.	0.	0.	0.
.125	0.49	72.	0.	0.	0.	0.	0.	0.	0.	0.	0.	0.
.187	0.23	13.	0.	0.	0.	0.	0.	0.	0.	0.	0.	0.
.250	0.42	88.	0.	0.	0.	0.	0.	0.	0.	0.	0.	0.
.312	0.58	59.	0.	0.	0.	0.	0.	0.	0.	0.	0.	0.
.375	0.49	37.	0.	0.	0.	0.	0.	0.	0.	0.	0.	0.
.437	0.41	58.	0.	0.	0.	0.	0.	0.	0.	0.	0.	0.

.500	0.71	-55.	0.	0.	0.	0.	0.	0.	0.	0.	0.	0.	0.
.562	0.84	-55.	0.	0.	0.	0.	0.	0.	0.	0.	0.	0.	0.
.625	0.65	-83.	0.	0.	0.	0.	0.	0.	0.	0.	0.	0.	0.
.687	0.48	60.	0.	0.	0.	0.	0.	0.	0.	0.	0.	0.	0.
.750	0.50	-29.	0.	0.	0.	0.	0.	0.	0.	0.	0.	0.	0.
.812	0.81	-12.	0.	0.	0.	0.	0.	0.	0.	0.	0.	0.	0.
.875	0.47	8.	0.	0.	0.	0.	0.	0.	0.	0.	0.	0.	0.
.937	0.50	-90.	0.	0.	0.	0.	0.	0.	0.	0.	0.	0.	0.
.000	0.79	81.	0.	0.	0.	0.	0.	0.	0.	0.	0.	0.	0.
.062	0.83	61.	0.	0.	0.	0.	0.	0.	0.	0.	0.	0.	0.
.125	0.39	17.	0.	0.	0.	0.	0.	0.	0.	0.	0.	0.	0.
.187	0.46	-56.	0.	0.	0.	0.	0.	0.	0.	0.	0.	0.	0.
.250	0.23	-37.	0.	0.	0.	0.	0.	0.	0.	0.	0.	0.	0.
.312	0.42	-79.	0.	0.	0.	0.	0.	0.	0.	0.	0.	0.	0.
.375	0.61	-83.	0.	0.	0.	0.	0.	0.	0.	0.	0.	0.	0.
.437	0.18	-8.	0.	0.	0.	0.	0.	0.	0.	0.	0.	0.	0.
.500	0.49	-7.	0.	0.	0.	0.	0.	0.	0.	0.	0.	0.	0.
.562	0.64	-20.	0.	0.	0.	0.	0.	0.	0.	0.	0.	0.	0.
.625	0.56	-6.	0.	0.	0.	0.	0.	0.	0.	0.	0.	0.	0.
.687	0.83	27.	0.	0.	0.	0.	0.	0.	0.	0.	0.	0.	0.
.750	0.49	-12.	0.	0.	0.	0.	0.	0.	0.	0.	0.	0.	0.
.812	0.31	60.	0.	0.	0.	0.	0.	0.	0.	0.	0.	0.	0.
.875	0.60	-16.	0.	0.	0.	0.	0.	0.	0.	0.	0.	0.	0.
.937	0.42	-41.	0.	0.	0.	0.	0.	0.	0.	0.	0.	0.	0.
.000	0.17	78.	0.	0.	0.	0.	0.	0.	0.	0.	0.	0.	0.
.062	0.69	66.	0.	0.	0.	0.	0.	0.	0.	0.	0.	0.	0.
.125	1.17	18.	0.	0.	0.	0.	0.	0.	0.	0.	0.	0.	0.
.187	1.82	-35.	0.	0.	0.	0.	0.	0.	0.	0.	0.	0.	0.
.250	0.73	-78.	0.	0.	0.	0.	0.	0.	0.	0.	0.	0.	0.
.312	0.22	3.	0.	0.	0.	0.	0.	0.	0.	0.	0.	0.	0.
.375	0.88	28.	0.	0.	0.	0.	0.	0.	0.	0.	0.	0.	0.
.437	2.74	37.	0.	0.	0.	0.	0.	0.	0.	0.	0.	0.	0.
.500	2.59	25.	0.	0.	0.	0.	0.	0.	0.	0.	0.	0.	0.

0 0 330.2

CASE 27-2 LITTLETON MASS 12/5/59 .2-.6 CPS
DEC 150,0,0,150,40,.5,1,0,0,0,0
PG 000000000000000000000000000000000000000000000000000000000000

POWER DENSITY SPECTRA

FREQ	H1	H2	E1	E2
	MS GAMMAS		MS MV/KM	
.012	.631E-03	.	.	.328E-01
.025	.235E-03	.	.	.208E-01
.050	.468E-04	.	.	.974E-02
.075	.279E-04	.	.	.125E-01
.100	.268E-04	.	.	.386E-01
.125	.268E-04	.	.	.553E-01
.150	.724E-04	.	.	.145E-00
.175	.824E-04	.	.	.201E-00
.200	.620E-04	.	.	.388E-00
.225	.752E-04	.	.	.110E 01
.250	.763E-04	.	.	.129E 01
.275	.490E-04	.	.	.713E 00
.300	.291E-04	.	.	.394E-00
.325	.270E-04	.	.	.290E-00
.350	.354E-04	.	.	.153E-00
.375	.379E-04	.	.	.158E-00
.400	.238E-04	.	.	.254E-00
.425	.106E-04	.	.	.227E-00
.450	.103E-04	.	.	.292E-00
.475	.976E-05	.	.	.302E-00
.500	.830E-05	.	.	.110E-00
.525	.770E-05	.	.	.349E-01
.550	.552E-05	.	.	.732E-01
.575	.319E-05	.	.	.749E-01
.600	.191E-05	.	.	.396E-01
.625	.530E-05	.	.	.642E-01
.650	.635E-05	.	.	.876E-01
.675	.223E-05	.	.	.392E-01
.700	.436E-06	.	.	.811E-02
.725	.556E-06	.	.	.534E-02
.750	.608E-06	.	.	.643E-02
.775	.829E-06	.	.	.806E-02
.800	.548E-06	.	.	.329E-02
.825	.116E-06	.	.	.662E-03
.850	.536E-07	.	.	.141E-02
.875	.108E-06	.	.	.197E-02
.900	.161E-06	.	.	.108E-02
.925	.160E-06	.	.	.263E-04
.950	.859E-07	.	.	.336E-03
.975	.933E-07	.	.	.660E-05
.000	.123E-06	.	.	.215E-03

COHERENCY ANALYSIS

FREQ	(H1,E2)		(H1,E1)		(H1,H2)		(H2,E1)		(H2,E2)		(E1,E2)	
	AMP	PHASE	AMP	PHASE	AMP	PHASE	AMP	PHASE	AMP	PHASE	AMP	PHASE
.012	0.71	41.	0.	0.	0.	0.	0.	0.	0.	0.	0.	0.
.025	0.66	37.	0.	0.	0.	0.	0.	0.	0.	0.	0.	0.
.050	0.49	25.	0.	0.	0.	0.	0.	0.	0.	0.	0.	0.
.075	0.84	-56.	0.	0.	0.	0.	0.	0.	0.	0.	0.	0.
.100	0.76	-20.	0.	0.	0.	0.	0.	0.	0.	0.	0.	0.
.125	0.39	-26.	0.	0.	0.	0.	0.	0.	0.	0.	0.	0.
.150	0.67	-44.	0.	0.	0.	0.	0.	0.	0.	0.	0.	0.
.175	0.87	-37.	0.	0.	0.	0.	0.	0.	0.	0.	0.	0.

.200	0.85	-5.	0.	0.	0.	0.	0.	0.	0.	0.	0.	0.
.225	0.81	-5.	0.	0.	0.	0.	0.	0.	0.	0.	0.	0.
.250	0.80	-19.	0.	0.	0.	0.	0.	0.	0.	0.	0.	0.
.275	0.80	-30.	0.	0.	0.	0.	0.	0.	0.	0.	0.	0.
.300	0.73	-36.	0.	0.	0.	0.	0.	0.	0.	0.	0.	0.
.325	0.75	-29.	0.	0.	0.	0.	0.	0.	0.	0.	0.	0.
.350	0.62	-17.	0.	0.	0.	0.	0.	0.	0.	0.	0.	0.
.375	0.55	8.	0.	0.	0.	0.	0.	0.	0.	0.	0.	0.
.400	0.65	-3.	0.	0.	0.	0.	0.	0.	0.	0.	0.	0.
.425	0.55	-31.	0.	0.	0.	0.	0.	0.	0.	0.	0.	0.
.450	0.23	-31.	0.	0.	0.	0.	0.	0.	0.	0.	0.	0.
.475	0.34	2.	0.	0.	0.	0.	0.	0.	0.	0.	0.	0.
.500	0.39	-5.	0.	0.	0.	0.	0.	0.	0.	0.	0.	0.
.525	0.68	-27.	0.	0.	0.	0.	0.	0.	0.	0.	0.	0.
.550	0.80	-25.	0.	0.	0.	0.	0.	0.	0.	0.	0.	0.
.575	0.85	-41.	0.	0.	0.	0.	0.	0.	0.	0.	0.	0.
.600	0.79	-49.	0.	0.	0.	0.	0.	0.	0.	0.	0.	0.
.625	0.85	-21.	0.	0.	0.	0.	0.	0.	0.	0.	0.	0.
.650	0.82	-20.	0.	0.	0.	0.	0.	0.	0.	0.	0.	0.
.675	0.43	-13.	0.	0.	0.	0.	0.	0.	0.	0.	0.	0.
.700	1.62	-28.	0.	0.	0.	0.	0.	0.	0.	0.	0.	0.
.725	0.78	-7.	0.	0.	0.	0.	0.	0.	0.	0.	0.	0.
.750	0.16	-80.	0.	0.	0.	0.	0.	0.	0.	0.	0.	0.
.775	0.51	-13.	0.	0.	0.	0.	0.	0.	0.	0.	0.	0.
.800	0.42	-18.	0.	0.	0.	0.	0.	0.	0.	0.	0.	0.
.825	1.01	42.	0.	0.	0.	0.	0.	0.	0.	0.	0.	0.
.850	0.67	81.	0.	0.	0.	0.	0.	0.	0.	0.	0.	0.
.875	0.44	9.	0.	0.	0.	0.	0.	0.	0.	0.	0.	0.
.900	0.23	55.	0.	0.	0.	0.	0.	0.	0.	0.	0.	0.
.925	3.39	22.	0.	0.	0.	0.	0.	0.	0.	0.	0.	0.
.950	1.60	7.	0.	0.	0.	0.	0.	0.	0.	0.	0.	0.
.975	5.05	-7.	0.	0.	0.	0.	0.	0.	0.	0.	0.	0.
.000	0.42	76.	0.	0.	0.	0.	0.	0.	0.	0.	0.	0.

0 0 330.6

CASE 27-3 LITTLETON MASS 12/5/59 .06-.2 CPS
DEC 166,0,0,166,40,1.,1,0,0,0,0,0
PG 000000000000000000000000000000000000000000000000000000000000

POWER DENSITY SPECTRA

FREQ	H1	H2	E1	E2
	MS GAMMAS		MS MV/KM	
.006	.119E-01	.	.	.528E 00
.012	.605E-02	.	.	.151E-00
.025	.689E-03	.	.	.564E 00
.037	.571E-02	.	.	.244E 01
.050	.107E-01	.	.	.392E 01
.062	.136E-01	.	.	.105E 02
.075	.152E-01	.	.	.176E 02
.087	.106E-01	.	.	.134E 02
.100	.404E-02	.	.	.723E 01
.112	.112E-02	.	.	.467E 01
.125	.400E-03	.	.	.248E 01
.137	.304E-03	.	.	.332E 01
.150	.256E-03	.	.	.389E 01
.162	.200E-03	.	.	.208E 01
.175	.156E-03	.	.	.134E 01
.187	.103E-03	.	.	.131E 01
.200	.834E-04	.	.	.785E 00
.212	.504E-04	.	.	.442E-00
.225	.218E-04	.	.	.285E-00
.237	.174E-04	.	.	.745E-01
.250	.137E-04	.	.	.163E-02
.262	.730E-05	.	.	.277E-01
.275	.275E-05	.	.	.206E-01
.287	.188E-05	.	.	.194E-01
.300	.201E-05	.	.	.213E-01
.312	.159E-05	.	.	.273E-03
.325	.590E-06	.	.	.717E-02
.337	.101E-06	.	.	.505E-02
.350	.247E-06	.	.	.302E-02
.362	.504E-06	.	.	.758E-03
.375	.354E-06	.	.	.341E-02
.387	.588E-07	.	.	.315E-02
.400	.205E-06	.	.	.166E-02
.412	.584E-07	.	.	.441E-02
.425	.142E-07	.	.	.352E-02
.437	.309E-07	.	.	.582E-02
.450	.627E-08	.	.	.664E-02
.462	.696E-08	.	.	.491E-02
.475	.260E-07	.	.	.944E-02
.487	.991E-07	.	.	.336E-02
.500	.130E-06	.	.	.165E-02

COHERENCY ANALYSIS

FREQ	(H1,E2)		(H1,E1)		(H1,H2)		(H2,E1)		(H2,E2)		(E1,E2)	
	AMP	PHASE	AMP	PHASE	AMP	PHASE	AMP	PHASE	AMP	PHASE	AMP	PHASE
.006	0.96	-5.	0.	0.	0.	0.	0.	0.	0.	0.	0.	0.
.012	0.24	-77.	0.	0.	0.	0.	0.	0.	0.	0.	0.	0.
.025	1.10	11.	0.	0.	0.	0.	0.	0.	0.	0.	0.	0.
.037	0.64	-2.	0.	0.	0.	0.	0.	0.	0.	0.	0.	0.
.050	0.28	-42.	0.	0.	0.	0.	0.	0.	0.	0.	0.	0.
.062	0.55	-18.	0.	0.	0.	0.	0.	0.	0.	0.	0.	0.
.075	0.82	-7.	0.	0.	0.	0.	0.	0.	0.	0.	0.	0.
.087	0.79	-12.	0.	0.	0.	0.	0.	0.	0.	0.	0.	0.

.100	0.63	-37.	0.	0.	0.	0.	0.	0.	0.	0.	0.	0.
.112	0.57	-29.	0.	0.	0.	0.	0.	0.	0.	0.	0.	0.
.125	0.71	7.	0.	0.	0.	0.	0.	0.	0.	0.	0.	0.
.137	0.66	-26.	0.	0.	0.	0.	0.	0.	0.	0.	0.	0.
.150	0.71	-29.	0.	0.	0.	0.	0.	0.	0.	0.	0.	0.
.162	0.69	-11.	0.	0.	0.	0.	0.	0.	0.	0.	0.	0.
.175	0.70	-12.	0.	0.	0.	0.	0.	0.	0.	0.	0.	0.
.187	0.55	-43.	0.	0.	0.	0.	0.	0.	0.	0.	0.	0.
.200	0.61	-63.	0.	0.	0.	0.	0.	0.	0.	0.	0.	0.
.212	0.67	-51.	0.	0.	0.	0.	0.	0.	0.	0.	0.	0.
.225	0.64	-3.	0.	0.	0.	0.	0.	0.	0.	0.	0.	0.
.237	0.75	33.	0.	0.	0.	0.	0.	0.	0.	0.	0.	0.
.250	0.32	70.	0.	0.	0.	0.	0.	0.	0.	0.	0.	0.
.262	0.57	79.	0.	0.	0.	0.	0.	0.	0.	0.	0.	0.
.275	0.44	-81.	0.	0.	0.	0.	0.	0.	0.	0.	0.	0.
.287	0.67	25.	0.	0.	0.	0.	0.	0.	0.	0.	0.	0.
.300	0.59	37.	0.	0.	0.	0.	0.	0.	0.	0.	0.	0.
.312	2.38	56.	0.	0.	0.	0.	0.	0.	0.	0.	0.	0.
.325	1.31	42.	0.	0.	0.	0.	0.	0.	0.	0.	0.	0.
.337	1.44	18.	0.	0.	0.	0.	0.	0.	0.	0.	0.	0.
.350	1.82	-87.	0.	0.	0.	0.	0.	0.	0.	0.	0.	0.
.362	4.60	-69.	0.	0.	0.	0.	0.	0.	0.	0.	0.	0.
.375	2.33	-76.	0.	0.	0.	0.	0.	0.	0.	0.	0.	0.
.387	3.60	77.	0.	0.	0.	0.	0.	0.	0.	0.	0.	0.
.400	1.69	48.	0.	0.	0.	0.	0.	0.	0.	0.	0.	0.
.412	2.43	30.	0.	0.	0.	0.	0.	0.	0.	0.	0.	0.
.425	5.68	20.	0.	0.	0.	0.	0.	0.	0.	0.	0.	0.
.437	1.90	16.	0.	0.	0.	0.	0.	0.	0.	0.	0.	0.
.450	4.68	11.	0.	0.	0.	0.	0.	0.	0.	0.	0.	0.
.462	7.46	40.	0.	0.	0.	0.	0.	0.	0.	0.	0.	0.
.475	3.17	59.	0.	0.	0.	0.	0.	0.	0.	0.	0.	0.
.487	1.93	28.	0.	0.	0.	0.	0.	0.	0.	0.	0.	0.
.500	2.72	-9.	0.	0.	0.	0.	0.	0.	0.	0.	0.	0.

0 0 331.0

CASE 27-4 LITTLETON MASS 12/5/59 .005-.02 CPS
DEC 120,0,0,120,40,10.,1,0,0,0,0,0
PG 0000000000000000000000000000000000000000000000000000000000000000

POWER DENSITY SPECTRA

FREQ	H1	H2	E1	E2
	MS GAMMAS		MS MV/KM	
.001	.200E 04	.	.	.266E 02
.001	.508E 03	.	.	.436E 02
.002	.751E 02	.	.	.228E 02
.004	.153E 03	.	.	.142E 02
.005	.310E 03	.	.	.132E 04
.006	.295E 03	.	.	.365E 04
.007	.277E 03	.	.	.396E 04
.009	.317E 03	.	.	.489E 04
.010	.205E 03	.	.	.546E 04
.011	.456E 02	.	.	.249E 04
.012	.244E 01	.	.	.460E 03
.014	.429E 01	.	.	.339E 03
.015	.281E 01	.	.	.204E 03
.016	.432E 01	.	.	.124E 03
.017	.489E 01	.	.	.123E 03
.019	.260E 01	.	.	.793E 02
.020	.128E 01	.	.	.122E 03
.021	.171E 01	.	.	.197E 03
.022	.111E 01	.	.	.109E 03
.024	.390E-00	.	.	.797E 02
.025	.358E-00	.	.	.131E 03
.026	.345E-00	.	.	.974E 02
.027	.331E-00	.	.	.303E 02
.029	.259E-00	.	.	.170E 02
.030	.788E-01	.	.	.125E 02
.031	.459E-01	.	.	.112E 02
.032	.629E-01	.	.	.113E 02
.034	.313E-01	.	.	.777E 01
.035	.161E-02	.	.	.119E 02
.036	.136E-01	.	.	.757E 01
.037	.125E-01	.	.	.263E 01
.039	.826E-02	.	.	.470E 01
.040	.259E-02	.	.	.416E 01
.041	.106E-01	.	.	.396E 01
.042	.516E-02	.	.	.544E 01
.044	.343E-02	.	.	.577E 01
.045	.176E-02	.	.	.323E 01
.046	.280E-02	.	.	.104E 01
.047	.177E-02	.	.	.372E-00
.049	.862E-02	.	.	.218E 01
.050	.108E-01	.	.	.435E 01

COHERENCY ANALYSIS

FREQ	(H1,E2)		(H1,E1)		(H1,H2)		(H2,E1)		(H2,E2)		(E1,E2)	
	AMP	PHASE	AMP	PHASE	AMP	PHASE	AMP	PHASE	AMP	PHASE	AMP	PHASE
.001	0.49	50.	0.	0.	0.	0.	0.	0.	0.	0.	0.	0.
.001	0.34	-3.	0.	0.	0.	0.	0.	0.	0.	0.	0.	0.
.002	0.62	-54.	0.	0.	0.	0.	0.	0.	0.	0.	0.	0.
.004	1.51	47.	0.	0.	0.	0.	0.	0.	0.	0.	0.	0.
.005	0.79	10.	0.	0.	0.	0.	0.	0.	0.	0.	0.	0.
.006	0.85	-12.	0.	0.	0.	0.	0.	0.	0.	0.	0.	0.
.007	0.86	-18.	0.	0.	0.	0.	0.	0.	0.	0.	0.	0.
.009	0.91	-0.	0.	0.	0.	0.	0.	0.	0.	0.	0.	0.

.010	0.94	3.	0.	0.	0.	0.	0.	0.	0.	0.	0.	0.
.011	0.86	-4.	0.	0.	0.	0.	0.	0.	0.	0.	0.	0.
.012	0.41	-86.	0.	0.	0.	0.	0.	0.	0.	0.	0.	0.
.014	0.70	-67.	0.	0.	0.	0.	0.	0.	0.	0.	0.	0.
.015	0.74	-71.	0.	0.	0.	0.	0.	0.	0.	0.	0.	0.
.016	0.61	-20.	0.	0.	0.	0.	0.	0.	0.	0.	0.	0.
.017	0.83	-34.	0.	0.	0.	0.	0.	0.	0.	0.	0.	0.
.019	0.99	-46.	0.	0.	0.	0.	0.	0.	0.	0.	0.	0.
.020	0.92	-35.	0.	0.	0.	0.	0.	0.	0.	0.	0.	0.
.021	0.88	-24.	0.	0.	0.	0.	0.	0.	0.	0.	0.	0.
.022	0.76	-2.	0.	0.	0.	0.	0.	0.	0.	0.	0.	0.
.024	0.75	9.	0.	0.	0.	0.	0.	0.	0.	0.	0.	0.
.025	0.94	-47.	0.	0.	0.	0.	0.	0.	0.	0.	0.	0.
.026	0.88	-77.	0.	0.	0.	0.	0.	0.	0.	0.	0.	0.
.027	0.97	70.	0.	0.	0.	0.	0.	0.	0.	0.	0.	0.
.029	1.05	88.	0.	0.	0.	0.	0.	0.	0.	0.	0.	0.
.030	1.20	-72.	0.	0.	0.	0.	0.	0.	0.	0.	0.	0.
.031	1.19	-42.	0.	0.	0.	0.	0.	0.	0.	0.	0.	0.
.032	1.18	-51.	0.	0.	0.	0.	0.	0.	0.	0.	0.	0.
.034	1.27	-71.	0.	0.	0.	0.	0.	0.	0.	0.	0.	0.
.035	1.63	69.	0.	0.	0.	0.	0.	0.	0.	0.	0.	0.
.036	0.89	-25.	0.	0.	0.	0.	0.	0.	0.	0.	0.	0.
.037	1.82	-12.	0.	0.	0.	0.	0.	0.	0.	0.	0.	0.
.039	1.63	11.	0.	0.	0.	0.	0.	0.	0.	0.	0.	0.
.040	2.65	17.	0.	0.	0.	0.	0.	0.	0.	0.	0.	0.
.041	1.57	15.	0.	0.	0.	0.	0.	0.	0.	0.	0.	0.
.042	2.53	-2.	0.	0.	0.	0.	0.	0.	0.	0.	0.	0.
.044	2.37	-16.	0.	0.	0.	0.	0.	0.	0.	0.	0.	0.
.045	2.04	-38.	0.	0.	0.	0.	0.	0.	0.	0.	0.	0.
.046	1.45	-67.	0.	0.	0.	0.	0.	0.	0.	0.	0.	0.
.047	3.30	-19.	0.	0.	0.	0.	0.	0.	0.	0.	0.	0.
.049	1.24	3.	0.	0.	0.	0.	0.	0.	0.	0.	0.	0.
.050	1.01	0.	0.	0.	0.	0.	0.	0.	0.	0.	0.	0.

0 0 331.3

Note:

In Case 27-5 the E2 power spectra must be divided by 11 because the gain was put in the machine as 300 when it should have been 1000.

CASE 27-5 LITTLETON MASS 12/5/59 .02-.06 CPS
DEC 166,0,0,166,40,5.,1,0,0,0,0,0
PG 0000000000000000000000000000000000000000000000000000000000000000

POWER DENSITY SPECTRA

FREQ	H1	H2	E1	E2
	MS GAMMAS		MS MV/KM	
.001	.381E 01	.	.	.556E 02
.002	.132E 01	.	.	.576E 02
.005	.206E-00	.	.	.590E 02
.007	.632E-01	.	.	.605E 02
.010	.700E-01	.	.	.480E 02
.012	.521E 00	.	.	.138E 03
.015	.723E 00	.	.	.294E 03
.017	.127E 01	.	.	.713E 03
.020	.241E 01	.	.	.208E 04
.022	.206E 01	.	.	.261E 04
.025	.857E 00	.	.	.185E 04
.027	.394E-00	.	.	.168E 04
.030	.374E-00	.	.	.140E 04
.032	.366E-00	.	.	.103E 04
.035	.439E-00	.	.	.101E 04
.037	.507E 00	.	.	.114E 04
.040	.363E-00	.	.	.121E 04
.042	.204E-00	.	.	.896E 03
.045	.130E-00	.	.	.550E 03
.047	.813E-01	.	.	.366E 03
.050	.588E-01	.	.	.259E 03
.052	.419E-01	.	.	.167E 03
.055	.246E-01	.	.	.137E 03
.057	.145E-01	.	.	.184E 03
.060	.157E-01	.	.	.189E 03
.062	.164E-01	.	.	.112E 03
.065	.100E-01	.	.	.530E 02
.067	.298E-02	.	.	.265E 02
.070	.135E-02	.	.	.679E 01
.072	.139E-02	.	.	.110E 01
.075	.932E-03	.	.	.206E 01
.077	.989E-03	.	.	.796E 01
.080	.970E-03	.	.	.165E 02
.082	.501E-03	.	.	.184E 02
.085	.229E-03	.	.	.122E 02
.087	.184E-03	.	.	.160E 02
.090	.185E-03	.	.	.226E 02
.092	.194E-03	.	.	.218E 02
.095	.113E-03	.	.	.252E 02
.097	.203E-03	.	.	.269E 02
.100	.326E-03	.	.	.245E 02

COHERENCY ANALYSIS

FREQ	(H1,E2)		(H1,E1)		(H1,H2)		(H2,E1)		(H2,E2)		(E1,E2)	
	AMP	PHASE	AMP	PHASE	AMP	PHASE	AMP	PHASE	AMP	PHASE	AMP	PHASE
.001	0.23	10.	0.	0.	0.	0.	0.	0.	0.	0.	0.	0.
.002	0.23	-29.	0.	0.	0.	0.	0.	0.	0.	0.	0.	0.
.005	0.31	-58.	0.	0.	0.	0.	0.	0.	0.	0.	0.	0.
.007	0.43	-44.	0.	0.	0.	0.	0.	0.	0.	0.	0.	0.
.010	0.17	26.	0.	0.	0.	0.	0.	0.	0.	0.	0.	0.
.012	0.88	-11.	0.	0.	0.	0.	0.	0.	0.	0.	0.	0.
.015	0.83	-10.	0.	0.	0.	0.	0.	0.	0.	0.	0.	0.
.017	0.81	-22.	0.	0.	0.	0.	0.	0.	0.	0.	0.	0.

.020	0.92	-20.	0.	0.	0.	0.	0.	0.	0.	0.	0.	0.
.022	0.95	-16.	0.	0.	0.	0.	0.	0.	0.	0.	0.	0.
.025	0.88	-17.	0.	0.	0.	0.	0.	0.	0.	0.	0.	0.
.027	0.78	-24.	0.	0.	0.	0.	0.	0.	0.	0.	0.	0.
.030	0.77	-31.	0.	0.	0.	0.	0.	0.	0.	0.	0.	0.
.032	0.84	-30.	0.	0.	0.	0.	0.	0.	0.	0.	0.	0.
.035	0.90	-28.	0.	0.	0.	0.	0.	0.	0.	0.	0.	0.
.037	0.93	-42.	0.	0.	0.	0.	0.	0.	0.	0.	0.	0.
.040	0.93	-50.	0.	0.	0.	0.	0.	0.	0.	0.	0.	0.
.042	0.91	-45.	0.	0.	0.	0.	0.	0.	0.	0.	0.	0.
.045	0.88	-25.	0.	0.	0.	0.	0.	0.	0.	0.	0.	0.
.047	0.84	-13.	0.	0.	0.	0.	0.	0.	0.	0.	0.	0.
.050	0.79	-38.	0.	0.	0.	0.	0.	0.	0.	0.	0.	0.
.052	0.93	-60.	0.	0.	0.	0.	0.	0.	0.	0.	0.	0.
.055	0.89	-53.	0.	0.	0.	0.	0.	0.	0.	0.	0.	0.
.057	0.90	-34.	0.	0.	0.	0.	0.	0.	0.	0.	0.	0.
.060	0.83	-27.	0.	0.	0.	0.	0.	0.	0.	0.	0.	0.
.062	0.71	-14.	0.	0.	0.	0.	0.	0.	0.	0.	0.	0.
.065	0.69	1.	0.	0.	0.	0.	0.	0.	0.	0.	0.	0.
.067	0.45	29.	0.	0.	0.	0.	0.	0.	0.	0.	0.	0.
.070	0.99	-84.	0.	0.	0.	0.	0.	0.	0.	0.	0.	0.
.072	0.86	45.	0.	0.	0.	0.	0.	0.	0.	0.	0.	0.
.075	0.51	-18.	0.	0.	0.	0.	0.	0.	0.	0.	0.	0.
.077	0.62	14.	0.	0.	0.	0.	0.	0.	0.	0.	0.	0.
.080	0.58	17.	0.	0.	0.	0.	0.	0.	0.	0.	0.	0.
.082	0.38	16.	0.	0.	0.	0.	0.	0.	0.	0.	0.	0.
.085	0.18	-44.	0.	0.	0.	0.	0.	0.	0.	0.	0.	0.
.087	0.16	-31.	0.	0.	0.	0.	0.	0.	0.	0.	0.	0.
.090	0.36	-41.	0.	0.	0.	0.	0.	0.	0.	0.	0.	0.
.092	0.57	-50.	0.	0.	0.	0.	0.	0.	0.	0.	0.	0.
.095	0.75	-71.	0.	0.	0.	0.	0.	0.	0.	0.	0.	0.
.097	0.59	-74.	0.	0.	0.	0.	0.	0.	0.	0.	0.	0.
.100	0.49	-73.	0.	0.	0.	0.	0.	0.	0.	0.	0.	0.

0 0 331.7
DPR M277 DATA OUTPUT IS FINISHED. THANK YOU

APPENDIX II

APPARENT RESISTIVITY CALCULATIONS

In this appendix the results of calculations for the apparent resistivity are included. The calculations were done using the formula

$$\rho_a = .2\ T\ \left(\frac{E}{H}\right)^2$$

$$= .^2/_f\ \left(\frac{PE}{PH}\right)$$

where T is the period in seconds, f the frequency in cps, PE the power density of the electric field, and PH that of the magnetic field. The data for the calculations were taken from the tables in Appendix I. Each table starts with the case number and frequency, followed by a merit number and the number of lags in the correlation analysis. The merit numbers are discussed in Chapter IV and run from 1 to 3 with 1 designating the best records and 3 the poorest.

The resistivities were only calculated in the pass band or at most one frequency band outside it. They were generally only calculated for data with good coherency.

Case 20-8 .02 - .04 cps
Merit No-2 20 lags

f	
.020 cps	20,800 ohm meters
.025	17,500
.030	10,500
.035	9350
.040	22,000
.045	44,000

Case 21-3 .04 - .06 cps
Merit No-2 20 lags

f	
.040 cps	3700 ohm meters
.045	4000
.050	2350
.055	1800
.060	2700
.065	4250

Case 21-4 .06 - .1 cps
Merit No-1 20 lags

f	
.050 cps	2940 ohm meters
.062	3900
.075	3400
.087	1870
.100	1450

Case 24-5 .02 - .06 cps
Merit No-3 20 lags

f	
.020 cps	360 ohm meters
.025	490
.030	550
.035	475
.040	370
.045	310
.050	410

Case 24-6 .06 - .2 cps
Merit No-2 20 lags

f	
.050 cps	10,600 ohm meters
.062	11,000
.075	17,400
.087	30,400
.100	22,500

Case 26-1 .02 - .06 cps
Merit No-1 20 lags

f	
.020 cps	2580 ohm meters
.040	8200
.045	7050
.050	5780
.055	2980
.060	6600

Case 26-2 .2 - .6 cps
Merit No-3 20 lags

f	
.20 cps	14,600 ohm meters
.25	12,000
.30	13,700
.35	14,000
.40	11,800

Case 26-3 .08 - .2 cps
Merit No-2 20 lags

f	
.125 cps	12,200 ohm meters
.150	9200
.175	9300
.200	13,500
.225	15,500

Case 26-4 .06 - .08 cps
Merit No-2 20 lags

f	
.050 cps	6320 ohm meters
.062	9200
.075	14700

Case 26-5 .02 - .04 cps
Merit No-1 20 lags

f	
.015 cps	1200 ohm meters
.020	1450
.025	1500
.030	1860
.035	2460

Case 26-6 .02 - .06 cps
Merit No-1 20 lags

f	
.015 cps	800 ohm meters
.020	860
.025	995
.030	1350
.035	1970
.040	2380
.045	2500
.050	2750
.055	3000
.060	3000

Case 26-7 .02 - .06 cps
Merit No-1 20 lags

f	
.010 cps	830 ohm meters
.015	1200
.020	1540
.025	1650
.030	1140
.035	840

Case 27-1 .6 - 1 cps
Merit No-3 20 lags

f	
.5 cps	1240 ohm meters
.625	980
.750	1280
.875	1970
1.000	2900

Case 27-1 .6 - 1 cps
Merit No-3 40 lags

f	
.5 cps	1650 ohm meters
.562	1360
.625	750
.687	520
.750	1560
.812	812
.875	1550
.937	1670
1.000	4500

Case 27-2 .2 - .6 cps
Merit No-2 20 lags

f	
.20 cps	7940 ohm meters
.25	11700
.30	9200
.35	4050
.40	5000
.45	9300
.50	7800
.55	4750
.60	5000

Case 27-2 .2 - .6 cps
Merit No-2 40 lags

f	
.200 cps	6250 ohm meters
.225	13000
.250	13600
.275	10500
.300	9000
.325	6600
.350	2500
.375	2220
.400	5350
.425	10000
.450	12500
.475	13000
.500	5300
.525	1730
.550	4830
.575	8200
.600	6900

Case 27-3 .06 - .2 cps
Merit No-1 20 lags

f	
.050 cps	1950 ohm meters
.075	2820
.100	3900
.125	7700
.150	16300
.175	13300

Case 27-3 .06 - .2 cps
Merit No-1 40 lags

f	
.062 cps	2500 ohm meters
.075	3100
.087	2800
.100	3600
.112	7400
.125	10000
.137	16000
.150	20000
.162	12800
.175	9800
.187	13500
.200	9400

Case 27-4 .005 - .02 cps
Merit No-2 20 lags

f	
.005 cps	228 ohm meters
.007	390
.010	520
.012	860
.015	1000
.017	400
.020	640

Case 27-4 .005 - .02 cps
Merit No-2 40 lags

f	
.005 cps	170 ohm meters
.006	360
.007	410
.009	340
.010	535
.011	990
.012	310
.014	1130
.015	970
.016	360
.017	300
.019	320
.020	950

Case 27-5 Merit No-1 f	.02 - .06 cps 20 lags
.015 cps	560 ohm meters
.020	860
.025	1400
.030	1880
.035	1400
.040	1400
.045	1740
.050	1720
.055	2060
.060	2800
.065	2300

Case 27-5 Merit No-1 f	.02 - .06 cps 40 lags
.015 cps	490 ohm meters
.017	600
.020	780
.022	1040
.025	1570
.027	2860
.030	2260
.032	1590
.035	1190
.037	1000
.040	1500
.042	1900
.045	1700
.047	1740
.050	1600
.052	1390
.055	1800
.057	4000
.060	3620
.062	2000
.065	1470

APPENDIX III

DERIVATIONS

In the pages that follow, the details of the derivations used in Chapter III are presented. They are subdivided into,

a) The conductivity structure is anisotropic and the fields linearly polarized.

b) The conductivity structure is inhomogeneous with one field linearly polarized.

c) The conductivity structure is either anisotropic or inhomogeneous and the fields are elliptically polarized.

a) For anisotropic conductivity structure and linearly polarized fields(text reference, page 67)

Two separate measurements, I and II, are made,

Then

$$1)\ H_2^{I} = \alpha_{21} E_1^{I} + \alpha_{22} E_2^{I}$$

$$2)\ H_2^{II} = \alpha_{21} E_1^{II} + \alpha_{22} E_2^{II}$$

$$3)\ H_1^{I} = \alpha_{11} E_1^{I} + \alpha_{12} E_2^{I}$$

$$4)\ H_1^{II} = \alpha_{11} E_1^{II} + \alpha_{12} E_2^{II}$$

Phase of α_{ij} is 45°

Multiplying 1) and 2) by E_1^{II} and E_1^{I} respectively

$$H_2^{I} E_1^{II} = \alpha_{21} E_1^{I} E_1^{II} + \alpha_{22} E_2^{I} E_1^{II}$$

$$H_2^{II} E_1^{I} = \alpha_{21} E_1^{II} E_1^{I} + \alpha_{22} E_2^{II} E_1^{I}$$

Solving

$$5)\ \frac{H_2^{I} E_1^{II} - H_2^{II} E_1^{I}}{E_2^{I} E_1^{II} - E_2^{II} E_1^{I}} = \alpha_{22}$$

Multiplying 1) and 2) by E_2^{II} and E_2^{I} respectively

$$H_2^{I} E_2^{II} = \alpha_{21} E_1^{I} E_2^{II} + \alpha_{22} E_2^{I} E_2^{II}$$

$$H_2^{II} E_2^{I} = \alpha_{21} E_1^{II} E_2^{I} + \alpha_{22} E_2^{II} E_2^{I}$$

Solving

$$6) \quad \alpha_{21} = \frac{H_2^{I} E_2^{II} - H_2^{II} E_2^{I}}{E_1^{I} E_2^{II} - E_1^{II} E_2^{I}}$$

Multiplying 3) and 4) by E_1^{II} and E_1^{I} respectively

$$H_1^{I} E_1^{II} = \alpha_{11} E_1^{I} E_1^{II} + \alpha_{12} E_2^{I} E_1^{II}$$

$$H_1^{II} E_1^{I} = \alpha_{11} E_1^{II} E_1^{I} + \alpha_{12} E_2^{II} E_1^{I}$$

Solving

$$7) \quad \alpha_{12} = \frac{H_1^{I} E_1^{II} - H_1^{II} E_1^{I}}{E_2^{I} E_1^{II} - E_2^{II} E_1^{I}}$$

Multiplying 3) and 4) by E_2^{II} and E_2^{I} respectively

$$H_1^{I} E_2^{II} = \alpha_{11} E_1^{I} E_2^{II} + \alpha_{12} E_2^{I} E_2^{II}$$

$$H_1^{II} E_2^{I} = \alpha_{11} E_1^{II} E_2^{I} + \alpha_{12} E_2^{II} E_2^{I}$$

Solving

$$8) \quad \alpha_{11} = \frac{H_1^{I} E_2^{II} - H_1^{II} E_2^{I}}{E_1^{I} E_2^{II} - E_1^{II} E_2^{I}}$$

b) The conductivity structure is inhomogeneous with one field linearly polarized. (Text reference, page 68.)

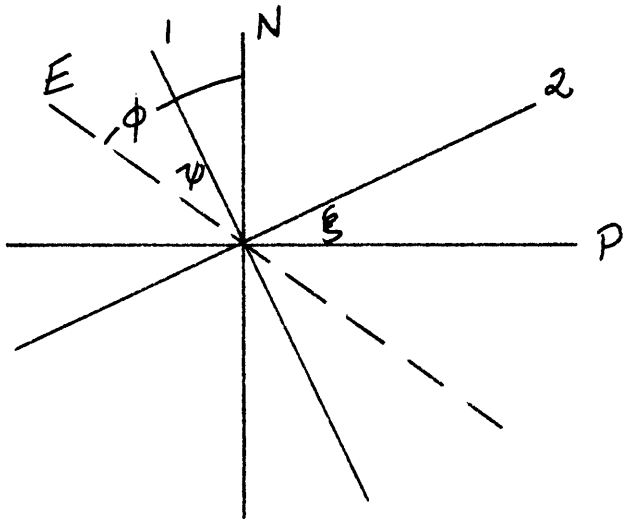

N & P are symmetry axes.

1 & 2 are measurement axes.

E is axis of linear polarization of electric signal.

$$H_p = E_N |\alpha_1| e^{i\phi_1}$$

$$H_N = -E_p |\alpha_2| e^{i\phi_2}$$

$$H_2 = H_p \cos\xi + H_N \sin\xi$$

$$H_1 = -H_p \sin\xi + H_N \cos\xi$$

$$H_2 = E_N \alpha_1 e^{i\phi_1} \cos\xi - E_p \alpha_2 e^{i\phi_2} \sin\xi$$

$$H_1 = -E_N \alpha_1 e^{i\phi_1} \sin\xi - E_p \alpha_2 e^{i\phi_2} \cos\xi$$

where absolute values of $\alpha_1 \neq \alpha_2$ are assumed

Substituting

$$E_N = E \cos\phi$$

$$E_p = -E \sin\phi$$

$$H_2 = E\{\cos\phi\ \alpha_1 e^{i\phi_1} \cos\xi - \sin\phi\ \alpha_2 e^{i\phi_2} \sin\xi\}$$

$$H_1 = E\{\cos\phi\ \alpha_1 e^{i\phi_1} \sin\xi + \sin\phi\ \alpha_2 e^{i\phi_2} \cos\xi\}$$

or if $\alpha_1 \neq \alpha_2$ are complex

$$9)\quad H_2 = E\{\cos\phi\ \alpha_1 \cos\xi - \sin\phi\ \alpha_2 \sin\xi\}$$

$$10)\quad H_1 = E\{\cos\phi\ \alpha_1 \sin\xi + \sin\phi\ \alpha_2 \cos\xi\}$$

We measure $H_1, H_2, E,$ and the phases in between,

so that

11) $H_1 = E a_1 e^{i\theta_m^1} = E\{Re\, a_1 + Im\, a_1\}$

12) $H_2 = E a_2 e^{i\theta_m^2} = E\{Re\, a_2 + Im\, a_2\}$

Equating real and imaginary parts in 9) and 10), we have

13) $Re\, a_2 = \cos\phi \cos\xi\, Re\,\alpha_1 - \sin\phi \sin\xi\, Re\,\alpha_2$

14) $Im\, a_2 = \cos\phi \cos\xi\, Im\,\alpha_1 - \sin\phi \sin\xi\, Im\,\alpha_2$

15) $Re\, a_1 = \cos\phi \sin\xi\, Re\,\alpha_1 + \sin\phi \cos\xi\, Re\,\alpha_2$

16) $Im\, a_1 = \cos\phi \sin\xi\, Im\,\alpha_1 + \sin\phi \cos\xi\, Im\,\alpha_2$

Using the fact that

$$\phi = \psi + \xi$$

$$Re\ a_2 = (\cos\psi\cos\xi - \sin\psi\sin\xi)\alpha_1\cos\xi\cos\phi_1 - (\sin\psi\cos\xi + \cos\psi\sin\xi)\alpha_2\sin\xi\cos\phi_2$$

(A)

17) $$Re\ a_2 = \left(\cos\psi\left\{1-\sin^2\xi\right\} - \sin\psi\sin\xi\sqrt{1-\sin^2\xi}\right)\alpha_1\cos\phi_1 - \left(\sin\psi\sin\xi\sqrt{1-\sin^2\xi} + \cos\psi\sin^2\xi\right)\alpha_2\cos\phi_2$$

(B)

(E)

18) $$Im\ a_2 = \left(\cos\psi\left\{1-\sin^2\xi\right\} - \sin\psi\sin\xi\sqrt{1-\sin^2\xi}\right)\alpha_1\sin\phi_1 - \left(\sin\psi\sin\xi\sqrt{1-\sin^2\xi} + \cos\psi\sin^2\xi\right)\alpha_2\sin\phi_2$$

(F)

Using equations 15 and 16

(C)

19) $$Re\ a_1 = \left(\cos\psi\sin\xi\sqrt{1-\sin^2\xi} - \sin\psi\sin^2\xi\right)\alpha_1\cos\phi_1 + \left(\sin\psi\left\{1-\sin^2\xi\right\} + \cos\psi\sin\xi\sqrt{1-\sin^2\xi}\right)\alpha_2\cos\phi_2$$

(D)

(G)

$$20)\ \mathrm{Im}\ a_1 = \left(\cos\psi\sqrt{1-\sin^2\xi}\,\sin\xi - \sin\psi\sin^2\xi\right)\alpha_1\sin\phi_1 + \left(\sin\psi\{1-\sin^2\xi\} + \cos\psi\sin\xi\sqrt{1-\sin^2\xi}\right)\alpha_2\sin\phi_2$$

(H)

Solving for $\alpha_2\cos\phi_2$ (i.e. $\mathrm{Re}\,\alpha_2$)

From 17)

$$21)\ \alpha_2\cos\phi_2 = \frac{-\mathrm{Re}\,a_2 + A\alpha_1\cos\phi_1}{B}$$

From 19)

$$22)\ \alpha_2\cos\phi_2 = \frac{\mathrm{Re}\,a_1 - C\alpha_1\cos\phi_1}{D}$$

Solving for $\alpha_2 \sin \phi_2$ (ie $\mathrm{Im}\, \alpha_2$)

From 18)

$$23)\quad \alpha_2 \sin \phi_2 = \frac{-\mathrm{Im}\, a_2 + E \alpha_1 \sin \phi_1}{F}$$

From 20)

$$24)\quad \alpha_2 \sin \phi_2 = \frac{\mathrm{Im}\, a_1 - G \alpha_1 \sin \phi_1}{H}$$

Combining 21) and 22)

$$25)\quad \alpha_1 \cos \phi_1 = \frac{B\, \mathrm{Re}\, a_1 + D\, \mathrm{Re}\, a_2}{AD + BC}$$

Combining 23) and 24)

$$26)\quad \alpha_1 \sin \phi_1 = \frac{F\, \mathrm{Im}\, a_1 + H\, \mathrm{Im}\, a_2}{HE + FG}$$

Using superscripts and subscripts I and II to indicate two measurements

$$(\alpha_1 \sin\phi_1)^{I} = (\alpha_1 \sin\phi_1)^{II}$$

and

$$(\alpha_1 \cos\phi_1)^{I} = (\alpha_1 \cos\phi_1)^{II}$$

27)
$$\left\{ \frac{B\,Re\,a_1 + D\,Re\,a_2}{AD + BC} \right\}_I =$$

$$\left\{ \frac{B\,Re\,a_1 + D\,Re\,a_2}{AD + BC} \right\}_{II}$$

and

$$28)\quad \left\{ \frac{F\,\mathrm{Im}\,a_1 + H\,\mathrm{Im}\,a_2}{HE + FG} \right\}_{I} =$$

$$\left\{ \frac{F\,\mathrm{Im}\,a_1 + H\,\mathrm{Im}\,a_2}{HE + FG} \right\}_{II}$$

This gives two equations with the unknown $\sin\xi$; fourth order in $\sin\xi$.

A numerical test was carried out by picking values of for some fictitious data to see roughly the number of roots for $0^\circ < \xi < 90^\circ$.

The values chosen were:

Measurement I		Measurement II	
$\psi_I = 30°$	$a_1 = 1$	$\psi_{II} = 60°$	$a_1 = 1/2$
$\theta_m^{I_1} = 60°$	$a_2 = 1/2$	$\theta_m^{II_1} = 45°$	$a_2 = 1$
$\theta_m^{I_2} = 45°$		$\theta_m^{II_2} = 30°$	

Then for Case I

A $.866(1-\sin^2\xi) - .5\sin\xi\sqrt{1-\sin^2\xi}$

B $.5\sin\xi\sqrt{1-\sin^2\xi} + .866\sin^2\xi$

C $.866\sin\xi\sqrt{1-\sin^2\xi} - .5\sin^2\xi$

D $.5(1-\sin^2\xi) + .866\sin\xi\sqrt{1-\sin^2\xi}$

E $.866(1-\sin^2\xi) - .5\sin\xi\sqrt{1-\sin^2\xi}$

F $.5\sin\xi\sqrt{1-\sin^2\xi} + .866\sin^2\xi$

G $.866\sin\xi\sqrt{1-\sin^2\xi} - .5\sin^2\xi$

H $.5(1-\sin^2\xi) + .866\sin\xi\sqrt{1-\sin^2\xi}$

And for Case II

A $.5(1-\sin^2\xi) - .866\sin\xi\sqrt{1-\sin^2\xi}$

B $.866\sin\xi\sqrt{1-\sin^2\xi} + .5\sin^2\xi$

C $.5\sqrt{1-\sin^2\xi}\sin\xi - .866\sin^2\xi$

D $.866(1-\sin^2\xi) + .5\sin\xi\sqrt{1-\sin^2\xi}$

$$E \quad .5(1-\sin^2\xi) - .866\sin\xi\sqrt{1-\sin^2\xi}$$

$$F \quad .866\sin\xi\sqrt{1-\sin^2\xi} + .5\sin^2\xi$$

$$G \quad .5\sin\xi\sqrt{1-\sin^2\xi} - .866\sin^2\xi$$

$$H \quad .866(1-\sin^2\xi) + .5\sin\xi\sqrt{1-\sin^2\xi}$$

Using 27) and 28) and trial values for ξ

$$27)\ \{\ \}_I - \{\ \}_{II} = \Delta_1$$

$$28)\ \{\ \}_I - \{\ \}_{II} = \Delta_2$$

ξ	Δ_1	Δ_2
0°	−1.320	−.590
45°	+5.71	+5.70
90°	−.59	−.30

c) Conductivity structure either anisotropic or inhomogeneous with elliptic fields (text reference, page 70)

Again

$$H_2 = E_N \alpha_1 e^{i\phi_1}\cos\xi + E_p \alpha_2 e^{i\phi_2}\sin\xi$$

$$H_1 = -E_N \alpha_1 e^{i\phi_1}\sin\xi + E_p \alpha_2 e^{i\phi_2}\cos\xi$$

Then, substituting for E_N and E_ρ in terms of E_1 and E_2

$$29)\quad H_2 = \{E_1 \cos\xi + E_2 \sin\xi\}\,\alpha_1 e^{i\phi_1}\cos\xi \quad (R)$$
$$+ \{-E_1 \sin\xi + E_2 \cos\xi\}\,\alpha_2 e^{i\phi_2}\sin\xi \quad (L)$$

$$30)\quad H_1 = -\{E_1 \cos\xi + E_2 \sin\xi\}\,\alpha_1 e^{i\phi_1}\sin\xi \quad (M)$$
$$+ \{-E_1 \sin\xi + E_2 \cos\xi\}\,\alpha_2 e^{i\phi_2}\cos\xi \quad (N)$$

Measurements give

$$E_1 = H_2\, m_1\, e^{i\tau_1}$$
$$E_2 = H_2\, m_2\, e^{i\tau_2}$$
$$E_1 = H_1\, m_3\, e^{i\tau_3}$$
$$E_2 = H_1\, m_4\, e^{i\tau_4}$$

where m_i is amplitude factor and τ_i is phase.

Making these substitutions,

From 29)

$$31)\quad \alpha_1 e^{i\phi_1} = \frac{H_2 - \{L\}\alpha_2 e^{i\phi_2}\sin\xi}{\{K\}\cos\xi}$$

From 30)

$$32)\quad \alpha_1 e^{i\phi_1} = \frac{H_1 - \{N\}\alpha_2 e^{i\phi_2}\cos\xi}{-\{M\}\sin\xi}$$

and combining 31) and 32)

$$33)\quad \alpha_2 e^{i\phi_2} = \frac{H_1(\{K\})\cos\xi + H_2\{M\}\sin\xi}{\{L\}\{M\}\sin\xi + \{N\}\{K\}\cos\xi}$$

with two measurements

$$34)\quad \left\{\frac{H_1\{K\}\cos\xi + H_2\{M\}\sin\xi}{\{L\}\{M\}\sin\xi + \{N\}\{K\}\cos\xi}\right\}_{I} -$$

$$\left\{\frac{H_1\{K\}\cos\xi + H_2\{M\}\sin\xi}{\{L\}\{M\}\sin\xi + \{N\}\{K\}\cos\xi}\right\}_{II} = 0$$

34) is again fourth order in $\sin\xi$ if $\cos\xi$ is set equal to $\sqrt{1-\sin^2\xi}$. The number of roots was not tested, but it probably has multiple roots for $0^\circ < \xi < 90^\circ$.

BIOGRAPHICAL NOTE

T. Cantwell was born and attended school in Kenmore, New York. He received a B.S. in Chemical Engineering at M.I.T. in 1948, and an M.B.A. from Harvard in 1951. Since 1952 he has been employed by M.I.T. in the Industrial Liaison Office, as the project engineer on the M.I.T. Nuclear Reactor, and most recently as a Research Associate in the Department of Geology and Geophysics.

BIBLIOGRAPHY

Bendat, J.S., 1958, Principles and Applications of Random Noise Theory, John Wiley and Sons, 431 pp.

Blackman, R.B. and Tukey, J.W., 1958, The Measurement of Power Spectra, Dover Publications, 190 pp.

Burkhart, K., 1955, Micropulsations of Earth Currents and of the Horizontal Component of the Earth's Magnetic Field, Zeitschrift fur Geophysik, 57-73.

Cagniard, L., 1953, Basic Theory of the Magnetotelluric Method, Geophysics, 8, 605-635.

Cagniard, L., 1956, Electricite Tellurique, Handbuch der Physik, 47, 407-469.

Campbell, W.H., 1959, Studies of Magnetic Field Micropulsations with Periods of 5 to 30 Seconds, J. Geophys. Res., 64, 1819-1826.

Clemmow, P.C., 1953, Radio Propagation over a Flat Earth Across a Boundary Separating Two Media, Phil. Trans. Roy. Soc. Lond., A246, 1-55.

Davenport, W.B. and Root, W.L., 1958, Random Signals and Noise, McGraw Hill Book Co., 393 pp.

Deal, O.E., 1955, The Observation of Very Low Frequency Electromagnetic Signals of Natural Origin, Ph.D. Thesis, UCLA.

Duffus, H.J. and Shand, J.A., 1958, Some Observations of Geomagnetic Micropulsations, Canadian J. of Physics, 36, 508-526.

Duffus, H.J. et al, 1959, Geographical Variations in Geomagnetic Micropulsations, J. of Geophys. Res., 64, 581-583.

Dulaney, E.N., 1959, Personal Communication.

Enenshtein, B.S. and Aronov, L.E., 1957, Experimental Research into the Natural Electromagnetic Field of the Earth in the Frequency Spectrum 2-300 cps, Bull. Acad. of Sci. USSR, Geophysics Series, 68-78, AGU English Translation.

Goldberg, P.A., 1953, Observations of Short Period Fluctuations in the Geomagnetic Field, Ph.D. Thesis, UCLA.

Hatakeyama, H. and Hirayama, M., 1934, On the Phase Difference Between the Pulsation of Terrestrial Magnetism and of Earth Current, J. of Met. Soc. of Japan, 12, 449-459.

Holmberg, E.R.R., 1951, A Discussion of the Origin of Rapid Periodic Fluctuations of the Geomagnetic Field and a New Analysis of Observational Material, Ph.D. Thesis, London Univ.

Hughes, H., 1953, The Electrical Conductivity of the Earth's Interior, Ph.D. Thesis, Univ. of Cambridge.

Jackson, L.C., 1944, Wave Filters, Methuen & Co., Ltd., 107 pp.

Karal, F.C. and Karp, S., 1959, Diffraction of a Plane Wave by a Right Angle Wedge, New York Univ. Report No. EM-123.

Karp, S., 1959, Two Dimensional Greens Function for a Right Angle Wedge under an Impedance Boundary Condition, New York Univ. Report No. EM-129.

Kunetz, G., 1952, Enregistrements Des Courants Telluriques a l'Occasion de l'Eclipse de Soleil du Fevrier 1952, Compagnie Generale de Geophysique Publication, 1-9.

Kunetz, G., 1953, Correlation et recurrance des variations des courants tellurique et du champ magnetique, Presentation to 72nd Session of The French Association for the Advancement of Science, Proceedings, 240-243.

Kunetz, G. and D'Erceville, I., 1959, Some Observations Regarding Natural Electromagnetic Fields in Applied Geophysics, Paper at Soc. Explor. Geophys. Los Angeles Meeting.

Lipskaia, N.V., 1953, Some Relationships Between the Harmonic Periodic Variations of Terrestrial Electromagnetic Fields, Bull. Acad. Sci. USSR, Geophysics Series 1, 41-47.

MacDonald, G.J.F., 1959, Calculations on the Thermal Heating of the Earth, J. Geophys. Res., 64, 1967-2000.

Madden, T.R., 1959, Personal Communication.

Maple, E., 1959, Geomagnetic Oscillations at Middle Latitudes, Parts I and II, J. Geophys. Res., 64, 1395-1409.

Maple, E., 1959, Personal Communication.

Neves, A.S., 1957, The Magnetotelluric Method in Two Dimensional Structures, Ph.D. Thesis, M.I.T.

Niblett, E.R., 1959, An Estimate of the Variation of Electric Conductivity with Depth by the Magnetotelluric Method, Paper at Soc. Explor. Geophys. Los Angeles Meeting.

Rikitake, T., 1951, Changes in Earth Currents and Their Relation to the Electric State of the Earth's Crust, Tokyo Univ. Earthquake Res. Bull., 29, 271-276.

Robinson, E.A., 1954, Predictive Decomposition of Time Series with Applications to Seismic Exploration, M.I.T. GAG Report No. 7.

Rubens, S.M., 1945, Surface Coil for Producing a Uniform Magnetic Field, 16, 243-245.

Schlumberger, M. and Kunetz, G., 1946, Variations rapides simultanees du champ tellurique en France et a Madagascar, C. R. Acad. Sci. Paris, 223, 551-553.

Scholte, J.G. and Veldkamp, J., 1955, Geomagnetic and Geoelectric Variations, Jour. Atmos. and Terr. Physics, 6, 33-45.

Simpson, S.M., 1959, Personal Communication.

Simpson, S.M., 1959, On the Computation of Autocorrelations and Spectra, Unpublished report.

Slichter, L.B., 1955, Geophysics Applied to Prospecting for Ores, Fiftieth Anniversary Volume, Economic Geology, 953-957.

Sommerfeld, A., 1952, Electrodynamics, Lectures on Theoretical Physics, Vol. III, Academic Press, 92-95.

Sucksdorff, E., 1939, Giant Pulsations Recorded at Sodankyla During 1914-1938, Terr. Mag. and Atmos. Elect., 44, 157-170.

Tikhonov, A.N. and Shakhsuvarov, D.N., 1956, The Possibility of Utilizing the Impedance of the Natural Electromagnetic Field of the Earth for Studying its Upper Strata, Bull. Acad. Sci. USSR, Geophysics Series, 4, 410-418.

Wait, J.R., 1954, On the Relations Between Telluric Currents and the Earth's Magnetic Field, Geophysics, 19, 281-289.

Ward, S.H., 1959, AFMAG - Airborne and Ground, Geophysics, 24, 761-789.

Ward, S.H. et al, 1958, Prospecting by Use of Natural Alternating Magnetic Fields of Audio and Sub-Audio Frequencies, Transactions CIMM, 61, 261-268.

Watanabe, T., 1959, Morphology of the Geomagnetic Pulsation, Jour. of Geomag. and Geoelect., 10, 177-184.

Webster, T.F., 1957, An Experimental Investigation of Telluric and Magnetotelluric Phenomena, M.S. Thesis, U. of Alberta.

Zharkov, V.N., 1958, On the Electrical Conductivity and Temperature of the Earth's Mantle, Bull. Acad. Sci. USSR, Geophysics Series, AGU English Translation, 260-266.

Compagnie Generale de Geophysique, 1955, Geophysical Prospecting, 3, Supplement 3.

Hauck, A.M., 1959, Personal Communication.

Lahiri, B.N. and Price, A.T., 1939, Electromagnetic Induction in Non-Uniform Conductors, and The Determination of the Conductivity of the Earth from Terrestrial Magnetic Variations, Phil. Trans. Roy. Soc. London, A, 237, 509-540.

McDonald, K.L., 1957, Penetration of the Geomagnetic Field Through a Mantle with Variable Conductivity, J. Geophys. Res., 62, 117-141.

Slichter, L.B., 1934, An Engineering Problem in Geophysics, Tech Engineering News, 8-9.

Tozer, D.C., 1959, The Electrical Properties of the Earth's Interior, Physics and Chemistry of the Earth, Vol. 3, 414-436.